CompCytogen 13(3): 197–210 (2019)
doi: 10.3897/CompCytogen.v13i3.34732
http://compcytogen.pensoft.net

RESEARCH ARTICLE

COMPARATIVE Cytogenetics
A peer-reviewed open-access journal
International Journal of Plant & Animal Cytogenetics, Karyosystematics, and Molecular Systematics

Dysfunction telomeres in embryonic fibroblasts and cultured *in vitro* pluripotent stem cells of *Rattus norvegicus* (Rodentia, Muridae)

Natalya S. Zhdanova[1], Evgenia A. Vaskova[1], Tatyana V. Karamysheva[1], Julia M. Minina[1], Nykolay B. Rubtsov[1], Suren M. Zakian[1,2,3]

1 *The Federal Research Center Institute of Cytology and Genetics SB RAS, Acad. Lavrentiev Ave. 10, Novosibirsk 630090, Russia* **2** *E.N. Meshalkin National medical research center, Ministry of Health of the Russian Federation, Rechkunovskaya st. 15, 630055, Novosibirsk, Russia* **3** *Institute of Chemical Biology and Fundamental Medicine SB RAS, Acad. Lavrentjeva av. 8, 630090, Novosibirsk, Russia*

Corresponding author: *Julia M. Minina* (minina_jul@bionet.nsc.ru)

Academic editor: *Alsu Saifitdinova* | Received 25 March 2019 | Accepted 24 June 2019 | Published 29 July 2019

http://zoobank.org/1CDD3226-5079-4F3B-AA0A-F010AA63316A

Citation: Zhdanova NS, Vaskova EA, Karamysheva TV, Minina JM, Rubtsov NB, Zakian SM (2019) Dysfunction telomeres in embryonic fibroblasts and cultured *in vitro* pluripotent stem cells of *Rattus norvegicus* (Rodentia, Muridae). Comparative Cytogenetics 13(3): 197–210. https://doi.org/10.3897/CompCytogen.v13i3.34732

Abstract

We studied the level of spontaneous telomere dysfunction in Rattus norvegicus (Berkenhout, 1769) (Rodentia, Muridae) embryonic fibroblasts (rEFs) and in cultured in vitro rat pluripotent stem cells (rPSCs), embryonic stem cells (rESCs) and induced pluripotent stem cells (riPSCs), on early passages and after prolonged cultivation. Among studied cell lines, rESCs showed the lowest level of telomere dysfunction, while the riPSCs demonstrated an elevated level on early passages of cultivation. In cultivation, the frequency of dysfunctional telomeres has increased in all studied cell lines; this is particularly true for dysfunctional telomeres occurring in G1 stage in riPSCs. The obtained data are mainly discussed in the connection with the specific structure of the telomere regions and their influence on the differential DNA damage response in them.

Keywords

dysfunctional telomeres, rat, embryonic fibroblasts, ESC, iPSC

Introduction

Telomeres are specialized structures on animal chromosome ends; they preserve chromosomes from degradation and end-to-end fusions contributing to genome stability and play an important role in the maintenance of chromosome integrity. The lagging strand of telomeric DNA consists of repeat arrays of TTAGGG and are ended by G-rich overhang, which inserts into double strand telomere region forming t-loop. As a result, the chromosome ends are no longer recognized as DSBs (Double Strand Breaks). In addition, telomeres are protected from inappropriate recombination by a specialized protein complex shelterin consisting of six proteins (de Lange 2005, 2018). Telomere shortening or any DNA lesions, disruption of telomere capping or any telomere deprotection contribute to telomere dysfunction and further replicative senescence, apoptosis, frequent chromosomal rearrangements, degenerative diseases and cancer (Karlseder et al. 2002, Kaul et al. 2011, Cesare et al. 2013).

It has been shown earlier that one unrepaired DSB in a whole genome is able to direct cells towards the replicative senescence (di Leonardo et al. 1994). However, the normal human cells proved to be resistant to four spontaneous DDR+ telomeres (dysfunctional telomeres, DNA Damage Response) arose in G1 cell phase (Kaul et al. 2011). Nevertheless, we revealed 24 of such telomeres per metaphase in the well dividing primary *Sorex granarius* (Miller, 1910) (Eulipotyphla, Soricidae) fibroblasts without of hallmarks of growth crisis (Zhdanova et al. 2014). The data about the level of telomere dysfunction in other mammalian species and in different tissue including pluripotent stem cells are restricted.

Recently, it was shown that if the chromosomes are tolerant to end-to-end fusions, then DDR of these telomeres differs from DDR in the entire genome. Such dysfunctional telomeres display differential ATM (Ataxia Telangiectasia Mutated, serine/threonine protein kinase) signaling containing not phosphorylated CHK2 (Check point 2 protein) and partial telomere deprotection with sufficient TRF2 (Telomere Repair Factor 2, component of sheltrin complex) (Cesare et al. 2013, Cesare 2014). Moreover, to overcome the replication fork stagnation near the looping structures of telomeric DNA, the cells can use a special mode of DNA replication combined with reparation pathways (Sakofsky and Malkova 2017, Sobinoff and Pickett 2017). In this way, the mechanisms involved in the occurrence of spontaneous telomere dysfunction appear to depend on the unusual structure of telomeric DNA and the disturbances in telomere specific safeguard protein complex.

γ-H2AX is usually used for detection of both manifest and invisible non repaired DNA breaks and also for visualization of deprotected telomeres (Martin et al. 2014, Cesare et al. 2013). γ-H2AX is a phosphorylated histone H2AX, a variant of canonical H2A histone, found in all studied eukaryotes. Being the early marker of DDR γ-H2AX is rapidly accumulated around the above disturbance. It plays an important role in the recruitment of other DNA repair-related proteins and especially in the retention of repair factors after their initial involvement (Celeste et al. 2003). Colocalized with telomeric DNA in interphase and on metaphase chromosomes, γ-H2AX forms foci, TIFs (Telomere dysfunction-Induced Foci) and Meta-TIFs, correspond-

ingly (Rogakou et al. 1998, Pilch et al. 2003, Pinto and Flaus 2010). To assess the level of telomere dysfunction, Meta-TIFs are suitable rather than TIFs (Kaul et al. 2011).

Here we study the level of spontaneous telomere dysfunction in *Rattus norvegicus* (Berkenhout, 1769) embryonic fibroblasts (rEFs) and in cultured *in vitro* rat pluripotent stem cells (rPSCs), embryonic stem cells (rESCs) and induced pluripotent stem cells (riPSCs), on early passages and after prolonged cultivation. Most of the metaphases of these cell lines showed dysfunctional telomeres occurring before and after DNA replication, the last prevailed. The rESCs on the early passages of cultivation showed the lowest level of telomere dysfunction, while the riPSC lines demonstrated an elevated level. The level of telomere dysfunction increased in all studied cell lines after prolonged cultivation, especially noticeable increase in the level of telomere dysfunction arisen after G1. In addition, we have revealed a preferred accumulation of such dysfunction telomeres in riPSC lines than in rESCs. Note also the significant heterogeneity of the level of spontaneous telomere dysfunction between lines in the studied groups.

Material and Methods

Generation of riPSC and cell cultures

Four rEF lines were obtained from *R. norvegicus* 12-day embryos of laboratory strains Wag (RNFM1 and RNFF1 lines) and Brattleboro Wag (RWF1 and RWM1 lines). Three rESC lines (RES6, RES27, and RES28) were isolated from blastocysts of different Wag rats. Three riPSC lines (NF13, QV28, and MR39) were established as clonal lines from RNFF1 on 6 passage of cultivation by transduction. Briefly, rEFs were seeded at 10^4 cells/cm^2 in a six-well plate. One hour before transduction, the growth medium was supplemented with 4 mg/ml hexadimethrine bromide (Polybrene, H9269; Sigma) and the virus particles diluted in culture medium were added to wells for 18 hours (Vaskova et al. 2015). Then the culture medium was replaced with a fresh medium with doxycycline (44577; Sigma) at a final concentration of 2 mg/ml. Four days later, cells were plated on a 10-cm culture dish containing inactivated by mitomycin mouse EFs and cultured in the riPSC medium (Vaskova et al. 2015). The rESC and riPSC lines were able to differentiate into derivatives of the three germ layers (Vaskova et al. 2015). The rEF lines contained 63–67 percent of diploid metaphases, rESCs – 47–72, and riPSCs – 49–55, correspondingly. Single different Rb fusions were observed only in RES26 line (data are not presented).

Immunochemistry and Fluorescencent *in situ* hybridization (FISH)

Meta-TIFs were visualized after immunochemistry with γ-H2AX antibodies and subsequent FISH (Fluorescent *In Situ* Hybridization) procedure with probe to telomeric DNA. Preparation of metaphase spreads for experiment was performed as described in

Zhdanova et al. (2014). Briefly, adherent cultures were treated with colcemid (20 ng/ml, Sigma-Aldrich) for one hour. Cell suspensions were applied to polylisine coated slides (Thermo scientific) by cytospine centrifugation (Cytocentrifuge 7620, Wescor) at 1500 rpm for 7 min after hypotonic cell treatment with 75mM KCl. Then the slides were fixed by incubation in 4% paraformaldehyde in PBS for 10 min and permeabilized in buffer containing 120mM KCl, 20mM NaCl; 10mM Tris HCl (pH 7.5) with 0.1% Triton X-100 (Sigma-Aldrich) for 15 min at RT. The Meta-TIFs were detected with primary mouse anti- γ-H2AX antibodies (dilution 1:50, Millipore) and secondary donkey anti-mouse antibodies conjugated with Cy3 (dilution 1:100; Millipore) during 1 h at 37 °C every. The slides were re-fixed with 4% paraformaldehyde in PBS for 10 min at RT to save the fluorescent signals during conventional FISH procedure. FISH with a high sensitive telomere PNA (peptide nucleic acid) probe $(CCCATT)_3$ conjugated with FITC (Applied Biosystems) was performed as previously described (Zhdanova et al. 2014). Slides were counterstained with DAPI and mounted in Vectashield medium (Vector Laboratories). 45–90 metaphases were analyzed for each cell line.

Data analysis

Microscopic analysis and image registration were carried out using an AxioPlan 2 Imaging microscope (Zeiss), equipped with filter sets No. 49 (Zeiss),SP101 FITC and 103v1 (Chroma Technology), CCD-camera (CV M300, JAI Corporation, Japan) and running ISIS5 software (METASystems GmbH). Microscopy was performed in the Microscopic Centre of The Federal Research Center Institute of Cytology and Genetics of SB RAS, Novosibirsk, Russia. Statistics were performed using the t-test in STATISTICA 10. The results are presented as mean ±SD.

Results

The determination of *R. norvegicus* telomere status was based on the accumulation of γ-H2AX histone in telomeres of metaphase chromosomes (Meta-TIF). A fluorescent signal located on one of the two sister chromatids demonstrates the chromatid type of dysfunction (Meta-TIF of chromatid type) that has arisen after DNA replication while signals located on both sister chromatids on the one chromosomal arm confirm the chromosome type dysfunction (Meta-TIF of chromosome type) arose in prereplication period (Cesare et al. 2009, Kaul et al. 2011) (Fig. 1). For characterization of telomere dysfunction in rat lines, the following parameters were applied: number of the metaphases containing Meta-TIFs in percent; number of the metaphases containing Meta-TIFs of chromatid type in percent; number of the metaphases containing Meta-TIFs with dysfunction of chromosome type in percent; average number of Meta-TIFs per metaphase; average number of Meta-TIFs of chromosome type per metaphase and number of the metaphases carrying five and more Meta-TIFs of chromosome type in percent.

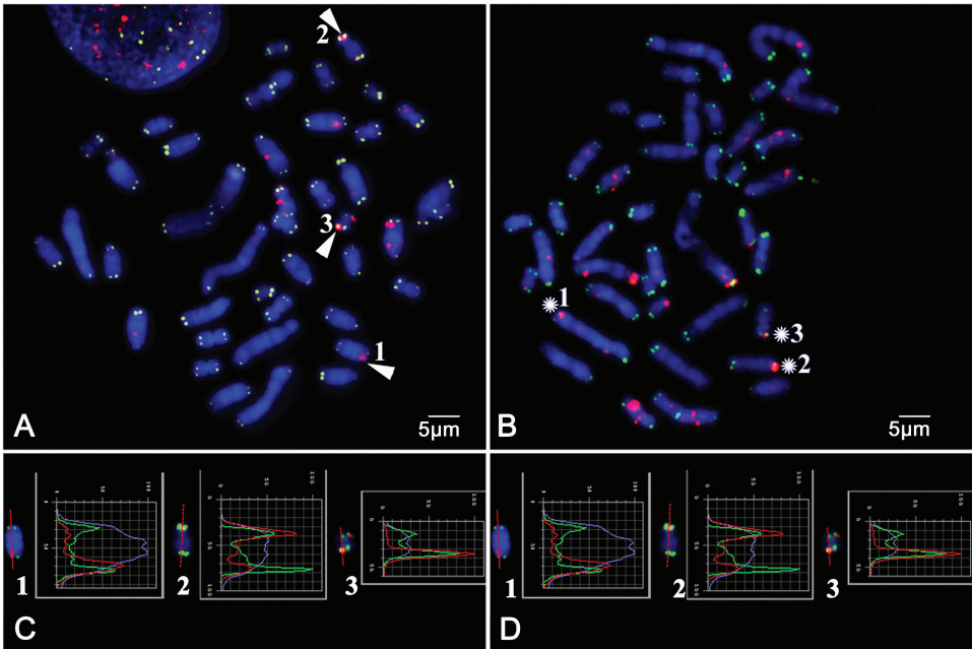

Figure 1. Immunochemistry with antibodies to ɤ-H2AX (red) and further FISH with telomeric PNA probe $(CCCTAA)_3$ conjugated with FITC (green). Chromosomes stained DAPI (blue) **A** The metaphase spread of RNFF1 cell line on 9th passage **B** The metaphase spread of MR39 cell line on 6th passage. The arrows and asterisks indicate dysfunctional telomeres **C – D**. Curves of signal intensities along the length of telomeres containing dysfunctional telomeres on individual chromosomes from **A–B** respectively. Scale bars: 5 μm

The obtained data are presented in Table 1 and Fig. 1–2, including histograms of distribution of metaphases according to a number of Meta-TIFs with chromosome type dysfunction in the most interesting lines. Here, in the text we discussed the most informative data.

The level of spontaneous telomere dysfunction in rat embryonic fibroblasts (rEFs)

Most of metaphases of rEFs (97 percent) on 5–9th passage of cultivation contained Meta-TIFs (Table 1) with a predominance of chromatid type. 72±5.6 % of metaphases demonstrated Meta-TIFs of chromatid type, while just 31±6.2 %, of chromosome type. A mean number of Meta-TIFs per metaphase was 2.76±0.77 (1.46–4.53) on average; of them, 0.40±0.13 were Meta-TIFs of chromosome type. Only 1.75±1.03 metaphases on average had five or more Meta-TIFs of chromosome type.

The rEFs grown to 23–29 passages showed an increase of almost all values used for characterization of telomere dysfunction (Table 1, Fig. 2). These lines are characterized by 6-fold an average increase in the number of metaphases with 5 and more Meta-TIFs

Table 1. The level of spontaneous dysfunctional (DDR+) telomeres in rat embryonic fibroblasts (rEFs) and cultured *in vitro* pluripotent stem cells of rat: embryonic stem cells (rESCs) and induced pluripotent stem cells (riPSCs).

Cell lines; passage	No. of metaphases in % with Meta-TIFs			Avr. No. of Meta-TIFs per metaphase		No. of metaphases in % with 5 and more Meta-TIFs of chromosome type
	Total	Chromatid type	Chromosome type	Total	Chromosome type	
			rEFs			
RWF1, 6	100	57	48	3.60 (2–10)	0.68	0
RWF1, 29	100	59	71	2.66 (1–10)	1.31	12
RWM1, 5	100	72	18	4.53 (2–17)	0.07	3
RWM1, 25	72	72	65	3.83 (0–18)	1.86	9
RNFM1; 9	95	81	28	1.46 (0–8)	0.54	4
RNFM1, 23	92	72	32	3.79 (0–15)	1.05	11
RNFF1, 9	93	80	31	1.46 (0–5)	0.31	0
RNFF1, 26	86	52	65	4.81 (0–19)	1.88	12
RNFF1, 41	98	71	89	10.20 (0.30)	4.32	30
rEFs; 5–9	#97±1.80	72±5.60	*#31±6.20	2.76±0.77	*0.40±0.13	*1.75±1.03
rEFs; 23–29	87±5.90	64±2.0	*58±8.90	3.77±0.44	*1.52±0.20	*11.0±0.70
			rESCs			
RES6; 10	92	92	29	0.90 (0–5)	0.04	1
RES27; 10	82	67	42	1.12 (0–5)	0.18	2
RES27; 42	100	41	97	14.41 (1–27)	5.47	52
RES28; 9	77	62	37	0.72 (0–3)	0.20	5
RES28; 28	96	77	84	3.55 (0–9)	0.51	9
rESCs; 9–10	#84±3.80	74±8.0	36±3.30	##0.91±0.l0	0.14±0.04	2.7±1.04
			riPSCs			
NF13; 6	90	75	43	3.05 (0–13)	0.89	2
NF13; 15	100	56	88	12.36 (1–22)	3.59	33
QV28; 4	96	73	66	3.77 (0–15)	1.94	12
QV28; 15	96	57	69	4,96 (0–25)	2.12	13
MR39; 6	78	73	57	1.77 (0–5)	0.39	9
MR39, 22	91	67	89	7.97 (0–43)	3.17	31
riPSCs, 4–6	88±5.30	**74±0.70	**#55±6.70	##2.86±0.58	**1.07±0.46	7.7±2.97
riPSCs, 15–22	95±2.60	**60±3.50	**82±6.50	8.43±2.15	**2.96±0.43	25.7±6.37

* and ** – mark indicators differing significantly (P≥0.95) on early stages and prolonged cultivation of rEFs and riPSCs, correspondingly.
# – marks indicators differing significantly (P≥0.95) on early stages of cultivation of rEFs and rESCs, rEFs and riPSCs also, correspondingly.
– marks indicators differing significantly (P≥0.95) on early stages of cultivation of rESCs and riPSCs. The results are presented as mean ± SD.

of chromosome type (11.0±0.70 % an average). Such as RNFF1 on 9th passage did not contain metaphases with five and more Meta-TIFs of chromosome type while on 26th and 41st passage, this line had 12 and 30 percent of such metaphases, respectively. Their maximum number was 35. In this way, during the cultivation, the rEFs tend to accumulation of dysfunctional telomeres, and especially telomeres with Meta-TIFs of chromosome type. The values relating to Meta-TIFs of chromosome type differed significantly (P<0.05) between lines on 5–9th and 23–29th passages, correspondingly. At

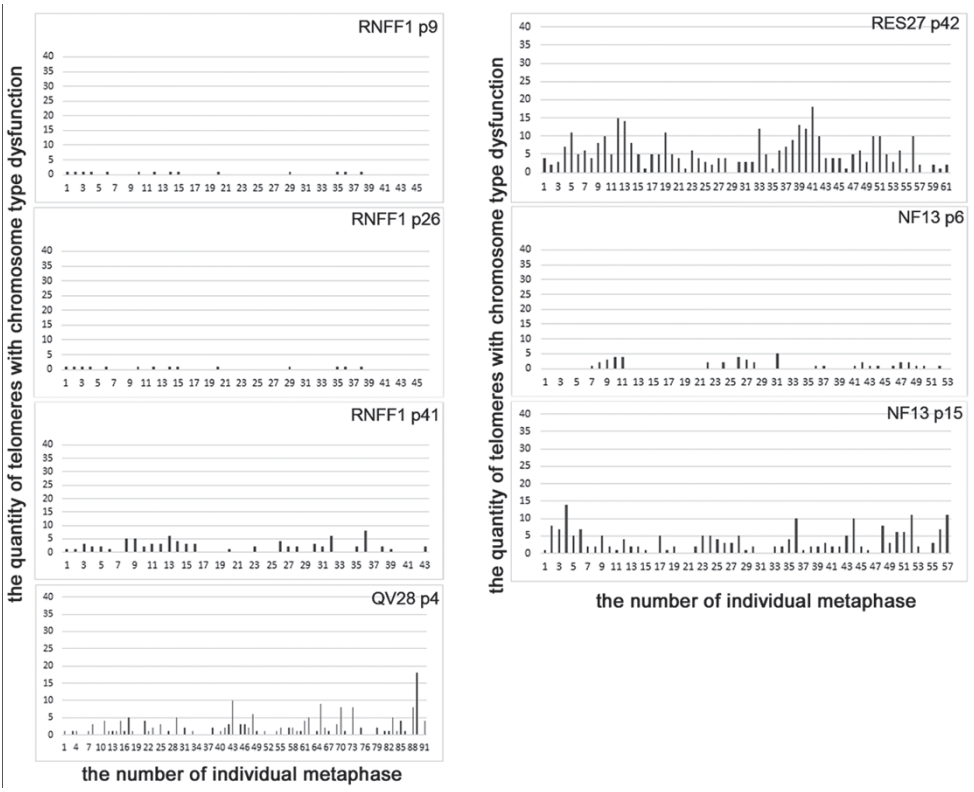

Figure 2. The histograms of distribution of metaphases according to a number of telomeres with chromosome type dysfunction in more interested analyzed cell lines :RNFF1 – rat embryonic fibroblasts (rEF); RES27 – rat embryonic stem cells (rESC); NF13, Q28 – induced pluripotent stem cells of rat (riPSC). P – passage. Axis x – the number of individual metaphases. Axis y – the quantity of telomeres with chromosome type dysfunction in individual metaphases.

the same, there observe wide disparities between studied lined in both groups on early passages and after prolonged cultivation. For instance, an average number of Met-TIFs on metaphase were 1.46 in RNFF1 on 9th passage of cultivation and 4.53 in RWM1, on 5th passage, and 2.66, in RWF1 on 29th passage.

The standard method of embryonic fibroblasts generation suggests a presence of fibroblasts at different stages of differentiation, as well as the other types of cells in primary cultures; as a rule, further cultivation leads to changes in cell content. These factors appear can affect the level of telomere dysfunction in the lines.

The level of spontaneous telomere dysfunction in rat pluripotent stem cells (rPSCs)

Similar to the rEFs, most of rESC metaphases at an early stage of cultivation contain Meta-TIFs, and Meta-TIFs of chromatid type are predominated (Table 1, Fig. 2). These lines on 9–10th passages of cultivation are uniform group; and the level of telomere dysfunction in them is significantly lower than in rEFs on early passages ($P<0.05$). In rESCs, the average number of Meta-TIFs of chromosome type per meta-

phase was 0.14±0.04 an average, and 1–5 percent of metaphases contained five and more of such Meta-TIFs. During cultivation, the number of Meta-TIFs on metaphase has increased. RES28 showed 9 percent metaphases containing five and more Meta-TIFs of chromosome type on 29th passage and 5 percent on 9th passage. RES27 on 42nd passage contained 52 percent of such metaphases, whereas on 10th passage only 2 percent. The maximum number of such Met-TIFs on metaphase was 18.

riPSCs were established from RNFF1 on 6th passage of cultivation. This line had the least number of dysfunctional telomeres among the rEFs (Table 1, Fig. 2). However, contrary to both parental lines and studied here rESCs, riPSCs even at early stages of cultivation demonstrated the elevated level of Meta-TIFs and was not uniform group. In riPSCs, the average number of Meta-TIFs on the metaphases was 2.86±0.58, and 2–12 percent of metaphases had five and more Meta-TIFs of chromosome type. In parental line on 9th passage, these indicators were 1.46 (0–5) and 0, correspondingly; and in rECSs, 0.91±0.10 on average and 1–5, correspondingly.

Similar to the other studied cell lines, the level of telomere dysfunction in the riPSCs has increased during cultivation. Some indicators characterized Meta-TIFs of both types differed significantly ($P<0.05$) in riPSCs on 4–6th and 15–22nd passages of cultivation (Table 1). MR39 on 22nd passage contained 31 percent of metaphases with five and more Meta-TIFs of chromosome type whereas 9 percent of such metaphases were observed on 6th passage of this line cultivation. NF1 looked like a MR39 while this indicator has shown little variation during cultivation of QV28. Only one indicator, the mean number of Meta-TIFs of chromosome type on metaphase, differ significantly ($P<0.05$) in the rESCs and the riPSCs; and one indicator, the number of metaphases with Meta-TIFs of chromosome type, was significantly higher ($P<0.05$) in the riPSCs, than in the rEFs. In general, the pattern of telomere dysfunction in the riPSCs is looking closer to those in the rEFs than in the rESCs.

Discussion

The rat cells, embryonic fibroblasts and cultured *in vitro* pluripotent stem cells showed low levels of spontaneous telomere dysfunction at the early stages of cultivation. The least level of telomere dysfunction characterized the rESCs whereas the riPSCs demonstrated elevated level. This applies to both types of dysfunction, chromatid and chromosomal, but increasingly to the chromosome type. For instance, the mean number of metaphases containing five and more Meta-TIFs of chromosome type in riPSCs exceeded that in normal human cells while the mean number of such Meta-TIFs on metaphase did not (Kaul et al. 2011). The dynamics of telomere dysfunction accumulation is likely to testify about the appearance of cell population prone to accumulation of higher number of Meta-TIFs of chromosome type at early stages of riPSC cultivation, and their number is increases with further cultivation. On 15–22nd passage, already quarter of riPSC metaphases contained five and more Meta-TIFs with dysfunction of chromosome type; some cells demonstrated 10 and more such telomeres.

It was reported that after reprogramming mouse/human iPSCs retain some epigenetic characteristics of donor tissue and accumulate errors of DNA methylation during the reprogramming process. Transcriptome profiles vary in iPSCs obtained not only from cells of different fibroblast lines but also in genetically matched cells. In practice, iPSCs generated from different cells of heterogeneous primary embryonic fibroblasts may have significant differences, both functional and molecular (Kim et al. 2010, Wang et al. 2012, Schuster et al. 2015, Ivanov et al. 2016, Kim and Costello 2017, Noguchi et al. 2017). We observed similar trends in the level of spontaneous telomere dysfunction in distinct riPSC lines.

The comparison of iPSCs with ESCs, which is considered the ideal for *in vitro* pluripotency, shows small but distinctive dissimilarities between them in transcribed genes, epigenetic landscapes, differentiation potential, and mutation load and so on. As a whole, ESCs give the highest chance for successful subsequent differentiation when compared with iPSCs. This supports the fact that iPSCs are generally less efficient in generating a high percentage of chimeras and live mice in tetraploid complementation. And even in the reprogramming process, only a fraction of colonies considered good quality iPSC (Stadtfeld et al. 2010, Bilic and Belmonte 2012). The key features of reprogramming process during generation of rPSCs and riPSCs may underlie the telomere status in them. Since the differentiating of pluripotent cells from fibroblast progenitors is a potentially transformative tool in personalized medicine, the deeper monitoring of their attributes, including the spontaneous level of telomere dysfunction, is required, prior to the clinical implementation of pluripotent stem cell-based therapy.

The nature of spontaneous telomere dysfunction is not yet fully understood, however clear that it differs from those in the whole genome. The distinctive features of telomeres, composition of and amount of telomeric DNA and also the presence of special safeguard protein complex, result in the special mode of telomere replication and reparation of telomere DSB and other lesions. G-quadruplexes and other looping structures are in telomeric DNA in abundance (Gilson and Geli 2007). To overcome the replication stress arising after the replication fork stagnation near them, telomeres use the reparation pathways including homologous recombination and break-induced replication (BIR) in addition to the conventional mechanism of DNA replication with the help of Okazaki fragments (Sakofsky and Malkova 2017). The use of reparation pathways in the replication invariably has led to increased level of spontaneous telomere dysfunction. Sobinoff and Pickett (2017) named this mode of replication "a homology-directed recombination-dependent replication pathway that utilizes telomeric templates for synthesis". The utilization of this mode in the case of ALT (Alternative Telomere Lengthening) activity (Cesare and Reddel 2010) considered in details (Sobinoff and Pickett 2017). The main feature of ALT cells is a recombinogenic large heterogenic telomeres (Henson and Reddel 2010). Normal mammalian cells are capable also to both intra- and extrachromosomal recombination using a mechanism similar to the use of ALT activity (Newmann et al. 2013, Dilley et al. 2016, Sakofsky and Malkova 2017) especially if they contain elongated telomeres as in ALT cells We observed unusual pattern of replication of large *S. granarius* (Miller, 1910) telomeres, containing 213 kb of telomeric repeats on average (Zhdanova et al. 2005, Minina et al. 2018).

Most mammal species are known to have telomeres less than 20 kb in length (Gomes et al. 2011). We previously described one of shrew species *S. granarius* with large recombinogenic telomeres, showing a high level of spontaneous telomere dysfunction (Zhdanova et al. 2005, 2014); wherein in the whole genome, the single DDRs are observed only in the regions of Robertsonian fusions. The rat is also a species with large telomeres, about 40 kb in fibroblasts of adult animals and about 100 kb in embryonic fibroblasts (Cherif et al. 2003, Gomes et al. 2011). It has been shown that small mammalian species with large telomeres do not use replicative senescence, and their fibroblasts can divide continuously *in vitro* (Gomes et al. 2011). We observed the nonstop division of rat embryonic fibroblast *in vitro* for half year and did not see the features of growth crisis after division of primary *S. granarius* fibroblasts for two years (Zhdanova et al. 2014). Probably, accumulation of dysfunctional telomeres in cultured primary rat and *S. granarius* fibroblasts does not lead to growth crisis and correlate with elongated telomeres.

A special protein complex shelterin protects telomeres from inappropriate recombination (de Lange 2009). In this regard, the telomere state model was developed, assuming the telomeres in protected and in a few distinct deprotected states implemented to telomere control of cellular proliferation (Karlseder et al. 2002, Cesare et al. 2009, 2013, Kaul et al. 2011). It is assumed that the induction of any alterations in shelterin components or deprotection affects the telomere dysfunction. It has been shown that a partial deprotected states activate differential ATM signaling with dephosphorylated Chk2, which do not activates G2-M checkpoint and also NHEJ pathway and end-to-end chromosome fusion, if such deprotected telomeres retain sufficient TRF2 (Telomere Repeat binding Factor 2, one of six components of shelterin). However, such telomeres activate DDR signaling and recruit ɤ-H2X (Kaul et al. 2011, Cesare 2014). If TRF2 deficit takes place, the activation of NHEJ, chromosome ends fusion with the following genome instability, a cell growth crisis, and cell death occur. Unlike whole genome, only five arisen in G1 partially deprotected telomeres with DDR signaling are able to induce replicative senescence in human cells and a more such telomeres can be accumulated without impact on growth cells in the absence of p53 signaling (Kaul et al. 2011, Cesare 2014). The telomere lengthening may contribute to decreasing of shelterin component density, including TRF2. Since ALT cells have larger telomeres and, as a rule, inactive p53 the partially deprotected telomeres may be involved in the occurrence of telomere dysfunction in them (Karlseder et al. 2002, Gocha et al. 2013, Cesare 2014) Possibly, the large telomeres at normal mammalian cells may also demonstrate the decreasing level of shelterin component density with the following resistance to elevated level of telomere dysfunction. In addition, the ability of telomere DDR signaling to persist through mitosis irrespective of telomerase activity in cells has been observed. (Hewitt et al. 2012, Fumagalli et al. 2013). These features of telometic DNA may play a role in the accumulation of dysfunctional telomeres in dividing cells as we see in the rat cells.

Spontaneous telomere dysfunction or telomere signaling are associated with the special mode of telomeric DNA replication and with a functioning of telomere safeguard complex shelterin, contributing to repression of NHEJ activation to avoid a numerous chromosomal rearrangements. They are involved in regulation of chromosome length and maintaining of genome stability.

Conclusion

Compared with rEFs and riPSCs, the rESCs showed a reduced frequency of spontaneous telomere dysfunction on early passages of cultivation while the riPSC lines demonstrated an elevated level; moreover, the level of dysfunction was very different in studied riPSC lines. As far as cultivation, the number of dysfunctional telomeres has increased in cells of all lines; this is especially true for riPSCs. riPSCs are a model system, the study of which shows how important in personalized medicine the deeper monitoring of human iPSC attributes including the level of spontaneous telomere dysfunction before clinical implementation.

Acknowledgement

This work was supported by budget project No 0324-2019-0041 of the Federal Research Center Institute of Cytology and Genetics of the Siberian Branch of the Russian Academy of Sciences and Russian Fond of Fundamental Investigation No 19-015-00084a.

References

Bilic J, Belmonte I (2012) Concise review: Induced pluripotent stem cells versus embryonic stem cells: close enough or yet too far apart? Stem Cells 30(1): 33–41. https://doi.org/10.1002/stem.700

Celeste A, Fernandez-Capetillo O, Kruhlak MJ, Pilch DR, Staudt DW, Lee A, Bonner RF, Bonner WM, Nussenzweig A (2003) Histone H2AX phosphorylation is dispensable for the initial recognition of DNA breaks. Nature Cell Biology 5(7): 675–579. https://doi.org/10.1038/ncb1004

Cesare AJ, Kaul Z, Cohen SB, Napier CE, Pickett HA, Neumann AA, Reddel RR (2009) Spontaneous occurrence of telomeric DNA damage response in the absence of chromosome fusions. Nature Structural and Molecular Biology 16(12): 1244–1251. https://doi.org/10.1089/scd.2015.0204

Cesare AJ, Reddel RR (2010) Alternative lengthening of telomeres: models, mechanisms and implications. Nature Reviews Genetics 11(5): 319–330. https://doi.org/10.1038/nrg2763

Cesare AJ, Hayashi MT, Crabbe L, Karlseder J (2013) The telomere deprotection response is functionally distinct from the genomic DNA damage response. Molecular Cell 51(2): 141–155. https://doi.org/10.1016/j.molcel.2013.06.006

Cesare AJ (2014) Mitosis, double strand break repair, and telomeres: a view from the end: how telomeres and the DNA damage response cooperate during mitosis to maintain genome stability. BioEssays 36(11): 1054–1061. https://doi.org/10.1002/bies.201400104

Cherif H, Tarry LJ, Ozanne SE, Hales CN (2003) Ageing and telomeres: a study into organ- and gender-specific telomere shortening. Nucleic Acids Research 31(5): 1576–1583. https://doi.org/10.1093/nar/gkg208

de Lange T (2005) Shelterin: the protein complex that shapes and safeguards human telomeres. Genes and Development 19(18): 2100–2110. https://doi.org/10.1101/gad.1346005

de Lange T (2009) How telomeres solve the end-protection problem. Science 326(5955): 948–952. https://doi.org/10.1126/science.1170633

de Lange T (2018) Shelterin-mediated telomere protection. Annual Review of Genetics 52: 19.1–19.25. https://doi.org/10.1146/annurev-genet-032918-021921

di Leonardo A, Linke SP, Clarkin K, Wahl GM (1994) DNA damage triggers a prolonged p53-dependent G1 arrest and long-term induction of Cip1 in normal human fibroblasts. Genes and Development 8: 2540–2551. https://doi.org/10.1101/gad.8.21.2540

Dilley RL, Verma P, Cho NW, Winters HD, Wondisford AR, Greenberg RA (2016) Break-induced telomere synthesis underlies alternative telomere maintenance. Nature 539(7627): 54–58. https://doi.org/10.1038/nature20099

Fumagalli M, Rossiello F, Clerici M, Barozzi S, Cittaro D, Kaplunov JM, Bucci G, Dobreva M, Matti V, Beausejour CM, Herbig U, Longhese MP, d'Adda di Fagagna F (2013) Telomeric DNA damage is irreparable and causes persistent DNA damage response activation. Nature Cell Biology 14(4): 355–365. https://doi.org/10.1038/ncb2466

Gilson E, Geli V (2007) How telomeres are replicated. Nature Reviews Molecular Cell Biology 8: 825–838. https://doi.org/10.1038/nrm2259

Gocha AR, Harris J, Groden J (2013) Alternative mechanisms of telomere lengthening: permissive mutations, DNA repair proteins and tumorigenic progression. Mutation Research 743–744: 142–150. https://doi.org/10.1016/j.mrfmmm.2012.11.006

Gomes NM, Ryder OA, Houck ML, Charter SJ, Walker W, Forsyth NR, Austad SN, Venditti C, Pagel M, Shay JW, Wright WE (2011) Comparative biology of mammalian telomeres: hypotheses on ancestral states and the roles of telomeres in longevity determination. Aging Cell 10(5): 761–768. https://doi.org/10.1111/j.1474-9726.2011.00718.x

Henson JD, Reddel RR (2010) Assaying and investigating Alternative Lengthening of Telomeres activity in human cells and cancers. FEBS Letters 584: 3800–3811. https://doi.org/10.1016/j.febslet.2010.06.009

Hewitt G, Jurk D, Marques FDM, Correia-Melo C, Hardy T, Gackowska A, Anderson R, Taschuk M, Mann J, Passos JF (2012) Telomeres are favoured targets of a persistent DNA damage response in ageing and stress-induced senescence. Nature Communications 3: 708. https://doi.org/10.1038/ncomms1708

Ivanov NA, Tao R, Chenoweth JG, Brandtjen A, Mighdoll MI, Genova JD, McKay RD, Jia Y, Weinberger DR, Kleinman JE, Hyde TM, Jaffe AE (2016) Strong components of epigenetic memory in cultured human fibroblasts related to site of origin and donor Age. PLOS Genetics 12(2): e1005819. https://doi.org/10.1371/journal.pgen.1005819

Karlseder J, Smogorzewska A, de Lange T (2002) Senescence induced by altered telomere state, not telomere loss. Science 295(55–64): 2446–2449. https://doi.org/10.1126/science.1069523

Kaul Z, Cesare AJ, Huschtscha LI, Neumann AA, Reddel RR (2011) Five dysfunctional telomeres predict onset of senescence in human cells. EMBO Reports 13(1): 52–59. https://doi.org/10.1038/embor.2011.227

Kim M, Costello J (2017) DNA methylation: an epigenetic mark of cellular memory. Experimental and Molecular Medicine 49(4): e322. https://doi.org/10.1038/emm.2017.10

Kim K, Doi A, Wen B, Ng K, Zhao R, Cahan P, Kim J, Aryee MJ, Ji H, Ehrlich LI, Yabuuchi A, Takeuchi A, Cunniff KC, Hongguang H, McKinney-Freeman S, Naveiras O, Yoon TJ, Irizarry RA, Jung N, Seita J, Hanna J, Murakami P, Jaenisch R, Weissleder R, Orkin SH (2010) Epigenetic memory in induced pluripotent stem cells. Nature 467(7313): 285–290. https://doi.org/10.1038/nature09342

Martin M, Terradas M, Hernandez L, Genesca A (2014) ɤ-H2AX foci on apparently intact mitotic chromosomes: Not signatures of misrejoining events but signals of unresolved DNA damage. Cell Cycle 13(19): 3026–3036. https://doi.org/10.4161/15384101.2014.947786

Minina JM, Karamysheva TV, Rubtsov NB, Zhdanova NS (2018) Replication timing of large *Sorex granarius* (Soricidae, Eulipotyphla) telomeres. Protoplasma 255: 1477–1486. https://doi.org/10.1007/s00709-018-1244-y

Neumann AA, Watson CM, Noble JR, Pickett HA, Tam PP, Reddel RR (2013) Alternative lengthening of telomeres in normal mammalian somatic cells. Genes and Development 27(1): 18–23. https://doi.org/10.1101/gad.205062.112

Noguchi H, Miyagi-Shiohira C, Nakashima Y (2017) Induced tissue-specific stem cells and epigenetic memory in induced pluripotent stem cells. Experimental and Molecular Medicine 49: e322. https://doi.org/10.1038/emm.2017.10

Pilch DR, Sedelnikova OA, Redon C, Celeste A, Nussenzweig A, Bonner WM (2003) Characteristics of gamma-H2AX foci at DNA double-strand breaks sites. Biochemistry and Cell Biology. 81(3): 123–129. https://doi.org/10.1139/o03-042

Pinto DM, Flaus A (2010) Structure and Function of Histone H2AX. Sub-Cellular Biochemistry 50: 55–78. https://doi.org/10.1007/978-90-481-3471-7_4

Rogakou EP, Pilch DR, Orr AH, Ivanova VS, Bonner WM (1998) DNA double stranded breaks induce histone H2AX phosphorylation on serine 139. The Journal of Biological Chemistry 273(10): 5858–5868. https://doi.org/10.1074/jbc.273.10.5858

Sakofsky CJ, Malkova A (2017) Break induced replication in eukaryotes: mechanisms, functions, and consequences. Critical Reviews in Biochemistry and Molecular Biology 52(4): 395–413. https://doi.org/10.1080/10409238.2017.1314444

Schuster J, Halvardson J, Pilar Lorenzo L, Ameur A, Sobol M, Raykova D, Annerén G, Feuk L, Dahl N (2015) Transcriptome profiling reveals degree of variability in induced pluripotent

stem cell lines: Impact for human disease modeling. Cell Reprogramming 17(5): 327–37. https://doi.org/10.1089/cell.2015.0009

Sobinoff AP, Pickett HA (2017) Alternative lengthening of telomeres: DNA repair pathways converge. Trends in Genetics 33(12): 921–932. https://doi.org/10.1016/j.tig.2017.09.003

Stadtfeld M, Apostolou E, Akutsu H, Fukuda A, Follett P, Natesan S, et al. (2010) Aberrant silencing of imprinted genes on chromosome 12qF1 in mouse induced pluripotent stem cells. Nature 465(7295): 175–181. https://doi.org/10.1038/nature09017

Vaskova EA, Medvedev SP, Sorokina AE, Nemudryy AA, Elisaphenko EA, Zakharova IS, Shevchenko AI, Kizilova EA, Zhelezova AI, Evshin IS, Sharipov RN, Minina JM, Zhdanova NS, Khegay II, Kolpakov FA, Sukhikh GT, Pokushalov EA, Karaskov AM, Vlasov VV, Ivanova LN, Zakian SM (2015) Transcriptome characteristics and X-chromosome inactivation status in cultured rat pluripotent stem cells. Stem Cells and Development 24(24): 2912–2924. https://doi.org/10.1089/scd.2015.0204

Wang F, Yin Y, Ye X, Liu K, Zhu H, Wang L, Chiourea M, Okuka M, Ji G, Dan J, Zuo B, Li M, Zhang Q, Liu N, Chen L, Pan X, Gagos S, Keefe DL, Liu L (2012) Molecular insights into the heterogeneity of telomere reprogramming in induced pluripotent cells. Cell Research 22(4): 757–768. https://doi.org/10.1038/cr.2011.201

Zhdanova NS, Karamisheva TV, Minina J, Astakhova NM, Lansdorp P, Kammori M, Rubtsov NB, Searle JB (2005) Unusual distribution pattern of telomeric repeats in the shrews *Sorex araneus* and *Sorex granarius*. Chromosome Research 13(6): 617–625. https://doi.org/10.1007/s10577-005-0988-3

Zhdanova NS, Draskovic I, Minina JM, Karamysheva TV, Novo CL, Liu W-Y, Porreca RM, Gibaud A, Zvereva ME, Skvortsov DA, Rubtsov NB, Londono-Vallejo A (2014) Recombinogenic telomeres in diploid *Sorex granarius* (Soricidae, Eulipotyphla) fibroblast cells. Molecular and Cellular Biology 34(15): 2786–2799. https://doi.org/10.1128/MCB.01697-13

CompCytogen 13(3): 211–230 (2019)
doi: 10.3897/CompCytogen.v13i3.35346
http://compcytogen.pensoft.net

RESEARCH ARTICLE

COMPARATIVE Cytogenetics
A peer-reviewed open-access journal
International Journal of Plant & Animal Cytogenetics, Karyosystematics, and Molecular Systematics

Molecular cytogenetic characterization and phylogenetic analysis of four *Miscanthus* species (Poaceae)

Yan-Mei Tang[1], Liang Xiao[1], Yasir Iqbal[1], Jian-Feng Liao[1], Long-Qian Xiao[2], Zi-Li Yi[1], Chao-Wen She[2]

1 *College of Bioscience and Biotechnology, Hunan Agricultural University, Changsha, Hunan 410128, China*
2 *Key Laboratory of Research and Utilization of Ethnomedicinal Plant Resources of Hunan Province, Huaihua University, Huaihua, Hunan 418008, China*

Corresponding author: *Zili Yi* (yizili@hunau.net); *Chaowen She* (shechaowen@aliyun.com)

Academic editor: *Elena Mikhailova* | Received 11 April 2019 | Accepted 26 July 2019 | Published 9 August 2019

http://zoobank.org/B75EA899-EC28-442A-B448-27AE84359D5B

Citation: Tang YM, Xiao L, Iqbal Y, Liao JF, Xiao LQ, Yi ZL, She CW (2019) Molecular cytogenetic characterization and phylogenetic analysis of four *Miscanthus* species (Poaceae). Comparative Cytogenetics 13(3): 211–230. https://doi.org/10.3897/CompCytogen.v13i3.35346

Abstract

Chromosomes of four *Miscanthus* (Andersson, 1855) species including *M. sinensis* (Andersson, 1855), *M. floridulus* (Schumann & Lauterb, 1901), *M. sacchariflorus* (Hackel, 1882) and *M. lutarioriparius* (Chen & Renvoize, 2005) were analyzed using sequentially combined PI and DAPI (CPD) staining and fluorescence *in situ* hybridization (FISH) with 45S rDNA probe. To elucidate the phylogenetic relationship among the four *Miscanthus* species, the homology of repetitive sequences among the four species was analyzed by comparative genomic *in situ* hybridization (cGISH). Subsequently four *Miscanthus* species were clustered based on the internal transcribed spacer (ITS) of 45S rDNA. Molecular cytogenetic karyotypes of the four *Miscanthus* species were established for the first time using chromosome measurements, fluorochrome bands and 45S rDNA FISH signals, which will provide a cytogenetic tool for the identification of these four species. All the four have the karyotype formula of *Miscanthus* species, which is 2n = 2x = 38 = 34m(2SAT) + 4sm, and one pair of 45S rDNA sites. The latter were shown as strong red bands by CPD staining. A non-rDNA CPD band emerged in *M. floridulus* and some blue DAPI bands appeared in *M. sinensis* and *M. floridulus*. The hybridization signals of *M. floridulus* genomic DNA to the chromosomes of *M. sinensis* and *M. lutarioriparius* genomic DNA to the chromosomes of *M. sacchariflorus* were stronger and more evenly distributed than other combinations. Molecular phylogenetic trees showed that *M. sinensis* and *M. floridulus* were closest relatives, and *M. sacchariflorus* and *M. lutarioriparius* were also closely related. These findings were consistent with the phylogenetic relationships inferred from the cGISH patterns.

Keywords
Miscanthus, karyotype, fluorochrome banding, 45S ribosomal RNA genes (45S rDNA), *in situ* hybridization, internal transcribed spacers, phylogeny

Introduction

The genus *Miscanthus* (Andersson, 1855), belonging to the tribe Andropogoneae of family Poaceae, is a tall perennial grass with C4 photosynthesis (Stewart et al. 2009). It includes 14–20 species and has been considered as one of the most promising high-yield fiber-based energy crops (Christian et al. 2009, Brosse et al. 2012). China is a genetic center of diverse *Miscanthus* germplasm. Four *Miscanthus* species, *M. sinensis* (Andersson, 1855), *M. floridulus* (Schumann & Lauterb, 1901), *M. sacchariflorus* (Hackel, 1882) and *M. lutarioriparius* (Chen & Renvoize, 2005), are most widely distributed. These have high biomass yield and are prone to interspecific hybridization, which lead to high genetic diversity (Liu et al. 2013, Zhao et al. 2017).

M. sinensis has been already sequenced (*Miscanthus sinensis* v7.1 DOE-JGI, https://phytozome.jgi.doe.gov/) and is an important species for comparative genomics. Therefore, it is necessary to investigate the chromosomes of *M. sinensis* and other *Miscanthus* species and reveal their genomic homology. It will provide a reference for further development of specific probes based on the *M. sinensis* genome sequence for chromosomal localization in *Miscanthus* and related genera. *M. floridulus* is similar to *M. sinensis* in morphology. *M. lutarioriparius* is a native *Miscanthus* species of China (Chen and Renvoize 2006, Sheng et al. 2016, Yang et al. 2019). Some scholars have published it as a variant or subspecies of *M. sacchariflorus* (Liu 2009, Sun et al. 2010, Lu 2012, Hu 2015) because of their high similarity in morphology. In a word, the interspecific relationships of the four *Miscanthus* species are complex and their origins are unclear (Chen and Renvoize 2006, Tamura et al. 2016). Until now, taxonomic studies on *M. sinensis*, *M. floridulus*, *M. sacchariflorus* and *M. lutarioriparius* have been carried out by using morphological features (Chae et al. 2014, Yook et al. 2014), nuclear DNA content (Chae et al. 2014, Sheng et al. 2016), molecular markers (Chae et al. 2014, Yook et al. 2014, Tang et al. 2015), fluorescence *in situ* hybridization (FISH) (Takahashi and Shibata 2002, Takahashi et al. 2002), and spectroscopy (Jin et al. 2017). However, none of them could distinguish the four species from each other unequivocally. Karyotype, the characterization of a genome at the chromosomal level, is a valuable tool for species identification and evolution analysis (Silva et al. 2018). However, it is difficult to perform accurate karyotype analysis in *Miscanthus* species because of their little chromosomal differentiation and lack of distinct chromosomal landmarks. Chromosome banding by Giemsa staining, fluorochrome staining or FISH with repetitive DNA sequences can provide additional characteristics to discriminate the chromosomes in the cell complement (Filion 1974, Sumner 1990, Koornneef et al. 2003).

Fluorochrome banding techniques use fluorescent dyes preferentially binding to GC- or AT-rich DNA sequences to display different classes of heterochromatin on chromosomes (Sumner 1990). Among the techniques used, combined PI (propidium

iodide) and DAPI (4', 6 diamino-2-phenylindole dihydrochloride) staining (called CPD staining) can reveal simultaneously GC-rich and AT-rich regions along chromosomes with high precision and repeatability (Peterson et al. 1999, She et al. 2006, 2015, 2017). FISH with 5S and 45S rDNA probes have been widely applied in plants to determine the number and location of rDNA sites, and to provide effective markers for chromosome identification. Moreover, information on evolutionary relationships between species can be provided by comparing rDNA distribution characteristics between closely related species (Moscone et al. 1999, de Moraes et al. 2007, She et al. 2015, 2017). The combination of chromosome morphology, fluorochrome bands and FISH signals can be employed to construct molecular cytogenetic karyotype. It can reveal chromosome-level genome organization of a plant species, investigate the evolutionary relationships among related species, and integrate genetic and physical maps (Zhang et al. 2015, She et al. 2015, 2017). Cytogenetic studies in the four *Miscanthus* species were so far primarily restricted to chromosome counts and conventional karyotype descriptions (Chramiec-Głąbik et al. 2012, Chae et al. 2014). FISH has been applied in diploid *M. sinensis* and tetraploid *M. sacchariflorus*, but their molecular cytogenetic karyotypes have not been established as yet (Takahashi and Shibata 2002, Takahashi et al. 2002).

The internal transcribed spacer (ITS) regions of 45S rDNA have been used extensively for determining phylogenetic relationships at interspecific or intraspecific level because of its relatively high rate of mutation (Álvarez and Wendel 2003, Hao et al. 2004, Capua et al. 2017). Another direct method for examining genome relationships is comparative genomic *in situ* hybridization (cGISH), in which the labelled total genomic DNA of one species is hybridized to the chromosomes of another species without competitive DNA (Zoller et al. 2001). It generates hybridization signals in regions of conserved repetitive DNA sequences. Therefore, it can be used to identify the evolutionary relationships between species within a genus (Wolny and Hasterok 2009, She et al. 2015, Zhang et al. 2015). So far, the phylogenetic relationships among the four *Miscanthus* species were mainly carried out at the morphological, cellular and molecular levels (Chae et al. 2014, Yook et al. 2014). In previous studies, the ITS sequence was used to assess the phylogeny of the four *Miscanthus* species and the species of the *Saccharum* complex and other related genera (Hodkinson et al. 2002b, Chen et al. 2007, Liu et al. 2010), and the genome relationship between diploid *M. sinensis* and tetraploid *M. sacchariflorus* was examined by FISH with rDNA, genomic DNA and *Saccharum* centromeric repeats (Takahashi and Shibata 2002; Takahashi et al. 2002). However, there has been no study on the phylogenetic relationships of all the four species by combining molecular cytogenetic characterization with ITS sequence analysis.

In the current study, well spread mitotic metaphase chromosomes of four *Miscanthus* species were prepared using the modified flame-drying method. Chromosomes were characterized using sequential CPD staining and FISH with 45S rDNA probe. Detailed molecular cytogenetic karyotypes of these species were established using combined data of chromosome measurements, CPD bands, DAPI bands and 45S rDNA FISH signals. Meanwhile, cGISH was carried out to detect the homology of repetitive

DNAs among these species, and a comparative sequence analysis of the ITS regions in these species was also conducted. The data were collected and evaluated to gain insight about the phylogenetic relationships among the four *Miscanthus* species.

Material and methods

Plant material and DNA extraction

Twenty-four *Miscanthus* accessions comprised of 6 *M. sinensis*, 6 *M. floridulus*, 6 *M. sacchariflorus* and 6 *M. lutarioriparius* were selected from different provinces of China and planted in the *Miscanthus* germplasm nursery located at the Hunan Agricultural University (Table 1). All the materials were used for ITS sequence analysis. Meanwhile, for CPD staining, rDNA FISH, karyotype analysis and cGISH, No. 03 (*M. sinensis*), No. 10 (*M. floridulus*), No. 16 (*M. sacchariflorus*) and No. 21 (*M. lutarioriparius*) were used. *Imperata cylindrica* (Beauvois, 1812) was included as an outgroup for the ITS phylogenetic analysis, and its sequences (JN407505.1) were obtained from GenBank Database.

Total genomic DNA (gDNA) was extracted from fresh leaf tissue using the cetyltrimethylammonium bromide (CTAB) method described by Murray and Thompson (1980). The quality and concentration of DNA were measured by 1% agarose gel electrophoresis and a microplate reader (BioTek Instruments Inc, Winooski, USA).

Table 1. Geographical data of 24 Miscanthus accessions and GenBank Numbers of the ITS sequences

No.	Species	Orginal location	Longitude (E°)	Latitude (N°)	Altitude (m)	GenBank No.
01	*M. sinensis*	Huangshan, Anhui	118°15.78'	29°41.63'	ca 139	MK981280
02		Shenzheng, Guangdong	114°18.00'	22°35.27'	ca 27	MK981281
03		Wuhan, Hubei	104°24.46'	30°32.75'	ca 735	MK138895
04		Jiaohe, Jilin	127°33.00'	43°34.00'	ca 345	MK981282
05		Zibo, Shandong	117°50.11'	36°28.66'	ca 290	MK981283
06		Naxi, Sichuan	105°27.43'	28°37.61'	ca 400	MK981284
07	*M. floridulus*	Jinzhai, Anhui	115°43.30'	31°12.29'	ca 490	MK981285
08		Nanpin, Fujian	110°17.36'	26°13.72'	ca 97	MK981286
09		Qiongzhong, Hainan	109°54.03'	19°08.49'	ca 263	MK981287
10		Wuhan, Hubei	114°24.46'	30°32.75'	ca 45	MK138896
11		Wuzhou, Guangxi	111°22.35'	23°30.02'	ca 25	MK981288
12		Zhuhai, Guangdong	113°35.99'	22°16.87'	ca 2	MK981289
13	*M. sacchariflorus*	Jinzhai, Anhui	115°48.04'	31°12.29'	ca 480	MK981290
14		Chengde, Hebei	117°50.50'	40°54.03'	ca 351	MK981291
15		Ning'an, Heilongjiang	129°29.09'	44°23.84'	ca 203	MK981292
16		Wuhan, Hubei	114°19.78'	30°28.60'	ca 36	MK138897
17		Panshan, Liaoning	121°59.48'	41°14.57'	ca 20	MK981293
18		Fuxian, Shaanxi	109°27.10'	35°59.30'	ca 1246	MK981294
19	*M. lutarioriparius*	Tongling, Anhui	117°44.25'	30°51.69'	ca 15	MK981295
20		Xichuan, Henan	111°28.69'	33°06.71'	ca 168	MK981296
21		Wuhan, Hubei	114°19.52'	30°28.66'	ca 78	MK138898
22		Changsha, Hunan	113°01.93'	28°11.08'	ca 80	MK981297
23		Nanjing, Jiangsu	118°50.80'	32°04.37'	ca 250	MK981298
24		Hukou, Jiangxi	116°12.68'	29°44.48'	ca 9	MK981299

Chromosome preparation

Mitotic metaphase chromosomes were prepared by using the root tips according to the procedure described by She et al. (2006). The actively growing root tips were collected from potted plants and treated with saturated α-bromonaphthalene for 1.5 h at 28 °C, fixed in 3:1 (v/v) methanol/glacial acetic acid for at least 12 h at room temperature, and then stored at 4 °C until use. The fixed root tips were then washed in double distilled water and citrate buffer (0.01 mM citric acid-sodium citrate, pH 4.5) for 10 min each and incubated in a mixture of 2% cellulase R-10 (Yakult Pharmaceutical Industry, Tokyo, Japan), 2% pectolyase Y-23 (Yakult Pharmaceuticals), and 2% macerozyme R-10 (Sigma-Aldrich, Steinhem, Germany) in citric acid buffer at 28 °C for 2.5~3 h. Root tips were transferred to a glass slide along with the fixative and dissected using fine-pointed forceps. Finally, the slides were dried above a flame. Good preparations were selected by Olympus BX60 phase contrast microscope, and then stored at -20 °C.

Staining with CPD and DAPI

The CPD staining followed the procedure described in She et al. (2006). Chromosome preparations were treated with RNase A and pepsin then stained with a mixture of 3 μg/ml DAPI and 0.6 μg/ml PI (both from Sigma-Aldrich) in a 30% (v/v, using double-distilled water as solvent) solution of Vectashield H-1000 (Vector Laboratories Burlingame, USA). Preparations were examined under an Olympus BX60 epifluorescence microscope equipped with a CoolSNAP EZ CCD camera (Photometrics, Tucson, USA). The CCD camera was controlled using Ocular software (Molecular Devices, Sunnyvale, USA). Photographs were taken using a green excitation filter for PI and a UV excitation filter for DAPI. DAPI and PI grey-scale images of the same plate were merged to produce a CPD image. The final images were optimized for contrast and background using Adobe PHOTOSHOP CS8.0.

Probe DNA labeling

A 45S rDNA clone containing a 9.04-kb tomato 45S rDNA insert (Perry and Palukaitis 1990) were used as probe to localize the 18S-5.8S-26S ribosomal RNA gene. The DNAs (45S rDNA and gDNAs) of the four *Miscanthus* species were labeled with biotin-16-dUTP and digoxigenin-11-dUTP, respectively, using the Nick Translation Kit (Roche Diagnostics, Mannheim, Germany).

FISH

FISH with the 45S rDNA probe was carried out on the same slides previously stained with CPD. FISH with the *M. sinensis*, *M. floridulus*, *M. sacchariflorus* and *M. lutarioriparius*

genomic probes to the *M. sinensis* chromosomes. FISH with the *M. sacchariflorus*, *M. floridulus* and *M. lutarioriparius* genomic probes to the *M. sacchariflorus* chromosomes, and FISH with the *M. lutarioriparius* and *M. floridulus* genomic probes to the the *M. lutarioriparius* chromosomes were performed, respectively. The slides previously stained or hybridized were washed twice for 15 min each in 2 × SSC, dehydrated through an ethanol series (70%, 90% and 100%, 5 min each) and then used for hybridization. The *in situ* hybridization and detection were performed as described by She et al. (2006). Briefly, 40 μl of the hybridization mixture, which contained 20 μl 20% dextran sulfate, 1 μl ssDNA, 16 μl hybridization buffer (HB50, containing 50% deionized formamide and 50 mM sodium phosphate, pH 7.5) and 3 μl labeled DNA (final concentration 100–150 ng/slide), was added to each slide and covered with a 24 × 50 mm glass coverslip. Chromosomes and probe were denatured together on ThermoBrite S500-24 (Abbott Molecular, USA) at 80 °C for 3 min, and then were incubated at 37 °C for 24 h. Post-hybridization washing was performed in 0.1 × SSC two times for 15 min each at 42 °C, followed by rinsing in 2 × SSC three times for 5 min each at 42 °C and in TN buffer (containing 100 mM Tris-HCl and 150 mM NaCl, pH 7.5) for 5 min at room temperature. Hybridization signals were detected after incubating the slides with 100 μl TNB buffer (0.5% Roche blocking reagent in TN buffer) for 30 min at 37 °C, and followed by rinsing in TN buffer for 1 min at room temperature.

The biotin-labeled 45S rDNA was detected using Fluorescein Avidin D (Vector Laboratories). The digoxigenin-labeled gDNA was detected using Anti-digoxigenin-rhodamine (Roche Diagnostics). The specific steps were as follows: 100 μl of 1% Fluorescein Avidin D or Anti-digoxigenin-rhodamine, diluted with TNB buffer, was added to each slide and covered with a glass coverslip, and then were incubated at 37 °C in dark for 1 h. Afterwards, the coverslip was removed and rinsed with TN buffer three times for 5 min each in dark. Slides were counterstained with 3 μg/ml DAPI in a 30% solution of Vectashield H100 and subsequently examined under an epifluorescence microscope equipped with the CCD camera as mentioned above. Observations were made using a UV, blue and green excitation filters for DAPI, fluorescein, and rhodamine, respectively. Grey-scale images were digitally captured and merged by the Ocular software. The final images were adjusted with Adobe PHOTOSHOP CS8.0.

Karyotype analysis

For each species, five well-spread metaphase plates were measured using Adobe PHOTOSHOP CS8.0 to obtain the chromosome relative lengths (RL; % of haploid complement), arm ratios (AR = long arm/short arm), chromosome length ratio (longest chromosome length / shortest chromosome length), size of the fluorochrome band (expressed as a percentage of the karyotype length) and the percentage distance from the rDNA site to the centromere (di = d × 100/a; d = distance of the centre of the rDNA sites from the centromere; a = length of the corresponding chromosome arm) (Greil-

huber and Speta 1976). In addition, the total length of the haploid complement (TCL; i.e. karyotype length) was measured using the five metaphase cells with the highest degree of chromosome condensation. The arm ratio was used to classify the chromosomes according to the system described by Levan et al. (1964). Karyotype asymmetry was determined using the mean centromeric index (CI), the intrachromosomal asymmetry index (A1), the interchromosomal asymmetry index (A2) (Zarco 1986), the ratio of the length of all long arms in the chromosome set to the total chromosome length in set (As K%) (Arano 1963), the asymmetry index (AI) (Paszko 2006), and the categories of Stebbins (Stebbins 1971). The chromosomes were arranged in order of decreasing lengths. Idiograms were drawn based on chromosomes measurement data, fluorochrome bands and 45S rDNA FISH signals.

The PCR and sequencing

The rDNA-ITS regions (including ITS1, 5.8s and ITS2) of the four *Miscanthus* species were amplified using the universal primers ITS4 and ITS5 (ITS4 primer sequence: 5'-TCCTCCGCTTATTGATATGC-3', ITS5 primer sequence: 5'-GGAAGTAAAAGTCGTAACAAGG-3') (White et al. 1990). The total volume of the PCR amplification reaction was 25 µl, including 2.5 µl 10 × PCR buffer, 1.5 µl 25 mM $MgCl_2$, 0.5 µl 10 mM dNTP, 0.75 µl 10 µM of each primer, 0.5 µl Taq DNA polymerase (Sangon, Shanghai, China), 1.5 µl gDNA (30~50 ng/µl) and 17 µl ddH_2O. The amplification conditions were: pre-denatured at 95 °C for 4 min; denaturation at 94 °C for 45 s, annealing at 54 °C for 45 s, extension at 72 °C for 45 s, 38 cycles; and a final extension step of 10 min at 72 °C on a thermal cycler PTC-200. The PCR products were detected by 1% agarose gel electrophoresis. PCR products purification and ITS sequencing were performed by Sangon. The ITS sequences have been deposited in GenBank and the accession numbers are listed in Table 1.

DNA sequences and phylogenetic analyses

Each DNA sequence was spliced by bi-directional sequencing. Then, the similarity searches were performed using the NCBI (National Centre for Biotechnology Information), BLAST network service. Sequences were aligned with CLUSTAL W program. The MEGA 7.0 software (Kumar et al. 2016) was used for sequence analyses (estimating percentage of the G + C content, variable sites and parsimony informative sites). ITS sequences of *I. cylindrical* was used as the outer group plant, and phylogenetic analyses were carried out using the neighbour joining (NJ) and maximum parsimony (MP) methods. In the ITS phylogenetic tree, the confidence of each branch was tested using bootstrap (Felsenstein 1985), each performing 1 000 cycles to evaluate the systematic significance and reliability of each branch.

Results

Comparative karyotyping

The karyotype measurement data for the four *Miscanthus* species are listed in Suppl. material 1, Tables S1–S4. The general karyotype features and parameters for the four *Miscanthus* species are listed in Table 2. Representative mitotic chromosomes, karyotypes showing the fluorescent bands and ideograms are shown in Figs 1–3.

All the four *Miscanthus* species had diploid chromosome number of 2n = 2x = 38. The mitotic metaphase chromosomes with a mean chromosome length 3.59 μm for *M. sacchariflorus* and 4.53 μm for *M. floridulus*. The total length of the haploid complement (TCL) ranges from 68.15 μm to 86.13 μm, and the mean centromeric index (CI) of the complements varied slightly between 44.00 ± 4.97 and 44.81 ± 4.28. In contrast, *M. floridulus* has exhibited the large variation in chromosome length, whereas *M. sinensis* has displayed the large variation in centromeric index.

The karyotype formulas of the four *Miscanthus* species were same, composed of 34 metacentric (m) chromosomes and 4 submetacentric (sm) chromosomes with a secondary constriction located on the long arms of chromosome 1, namely 2n = 2x = 38 = 34m(2SAT) + 4sm. All the karyotypes of the four species studied fell into the categories 2B of Stebbins (1971). The ranges for Romero Zarco's (1986) asymmetry indices were as follows: A1 = 0.11–0.20 and A2 = 0.24–0.52. The As K% of Arano (1963) ranged from 55.25 to 55.85, and Paszko's (2006) asymmetry index (AI) ranged from 2.37 to 4.47. RRL, CI, A1 and As K% have shown close similarity among species. In contrast, TCL, A2, and AI have displayed relatively large variation among species. According to the AI values, the karyotype of *M. sacchariflorus* is the most symmetrical and that of *M. lutarioriparius* is the most asymmetrical among the four species.

Fluorescence banding patterns

After CPD staining, slightly different fluorochrome banding patterns were observed among the four *Miscanthus* species (Fig. 1–3; Table 3). The red CPD bands were recorded in all species, whereas blue DAPI bands were found only in *M. sinensis* and *M. floridulus*.

Table 2. Karyotypic parameters of four *Miscanthus* species.

Species	KF	TCL±SD (μm)	RRL	CI±SD	A1	A2	As K%	AI	Stebbin's types
M. sinensis	2n=2x=38=34m(2SAT)+4sm	73.92±2.87	3.53~8.23	44.00±4.97	0.20	0.27	55.85	3.06	2B
M. floridulus	2n=2x=38=34m(2SAT)+4sm	86.13±5.87	3.47~8.60	44.88±4.35	0.13	0.26	55.19	2.51	2B
M. sacchariflorus	2n=2x=38=34m(2SAT)+4sm	68.15±3.25	3.76~8.44	44.19±4.31	0.12	0.24	55.72	2.37	2B
M. lutarioriparius	2n=2x=38=34m(2SAT)+4sm	76.48±5.02	3.69~8.04	44.56±3.83	0.11	0.52	55.40	4.47	2B

KF, karyotype formula; TCL, total length of the haploid complement (i.e. karyotype length); RRL, ranges of chromosome relative length; CI, mean centromeric index; A1 and A2, intra-chromosomal asymmetry index and inter-chromosomal asymmetry index, respectively; As K%, ratio of the length of all long arms in chromosome set to total chromosome length; AI, karyotype asymmetry index.

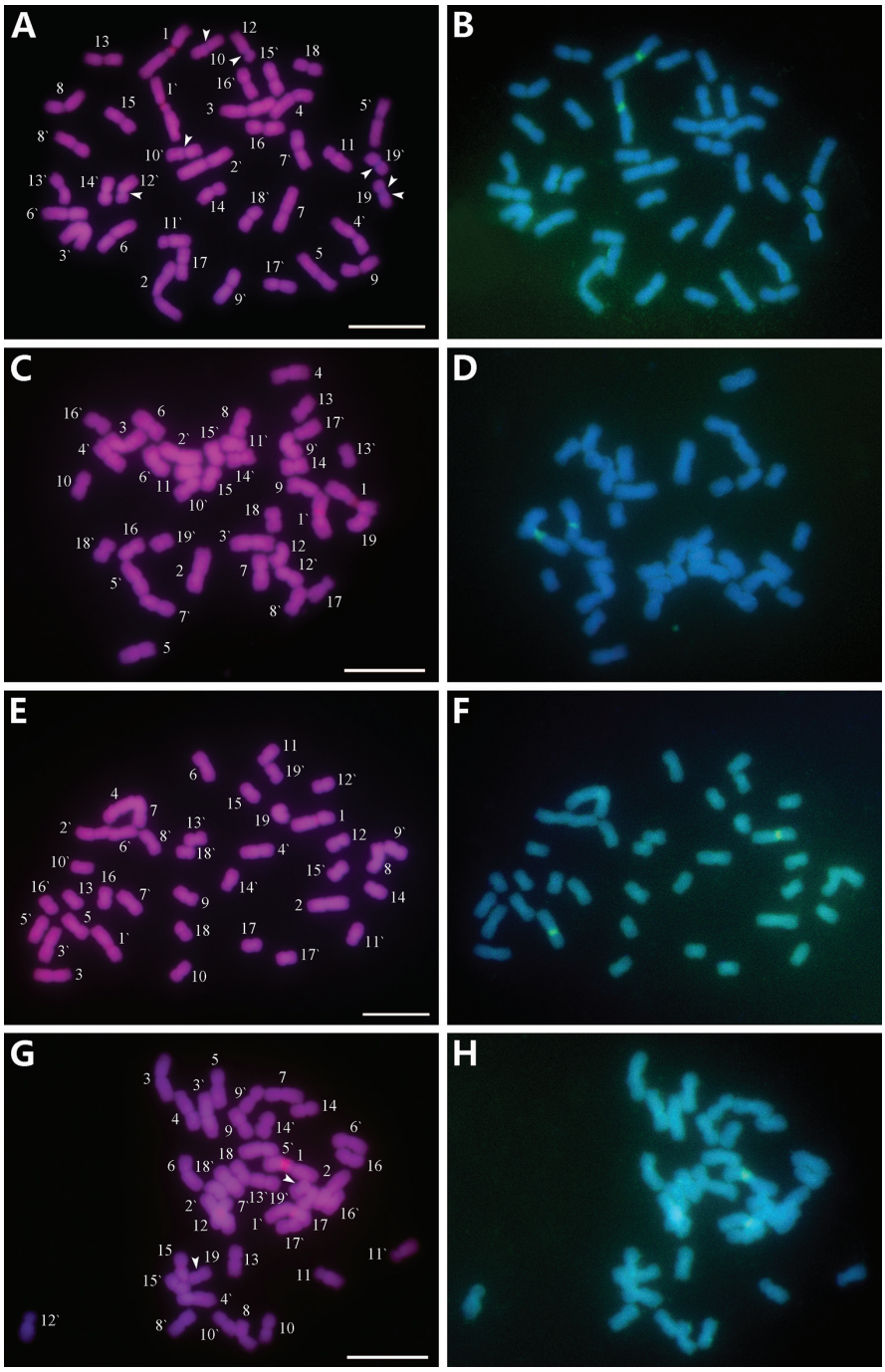

Figure 1. Mitotic chromosomes from *M. sinensis* (**A, B**), *M. sacchariflorus* (**C, D**), *M. lutarioriparius* (**E, F**) *M. floridulus* (**G, H**), stained with CPD staining and sequentially FISH with biotin-labelled 45S rDNA probe. **A, C, E** and **G** are chromosomes stained using CPD. The chromosome numbers were designated by karyotyping **B, D, F** and **H** are the chromosomes showing the 45S (green) signals. Arrowheads in **A** and **G** indicate the blue DAPI bands. Scale bars: 10 μm.

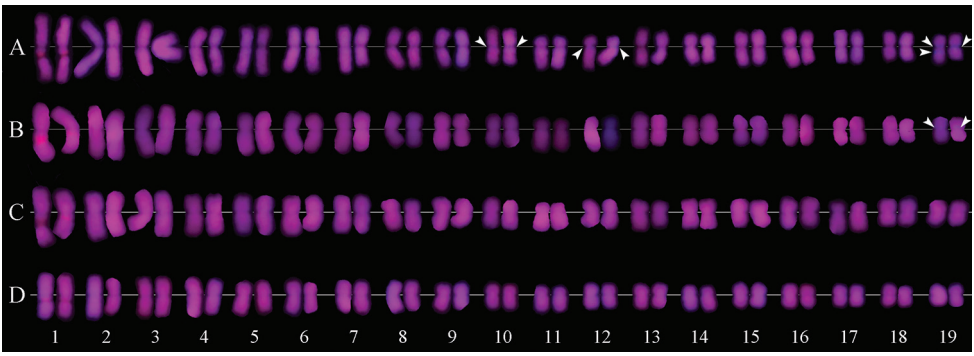

Figure 2. Karyotype showing CPD and DAPI bands of *M. sinensis* (**A**), *M. floridulus* (**B**), *M. sacchariflorus* (**C**), *M. lutarioriparius* (**D**). Arrowheads in **A** and **B** indicate the blue DAPI bands.

Table 3. The distribution of fluorochrome bands and 45S rDNA sites in the four *Miscanthus* species.

Species	Fluorochrome bands			Number (pair) and location of 45S rDNA sites[†§]
	Type	Distribution[†]	amount[‡] (%)	
M. sinensis	CPD	45S sites	0.93	One [1L-PROX (25.53%)]
	DAPI	10 CENS, 12L-PCENS, 19 CENS, 19L-PROX (one homologue)	1.94	
M. floridulus	CPD	45S sites, 15 PCEN (one homologue)	1.11	One [1L-PROX (29.43%)]
	DAPI	19S-PCEN	0.45	
M. sacchariflorus	CPD	45S sites	0.90	One [1L-PROX (32.07%)]
M. lutarioriparius	CPD	45S sites	0.75	One [1L-PROX (28.45%)]

[†] S and L represent the short and long arms, respectively; CEN, PCEN and PROX represent the centromeric, pericentromeric and proximal positions, respectively; figures ahead of the positions designate the chromosomal pair involved.

[‡] Amount of bands in the genome, expressed as a percentage of the karyotype length.

[§] The percentages in parenthesis indicate the percentage distance from the centromere to the rDNA site (di = d × 100/a; d = distance of the centre of the 45S sites from the centromere, a = length of the corresponding chromosome arm).

Results showed that only one pair of CPD bands in *M. sinensis*, *M. sacchariflorus* and *M. lutarioriparius* had occurred in the secondary constrictions on the long arms of chromosome 1, and were co-localized with the 45S rDNA-FISH hybridization sites (called rDNA CPD bands; Fig. 1A, E, G). There were three CPD bands in the *M. floridulus*: two bands correspond to the secondary constriction on the long arms of chromosome 1; the other band was a non-rDNA CPD band with weaker fluorescence, occurring in the pericentromeric region of a homologue of chromosome pair 15 (Fig. 1G). The rDNA CPD bands in *M. sinensis* and *M. lutarioriparius* were similar in size and intensity on the two homologous chromosomes, while those in *M. floridulus* and *M. sacchariflorus* displayed heterozygosity, the band on one chromosome was large and bright, whereas the band on the other homologue was small and weak. The CPD bands of *M. sinensis*, *M. floridulus*, *M. sacchariflorus* and *M. lutarioriparius* accounted for 0.93%, 1.11%, 0.90% and 0.75% of the karyotype length, respectively.

M. sinensis showed seven blue DAPI bands (Fig. 1A, 2A, 3A): two pairs of weak bands occurred in the centromeric regions of chromosomes 10 and the pericentromeric regions of the long arm of chromosome 12, three relatively strong bands occured on chromosome 19. Among the DAPI bands on pair 19, two were located in the

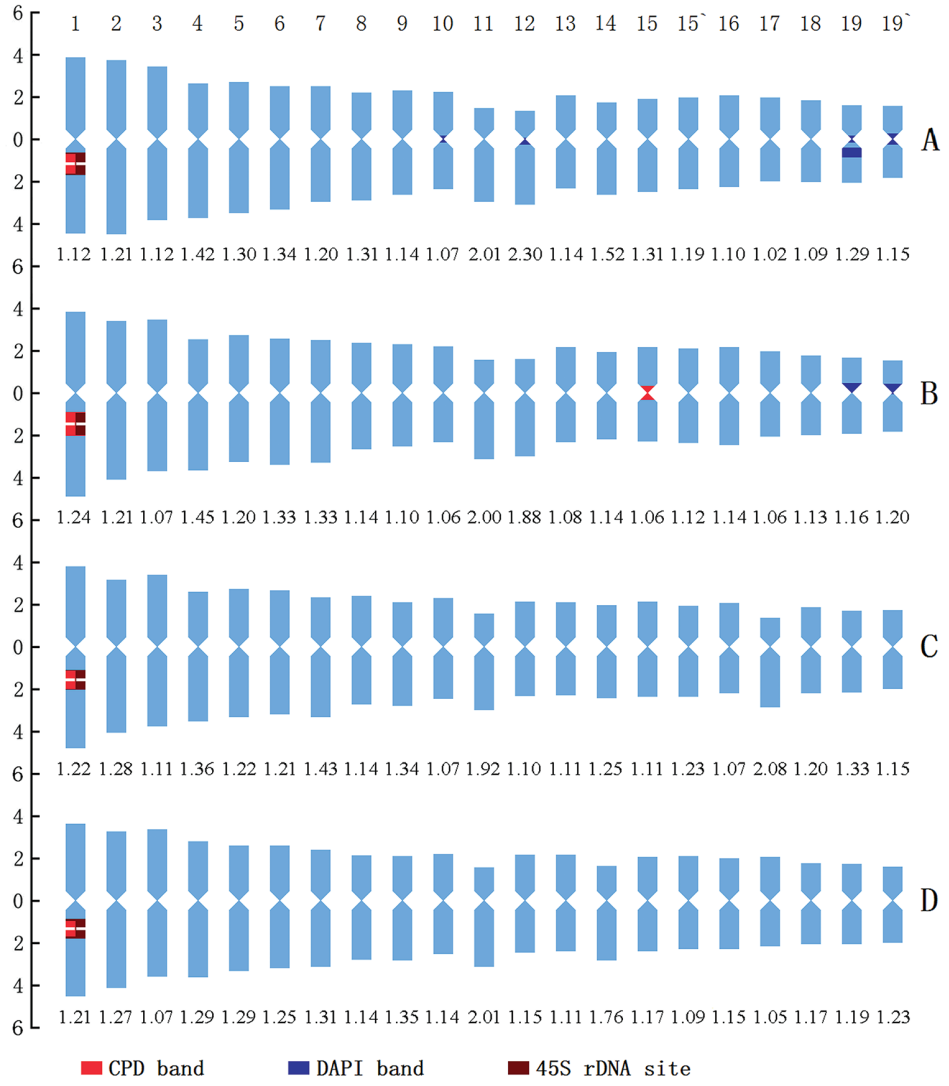

Figure 3. Idiograms of the four *Miscanthus* species that display the chromosome measurements, and the position and size of fluorochrome bands and 45 rDNA FISH signals. **A, B, C, D** indicate *M. sinensis*, *M. floridulus*, *M. sacchariflorus* and *M. lutarioriparius*, respectively. The ordinate scale on the left indicates the relative length of the chromosomes (i.e.% of haploid complement). The numerical values under each chromosome pair indicate the arm ratios of the respective chromosome pair. The numbers above panel **A** are chromosome numbers.

centromeric regions of both homologues, and one occured in the proximal region of the long arm of one homologue. *M. floridulus* had shown only one pair of weak DAPI bands in the pericentromeric regions on the chromosomes 19 (Fig. 1G, 2B, 3B). The DAPI bands of *M. sinensis* and *M. floridulus* accounted for 1.94% and 0.45% of the karyotype length, respectively.

FISH mapping of 45S rDNA

45S rDNA FISH showed that *M. sinensis*, *M. floridulus*, *M. sacchariflorus* and *M. lutarioriparius* had only one pair of 45S rDNA sites, which were located in the secondary constriction on the long arms of chromosome 1, and their percentage distances of 45S rDNA sites were 25.53 ± 1.17, 29.43 ± 1.12, 32.07 ± 0.49, 28.45 ± 0.89, respectively. The 45S rDNA sites of the four *Miscanthus* species corresponded to their respective CPD bands in both size and intensity, that is, the 45S rDNA signals of two homologues in *M. sinensis* and *M. lutarioriparius* were similar in size and intensity, while those in *M. floridulus* and *M. sacchariflorus* differed in size and intensity, displaying heterozygosity.

GISH signal patterns

The GISH results are shown in Fig. 4. Both self-GISH (sGISH; the genomic DNA of a species is applied to its own chromosomes) and cGISH generated hybridization signals

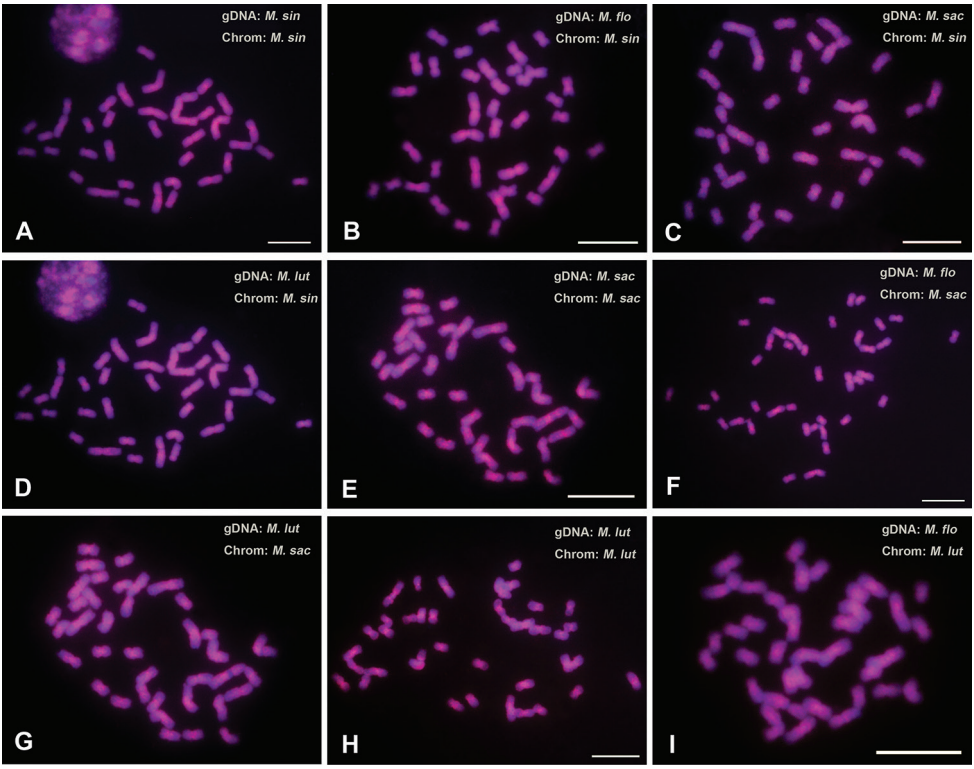

Figure 4. FISH with *M. sinensis* (**A**), *M. floridulus* (**B**), *M. sacchariflorus* (**C**) and *M. lutarioriparius* (**D**) genomic DNA probes (red) to *M. sinensis* chromosomes, FISH with *M. sacchariflorus* (**E**), *M. floridulus* (**F**) and *M. lutarioriparius* (**G**) genomic DNA probes (red) to *M. sacchariflorus* chromosomes, and FISH with *M. lutarioriparius* (**H**) and *M. floridulus* (**I**) genomic DNA probes (red) to *M. lutarioriparius* chromosomes. Scale bars: 10 μm.

in most regions of all chromosomes. Overall, the hybridization signals in the proximal and/or centromeric regions of the chromosomes were strong or very strong, while those in the proximal regions were relatively weak. In the GISHs to the *M. sinensis* chromosomes, the signals generated by *M. floridulus* gDNA (Fig. 4B) were stronger and more evenly distributed than those generated by *M. sacchariflorus* and *M. lutarioriparius* gDNAs (Fig. 4C, D), and more similar to the sGISH signals of *M. sinensis* (Fig. 4A). The hybridization signals of *M. floridulus* gDNA to the chromosomes of *M. sacchariflorus* (Fig. 4F) and *M. lutarioriparius* (Fig. 4I) were weaker than both the sGISH signals of *M. sacchariflorus* (Fig. 4E) and *M. lutarioriparius* (Fig. 4H), and the cGISH signals of *M. lutarioriparius* gDNA to *M. sacchariflorus* chromosomes (Fig. 4G) .

Phylogeny analysis based on ITS

Each ITS1-5.8S-ITS2 sequences were compared to the published sequences of *Miscanthus* and its related species, and the boundaries of the spacer regions were confirmed. The length and other characteristics of each ITS1-5.8S-ITS2 are given in Table 4. The entire ITS sequence (ITS1-5.8S-ITS2) of *I. cylindrica* that was used as the outgroup species was 684 bp in length, and its GC content was 63.89%.

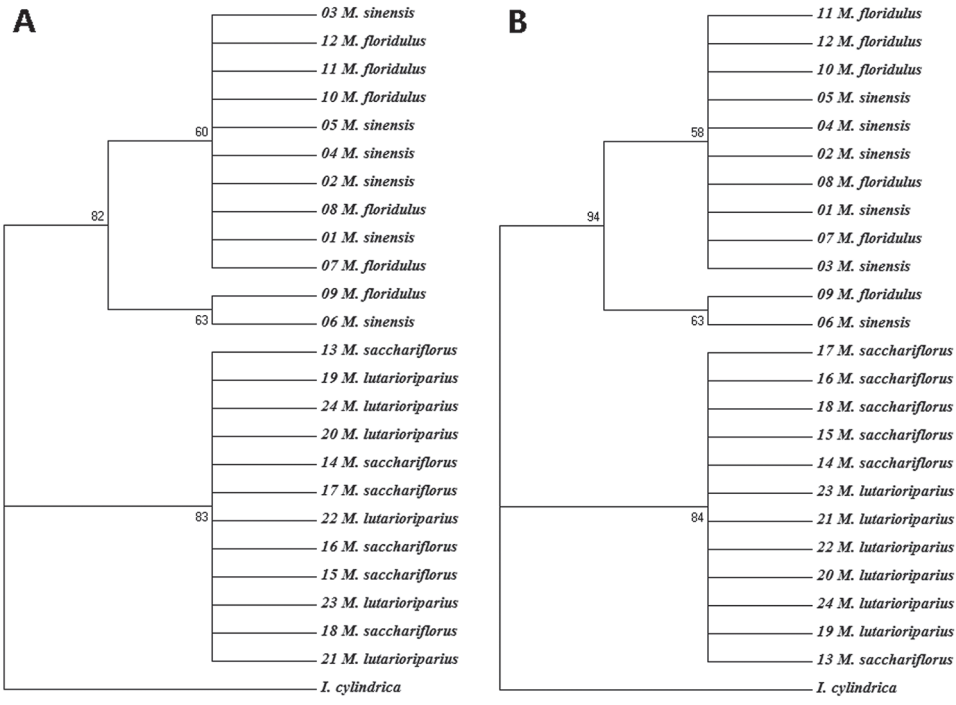

Figure 5. Rooted neighbour-joining (NJ) (**A**) and maximum-likelihood (ML) (**B**) tree based on the ITS1-5.8S-ITS2 sequences of the four *Miscanthus* species using the MEGA software (version 7.0) with *I. cylindrica* as an outgroup species. The numbers near the nodes indicate bootstrap values (in percentage).

Table 4. Features of the ITS1-5.8S-ITS2 sequences of the four *Miscanthus* species.

	Length range	G/C content range (%)	No. of indels	No. of variable sites	No. of informative sites	Transitions	Transversions	Ratio
ITS1	258–260	67.44–68.46	2	7	5	2	3	2:3
5.8S	157	56.05–56.69	0	1	0	0	1	0:1
ITS2	244–245	60.25 –61.63	1	8	3	1	6	1:6
complete	659–661	62.37–63.09	3	16	8	3	10	3:10

Neighbour joining (NJ) and maximum likelihood (ML) phylogenetic trees were developed based on the entire ITS sequences. The NJ and ML trees were very similar (Fig. 5), and the four *Miscanthus* species were divided into two categories: (i) group I contained *M. sinensis* and *M. floridulus*, which resulted in 82% (NJ) and 94% (ML) bootstrap values; (ii) group II included *M. sacchariflorus* and *M. lutarioriparius*, with 83% and 84% bootstrap values in NJ and ML trees, respectively. It was worth noting that in each branch the accessions of one species were not separated from those of another species (Fig. 5).

Discussion

Molecular cytogenetic karyotypes

In the present study, detailed karyotypes of *M. sinensis*, *M. floridulus*, *M. sacchariflorus* and *M. lutarioriparius* were established using a combination of chromosome measurements, fluorochrome bands and 45S rDNA FISH signals, which provided the primary molecular-cytogenetic characterization of the four *Miscanthus* energy plants for the first time.

Our results had shown that the molecular cytogenetic karyotypes were rather similar among the four *Miscanthus* species. For instance, their karyotype formula, the categories of Stebbins, and the number and location of the 45S rDNA sites were same and there were slight differences in RRL, CI, A1 and As K%. However, several differences in their karyotypes were recorded: (1) obvious differences in their TCL, A2 and AI. In particular, AI, which can more accurately reveal the heterogeneity of chromosome length and centromere index in karyotype (Paszko 2006), had significant differences among the four species. (2) A non-rDNA CPD band appeared in *M. floridulus*. (3) AT-rich heterochromatin (DAPI bands) occurred in *M. sinensis* and *M. floridulus* but not in *M. sacchariflorus* and *M. lutarioriparius*. (4) There appeared 45S rDNA heterozygosity in *M. floridulus* and *M. sacchariflorus* but not in *M. sinensis* and *M. lutarioriparius*. Therefore, the four *Miscanthus* species could be accurately distinguished from each other using the molecular-cytogenetic karyotypic data.

As our study revealed, the chromosome numbers of the four *Miscanthus* species were all 2n = 2× = 38, being consistent with those reported previously (Hodkinson et al. 2002a, Takahashi and Shibata 2002, Takahashi et al. 2002, Chramiec-Głąbik et al. 2012). The current karyotypes of the four *Miscanthus* species comprised

mainly of metacentric chromosomes, differing from the previous karyotypes, which had more submetacentric chromosomes, and even had acroentric chromosomes (Chramiec-Głąbik et al. 2012). Our study revealed that each species had a pair of satellite chromosomes, which were designated as chromosome 1. Previous studies also reported the presence of satellite chromosomes in *Miscanthus* species and revealed by FISH one pair of 45S rDNA sites in *M. sinensis*, but the serial number of the satellite chromosomes and the locations of the secondary constrictions were different (Takahashi and Shibata 2002, Takahashi et al. 2002, Chramiec-Głąbik et al. 2012). The deviations in karyotype were probably mainly due to differences in the material analysed, and difficulty in accurately pairing homologous chromosomes and distinguishing chromosomes by using the classical staining technique as applied before.

Phylogenetic relationships of the four *Miscanthus* species

The research on the evolutionary relationship among the four *Miscanthus* species could not be conducted using genomic information because the genome sequences of *M. floridulus*, *M. sacchariflorus* and *M. lutarioriparius* were currently unavailable. Therefore, at present the combination of molecular cytogenetic analysis with rDNA ITS and chloroplast DNA sequence analysis was an effective phylogenetic analysis pathway (She et al. 2015).

As mentioned above, the molecular cytogenetic karyotypes of the four *Miscanthus* species were very similar, indicating the high genome similarity and small genome differentiation among them. Furthemore, the cGISH signals were rather similar in intensity and distribution to the sGISH signals, further demonstrating the high similarity among the four *Miscanthus* genomes (Wolny and Hasterok 2009, She et al. 2015, Zhang et al. 2015). However, the differences in molecular cytogenetic karyotypes and cGISH signals among the four species also provided valuable evolution information: (1) AT-rich heterochromatin appeared in both *M. sinensis* and *M. floridulus*, but did not emerge in both *M. sacchariflorus* and *M. lutarioriparius*; (2) The hybridization signals of *M. floridulus* gDNA to *M. sinensis* chromosomes were stronger and more evenly distributed than those of *M. sacchariflorus* and *M. lutarioriparius* gDNA, whereas the hybridization signals of *M. floridulus* gDNA to *M. sacchariflorus* chromosomes were weaker than the hybridization signals of *M. lutarioriparius* gDNA to *M. sacchariflorus* chromosomes. This information indicates that there was a close phylogenetic relationship between *M. sinensis* and *M. floridulus*, and between *M. sacchariflorus* and *M. lutarioriparius*; the former two species were relatively distant from the latter two species.

In our study, the phylogenetic tree based on the ITS sequences had shown that, *M. sinensis* and *M. floridulus* clustered into one branch, and *M. sacchariflorus* and *M. lutarioriparius* clustered into another branch. It was consistent with not only the above molecular cytogenetic results, but also the previous clustering results based on morphology, molecular markers and the ITS sequence (Hodkinson et al. 2002b, Chen et al. 2007, Sun et al. 2010, Chae et al. 2014, Clark et al. 2014, Ge et al. 2017). In

addition, our clusering analysis revealed that the accessions of the two species in each branch were mixed and without distinct boundaries. These findings were consistent with the phylogenetic trees of *Miscanthus* and related genera inferred from ITS sequences (Hodkinson et al. 2002b, Chen et al. 2007, Liu et al. 2010), SSR markers (Ge et al. 2017), SNPs (Clark et al. 2014) and the dataset of genome size, ploidy level and genomic polymorphisms (Chae et al. 2014). To summarise, our clustering results have demonstrated that there was a very close phylogenetic relationship between *M. sinensis* and *M. floridulus*, and between *M. sacchariflorus* and *M. lutarioriparius* and they cannot be distinguished only based on the ITS sequences. However, as revealed in this study, the molecular cytogenetic karyotype analysis can effectively identify the four species.

Conclusion

Molecular cytogenetic karyotypes of *M. sinensis*, *M. floridulus*, *M. sacchariflorus* and *M. lutarioriparius* were established for the first time, which can effectively distinguish the four species. Molecular cytogenetic comparison revealed basic similarities and certain differences in genome organization among the four species. These findings will provide a reference for further development of specific probes based on *M. sinensis* genome sequence for chromosomal localization in the species of *Miscanthus* and related genera. The combined data of molecular cytogenetic and ITS sequence analysis indicated a close phylogenetic relationship between *M. sinensis* and *M. floridulus*, and between *M. sacchariflorus* and *M. lutarioriparius*, respectively. It can be concluded that former two species have relatively distant relationship compared with the latter two species.

Acknowledgements

The authors are indebted to the National Natural Science Fundation of China for funding this project (No. 31871693 and No. 31471557). And Hunan Provincial Department of Education Funding (18B116) has also provided financial support to carry out this study.

References

Álvarez I, Wendel JF (2003) Ribosomal ITS sequences and plant phylogenetic inference. Molecular Phylogenetics and Evolution 29: 417–434. https://doi.org/10.1016/S1055-7903(03)00208-2

Arano H (1963) Cytological studies in subfamily *Carduoideae* (Compositae) of Japan. IX. The karyotype analysis and phylogenic considerations on *Pertya* and *Ainsliaea* (2). Botanical Magazine Tokyo 76: 32–39. https://doi.org/10.15281/jplantres1887.76.32

Bennetzen JL (2000) Comparative sequence analysis of plant nuclear genomes: microcolinearity and its many exceptions. The Plant Cell 12: 1021–1029. https://doi.org/10.2307/3871252

Brosse N, Dufour A, Meng XZ, Sun QN, Ragauskas A (2012) *Miscanthus*: a fast-growing crop for biofuels and chemicals production. Biofuels Bioproducts and Biorefining-Biofpr 6: 580–598. https://doi.org/10.1002/bbb.1353

Capua ID, Maffucci F, Pannone R, Mazzocchi MG, Biffali E, Amato A (2017) Molecular phylogeny of *Oncaeidae* (Copepoda) using nuclear ribosomal internal transcribed spacer (ITS rDNA). PLoS One 12: 1–21. https://doi.org/10.1371/journal.pone.0175662

Chae WB, Hong SJ, Gifford JM, Rayburn AL, Sacks EJ, Juvik JA (2014) Plant morphology, genome size, and SSR markers differentiate five distinct taxonomic groups among accessions in the genus *Miscanthus*. GCB Bioenergy 6: 646–660. https://doi.org/10.1111/gcbb.12101

Chen SF, Dong SS, Wu W, Shi SH, Zhou PH (2007) Phylogenetics of *Triarrhena* and Related Genera Based on ITS Sequence Data. Journal of Wuhan Botanical Research 25: 239–244. [In Chinese] https://doi.org/10.3969/j.issn.2095-0837.2007.03.005

Chen SL, Renvoize SA (2006) *Miscanthus* Andersson. In: Wu ZY, Raven PH (Eds) Flora of China. Science Press, Beijing, 581–583.

Chramiec-Głąbik A, Grabowska-Joachimiak A, Sliwinska E, Legutko J, Kula A (2012) Cytogenetic analysis of *Miscanthus* × *giganteus* and its parent forms. Caryologia 65: 234–242. https://doi.org/10.1080/00087114.2012.740192

Christian DG, Yates NE, Riche AB (2009) Estimation of ramet production from *Miscanthus* × *giganteus* rhizome of different ages. Industrial Crops and Products 30: 176–178. https://doi.org/10.1016/j.indcrop.2009.02.007

Clark LV, Brummer JE, Glowacka K, Hall MC, Heo K, Peng JH, Yamada T, Yoo JH, Yu CY, Zhao H (2014) A footprint of past climate change on the diversity and population structure of *Miscanthus sinensis*. Annals of Botany 114: 97–107. https://doi.org/10.1093/aob/mcu084

de Moraes AP, dos Santos Soares Filho W, Guerra M (2007) Karyotype diversity and the origin of grapefruit. Chromosome Research 15: 115–121. https://doi.org/10.1007/s10577-006-1101-2

Deumling B, Greilhuber J (2004) Characterization of heterochromatin in different species of the *Scilla sibericagroup* (Liliaceae) by *in situ* hybridization of satellite DNAs and fluorochrome banding. Chromosoma 84: 535–555. https://doi.org/10.1007/BF00292854

Felsenstein J (1985) Confidence limits on phylogenies: an approach using the bootstrap. Evolution 39: 783–791. https://doi.org/10.1111/j.1558-5646.1985.tb00420.x

Filion WG (1974) Differential Giemsa staining in plants. Chromosoma 49: 51–60. https://doi.org/10.1007/BF00284987

Ge CX, Liu XM, Liu SM, Xu J, Li HF, Cui TT, Yao Y, Chen M, Yu WL, Chen CX (2017) *Miscanthus* sp.: Genetic Diversity and Phylogeny in China. Plant Molecular Biology Reporter 35: 600–610. https://doi.org/10.1007/s11105-017-1048-9

Greilhuber J, Speta F (1976) C-banded karyotypes in the *Scilla hohenackeri* group, *S. persica*, and *Puschkinia* (Liliaceae). Plant Systematics and Evolution 126: 149–188. https://doi.org/10.1007/BF00981669

Hao G, Yuan YM, Hu CM, Ge XJ, Zhao NX (2004) Molecular phylogeny of *Lysimachia* (Myrsinaceae) based on chloroplast *trnL-F* and nuclear ribosomal ITS sequences. Molecular Phylogenetics and Evolution 31: 323–339. https://doi.org/10.1016/S1055-7903(03)00286-0

Hodkinson TR, Chase MW, Takahashi C, Leitch IJ, Bennett MD, Renvoize SA (2002a) The use of DNA sequencing (ITS and *trnL-F*), AFLP, and fluorescent *in situ* hybridization to study allopolyploid *Miscanthus* (Poaceae). American Journal of Botany 89: 279–286. https://doi.org/10.3732/ajb.89.2.279

Hodkinson TR, Chase MW, Lledó MD, Salamin N, Renvoize SA (2002b) Phylogenetics of *Miscanthus*, *Saccharum* and related genera (Saccharinae, Andropogoneae, Poaceae) based on DNA sequences from ITS nuclear ribosomal DNA and plastid *trnL* intron and *trnL-F* intergenic spacers. Journal of Plant Research 115: 381–392. https://doi.org/10.1007/s10265-002-0049-3

Hu XH (2015) Collection and genetic variation of *Miscanthus lutarioriparius* germplasm resources. Ph.D. Dissertation, Hubei: Wuhan University, 97 pp. [In Chinese]

Jin XL, Chen XL, Xiao L, Shi CH, Chen L, Yu B, Yi ZL, Yoo JH, Heo K, Yu CY (2017) Application of visible and near-infrared spectroscopy to classification of *Miscanthus* species. PLoS One 12: e0171360. https://doi.org/10.1371/journal.pone.0171360

Koornneef M, Fransz P, Jong HD (2003) Cytogenetic tools for *Arabidopsis thaliana*. Chromosome Research 11: 183–194. https://doi.org/10.1023/A:1022827624082

Kumar S, Stecher G, Tamura K (2016) MEGA7: Molecular Evolutionary Genetics Analysis Version 7.0 for Bigger Datasets. Molecular biology and evolution 33: 1870–1874. https://doi.org/10.1093/molbev/msw054

Levan A, Fredga K, Sandberg AA (1964) Nomenclature for centromeric position on chromosomes. Hereditas 52: 201–220. https://doi.org/10.1111/j.1601-5223.1964.tb01953.x

Liu CC, Xiao L, Jiang JX, Wang WX, Gu F, Song DL, Yi ZL, Jin YC, Li LG (2013) Biomass properties from different *Miscanthus* species. Food and Energy Security 2: 12–19. https://doi.org/10.1002/fes3.19

Liu J (2009) Genetic diversity of *Triarrhena* germplasms in China revealed by SSR markers. PhD Thesis, Hunan Agricultural University, Hunan, 126 pp. [In Chinese]

Liu XL, Su HS, Ma L, Lu X, Ying XM, Cai Q, Fan YH (2010) Phylogenetic Relationships of Sugarcane Related Genera and Species Based on ITS Sequences of Nuclear Ribosomal DNA. Acta Agronomica Sinica 36: 1853–1863. [In Chinese] https://doi.org/10.3724/SP.J.1006.2010.01853

Lu YF (2012) Studies on systematics of genus *Miscanthus* (Poaceae) of China. PhD Thesis, Hunan Agricultural University, Hunan, 35 pp. [In Chinese]

Moscone EA, Klein F, Lambrou M, Fuchs J, Schweizer D (1999) Quantitative karyotyping and dual-color FISH mapping of 5S and 18S-25S rDNA probes in the cultivated *Phaseolus* species (Leguminosae). Genome 42: 1224–1233. https://doi.org/10.1139/g99-070

Murray MG, Thompson WF (1980) Rapid isolation of high molecular weight plant DNA. Nucleic Acids Research 8: 4321–4325. https://doi.org/10.1093/nar/8.19.4321

Paszko B (2006) A critical review and a new proposal of karyotype asymmetry indices. Plant Systematics and Evolution 258: 39–48. https://doi.org/10.1007/s00606-005-0389-2

Perry KL, Palukaitis P (1990) Transcription of tomato ribosomal DNA and the organization of the intergenic spacer. Molecular and General Genetics 221: 102–112. https://doi.org/10.1007/BF00280374

Peterson DG, Lapitan NLV, Stack SM (1999) Localization of single- and low-copy sequences on tomato synaptonemal complex spreads using fluorescence *in situ* hybridization (FISH). Genetics 152: 427–439. https://doi.org/10.1016/j.stem.2013.12.011

She CW, Jiang XH, Ou LJ, Liu J, Long KL, Zhang LH, Duan WT, Zhao W, Hu JC (2015) Molecular cytogenetic characterisation and phylogenetic analysis of the seven cultivated *Vigna* species (Fabaceae). Plant Biology 17: 268–280. https://doi.org/10.1111/plb.12174

She CW, Liu JY, Song YC (2006) CPD staining: an effective technique for detection of NORs and other GC-rich chromosomal regions in plants. Biotechnic and Histochemistry 81: 13–21. https://doi.org/10.1080/10520290600661414

She CW, Wei L, Jiang XH (2017) Molecular cytogenetic characterization and comparison of the two cultivated *Canavalia* species (Fabaceae). Comparative Cytogenetics 11: 579–600. https://doi.org/10.3897/compcytogen.v11i4.13604

Sheng JJ, Hu XH, Zeng XF, Li Y, Zhou FS, Hu ZL, Jin SR, Diao Y (2016) Nuclear DNA content in *Miscanthus* sp. and the geographical variation pattern in *Miscanthus lutarioriparius*. Scientific Reports 6: 34342. https://doi.org/10.1038/srep34342

Silva GS, Souza MM, de Melo CAF, Domingo UJ, Forni-Martins ER (2018) Identification and characterization of karyotype in *Passiflora* hybrids using FISH and GISH. BMC Genetics 19: 26. https://doi.org/10.1186/s12863-018-0612-0

Stebbins GL (1971) Chromosomal evolution in high plants. Addison-Wesley, London, 220 pp.

Stewart JR, Toma Y, Fernández FG, Nishiwaki A, Yamada T, Bollero G (2009) The ecology and agronomy of *Miscanthus sinensis*, a species important to bioenergy crop development, in its native range in Japan: a review. GCB Bioenergy 1: 126–153. https://doi.org/10.1111/j.1757-1707.2009.01010.x

Sumner AT (1990) Chromosome banding. Unwin Hyman, London, 155–186.

Sun Q, Lin Q, Yi ZL, Yang ZR, Zhou FS (2010) A taxonomic revision of *Miscanthus* s.l. (Poaceae) from China. Botanical Journal of the Linnean Society 164: 178–220. https://doi.org/10.1111/j.1095-8339.2010.01082.x

Takahashi C, Shibata F (2002) Analysis of *Miscanthus sacchanflorus* and *M. sinensis* chromosomes by fluorescence *in situ* hybridization using rDNA and total genomic DNA probes. Chromosome Science 6: 7–11. https://ci.nii.ac.jp/naid/110003723578

Takahashi C, Shibata F, Hizume M (2002) FISH detection of sugar cane centromeric repetitive sequences in the chromosomes of two *Miscanthus* species. Chromosome science 6: 1–5. https://ci.nii.ac.jp/naid/110003723577/en

Tamura K, Uwatoko N, Yamashita H, Fujimori M, Akiyama Y, Shoji A, Sanada Y, Okumura K, Gau M (2016) Discovery of natural interspecific hybrids between *Miscanthus Sacchariflorus* and *Miscanthus Sinensis* in southern Japan: morphological characterization, genetic structure, and origin. BioEnergy Research 9: 315–325. https://doi.org/10.1007/s12155-015-9683-1

Tang J, Daroch M, Kilian A, Jezowski S, Pogrzeba M, Mos M (2015) DArT-based characterisation of genetic diversity in a *Miscanthus* collection from Poland. Planta 242: 985–996. https://doi.org/10.1007/s00425-015-2335-z

White TJ, Bruns T, Lee S, Taylor J (1990) Amplification and direct seqencing of fungal ribosomal RNA genes for phylogenetics. In: Innis M, Gelfand D, Sninsky J, White T (Eds) PCR

Protocols: A Guide to Methods and Applications. Academic Press, San Diego, 315–322. https://doi.org/10.1016/B978-0-12-372180-8.50042-1

Wolny E, Hasterok R (2009) Comparative cytogenetic analysis of the genomes of the model grass *Brachypodium distachyon* and its close relatives. Annals of Botany 104: 873–881. https://doi.org/10.1093/aob/mcp179

Yang S, Xue S, Kang WW, Qian ZX, Yi ZL (2019) Genetic diversity and population structure of *Miscanthus lutarioriparius*, an endemic plant of China. PLoS ONE 14: 1–18. https://doi.org/10.1371/journal.pone.0211471

Yook MJ, Lim SH, Song JS, Kim JW, Zhang CJ, Lee EJ, Ibaragi Y, Lee GJ, Nah G, Kim DS (2014) Assessment of genetic diversity of Korean *Miscanthus* using morphological traits and SSR markers. Biomass and Bioenergy 66: 81–92. https://doi.org/10.1016/j.biombioe.2014.01.025

Zarco CR (1986) A new method for estimating karyotype asymmetry. Taxon 35: 526–530. https://doi.org/10.2307/1221906

Zhang YX, Cheng CY, Li J, Yang SQ, Wang YZ, Li Z, Chen JF, Lou QF (2015) Chromosomal structures and repetitive sequences divergence in *Cucumis* species revealed by comparative cytogenetic mapping. BMC Genomics 16: 730. https://doi.org/10.1186/s12864-015-1877-6

Zhao YL, Basak S, Fleener CE, Egnin M, Sacks EJ, Prakash CS, He GH (2017) Genetic diversity of *Miscanthus sinensis* in US naturalized populations. GCB Bioenergy 9: 965–972. https://doi.org/10.1111/gcbb.12404

Zoller JF, Yang Y, Herrmann RG, Hohmann U (2001) Comparative genomic *in situ* hybridization (cGISH) analysis on plant chromosomes revealed by labelled *Arabidopsis* DNA. Chromosome Research 9: 357–375. https://doi.org/10.1023/A:1016767100766

Supplementary material 1

Molecular cytogenetic characterization and phylogenetic analysis of four *Miscanthus* species (Poaceae)

Authors: Yanmei Tang, Liang Xiao, Yasir Iqbal, Jianfeng Liao, Longqian Xiao, Zili Yi, Chaowen She

Data type: species data

Explanation note: **Table S1.** Chromosome measurements of *M. sinensis*. **Table S2**. Chromosome measurements of *M. floridulus*. **Table S3.** Chromosome measurements of *M. sacchariflorus*. **Table S4.** Chromosome measurements of *M. lutarioriparius*.

Link: https://doi.org/10.3897/CompCytogen.v13i3.35346.suppl1

CompCytogen 13(3): 231–243 (2019)
doi: 10.3897/CompCytogen.v13i3.36112
http://compcytogen.pensoft.net

RESEARCH ARTICLE

COMPARATIVE Cytogenetics
A peer-reviewed open-access journal
International Journal of Plant & Animal Cytogenetics, Karyosystematics, and Molecular Systematics

Development of new cytogenetic markers for *Thinopyrum ponticum* (Podp.) Z.-W. Liu & R.-C. Wang

Pavel Yu. Kroupin[1,2], Victoria M. Kuznetsova[1,2], Ekaterina A. Nikitina[1], Yury Ts. Martirosyan[3], Gennady I. Karlov[1,2], Mikhail G. Divashuk[1,2]

1 *Laboratory of Applied Genomics and Crop Breeding, All-Russia Research Institute of Agricultural Biotechnology, Timiryazevskaya str. 42, Moscow 127550, Russia* **2** *Center of Molecular Biotechnology, Russian State Agrarian University-Moscow Timiryazev Agricultural Academy, Timiryazevskaya str. 49, Moscow 127550, Russia* **3** *Group of Aeroponic Plant Growing Technologies, All-Russia Research Institute of Agricultural Biotechnology, Timiryazevskaya str. 42, Moscow 127550, Russia*

Corresponding author: *Pavel Yu. Kroupin* (pavelkroupin1985@gmail.com)

Academic editor: *Xutong Wang* | Received 12 May 2019 | Accepted 22 July 2019 | Published 13 August 2019

http://zoobank.org/A3B54882-ED6D-4EDB-803E-4D6205B69CD6

Citation: Kroupin PYu, Kuznetsova VM, Nikitina EA, Martirosyan YuTs, Karlov GI, Divashuk MG (2019) Development of new cytogenetic markers for *Thinopyrum ponticum* (Podp.) Z.-W. Liu & R.-C. Wang. Comparative Cytogenetics 13(3): 231–243. https://doi.org/10.3897/CompCytogen.v13i3.36112

Abstract

Thinopyrum ponticum (Podpěra, 1902) Z.-W. Liu & R.-C.Wang, 1993 is an important polyploid wild perennial Triticeae species that is widely used as a source of valuable genes for wheat but its genomic constitution has long been debated. For its chromosome identification, only a limited set of FISH probes has been used. The development of new cytogenetic markers for *Th. ponticum* chromosomes is of great importance both for cytogenetic characterization of wheat-wheatgrass hybrids and for fundamental comparative studies of phylogenetic relationships between species. Here, we report on the development of five cytogenetic markers for *Th. ponticum* based on repetitive satellite DNA of which sequences were selected from the whole genome sequence of *Aegilops tauschii* Cosson, 1849. Using real-time quantitative PCR we estimated the abundance of the found repeats: P720 and P427 had the highest abundance and P132, P332 and P170 had lower quantity in *Th. ponticum* genome. Using fluorescence *in situ* hybridization (FISH) we localized five repeats to different regions of the chromosomes of *Th. ponticum.* Using reprobing multicolor FISH we colocalized the probes between each other. The distribution of these found repeats in the Triticeae genomes and its usability as cytogenetic markers for chromosomes of *Th. ponticum* are discussed.

Keywords

Thinopyrum ponticum, cytogenetic markers, repetitive DNA, fluorescence *in situ* hybridization, quantitative PCR, copy number

Introduction

Thinopyrum ponticum (Podpěra, 1902) Z.-W. Liu & R.-C.Wang, 1993 (=*Agropyron elongatum* Host ex P. Beauvois, 1812, 2n =10×=70) is an allodecaploid perennial grass used as a valuable pasture crop because of its heavy fibrous root system and good regrowth (Li and Wang 2009). *Th. ponticum* has high resistance to fungal and bacterial diseases, high productivity, and it is used as a donor of valuable genes because of its high cross-breeding with wheat. Such useful features as resistance to leaf and stem rust (Sepsi et al. 2008, Mago et al. 2018, Pei et al. 2018), *Fusarium* Link, 1809 head blight (Forte et al. 2014), dominant dwarfing gene (Chen et al. 2012), resistance to pre-harvest sprouting (Kocheshkova et al. 2017), yellow pigment in the endosperm (Pozniak et al. 2006), blue aleurone layer (Liu et al. 2018a), as well as perennial growth (Tsitsin 1978, Gazza et al. 2016) were transferred from *Th. ponticum* to the genome of bread wheat at the level of introgressions, additional and substituted lines, as well as partial amphidiploids by wide hybridization. Quick and accurate identification of the chromatin of *Th. ponticum* will make the use of elite genes in wheat breeding more efficient. Today, cytological methods and molecular markers are widely used to identify and monitor alien chromosomes or chromosome segments during crossing and selection.

The polyploid nature of *Th. ponticum* is still debatable, and the question about the possible origin of its subgenomes remains open to discussion. Chen et al. (1998) proposed the genomic formula JJJJsJs, and later Li and Zhang (2002) proposed the EeEbExStSt variant. The use of labeled DNA sequences as cytogenetic markers in the fluorescence *in situ* hybridization makes it possible to identify individual chromosomes and thus to establish phylogenetic relationships between genomes, understand the origin of subgenomes in allopolyploids, as well as to identify alien chromosomes in wide hybrids (Sepsi et al. 2008, He et al. 2017, Pei et al. 2018). Cytogenetic probes such as 5S rDNA (pTa794), 45S rDNA (pTa71), pAs1 (Afa family) and pSc119.2 that have become classical for bread wheat are used to identify the chromosomes of *Th. ponticum*. They are of used in the studies of the polyploid nature of *Th. ponticum* and the comparative characteristics of its subgenomes with subgenomes of closely related species (Li and Wang 2002, Brasileiro-Vidal et al. 2003). However, the available classical probes are not enough for the effective identification of chromosomes of *Th. ponticum* and it is necessary to develop new cytogenetic markers.

Repetitive DNA is the most promising for the development of chromosomal markers (Salina and Adonina 2018). Thus, new species- and chromosome-specific molecular-cytogenetic markers of *Th. ponticum* having both dispersed and tandem localization were developed (Yao et al. 2016, Liu et al. 2018a, Liu et al. 2018b). Simultaneous localization of multiple tandem repeats gives a pattern unique for each chromosome of *Th. ponticum*, different from wheat. This makes it possible to use repeats both newly identified wheatgrass-specific and common for wheatgrass and wheat in the cytogenetic characteristics of interspecific hybrids, as well as for fundamental evolutionary-phylogenetic studies (Mo et al. 2017, Komuro et al. 2013, Zhu et al. 2017; Lang et al. 2019). The development of genome-wide sequencing technologies made it possible to develop cytogenetic markers based on bioinformatic analysis of DNA sequences.

We have developed an algorithm to develop cytogenetic markers based on satellite DNA and identified five of the most copy satellite repeats in *Aegilops tauschii* Cosson, 1849 genome, which were successfully applied to A, B and D subgenomes of wheat and R of rye (Kroupin et al. 2019). In our study, this algorithm was used to study these five repeats in the genome of *Th. ponticum*. Their copy number was estimated using qPCR and FISH localization was carried out on the chromosomes of *Th. ponticum* of each of the five repeats.

Material and methods

Plant material

Plants of *Th. ponticum* (accession PI636523, Germplasm Research International Network, USA) were grown under optimum temperature and soil water conditions in a greenhouse.

Real-time quantitative PCR

Genomic DNA was extracted from plants according to the protocol in Bernatzky and Tanksley (1986). Real-time quantitative PCR (qPCR) was performed as in Yaakov et al. (2013) using LightCycler instrument (Roche Molecular Systems Inc., Pleasanton, CA, USA). The primers for each monomer were designed using Primer 3.0 v 4.1.0 (http://primer3.ut.ee) based on our previously published sequences (Kroupin et al. 2019). Each reaction was performed in a 15 µl volume consisting of 2.5 µl of reaction mix containing Eva Green (Syntol LTD, Moscow, Russia), serially diluted DNA template of *Th. ponticum* (10, 2, 0.4, and 0.08 ng), and 1.0 µl each of forward and reverse primer (10 pM/µl, Table 1). A single-copy VRN1 gene was used as a reference gene as described in Yaakov et al. (2013). The relative copy number of each repeat was calculated as described in Kroupin et al. (2019).

Fluorescence *in situ* hybridization (FISH)

A chromosome spread preparation was made according to Kroupin et al. (2011) using root tips collected from living plants. FISH was carried out following the procedure in Divashuk et al. (2016). For P720, P170, and P427 probes, the amplicons produced by PCR with the primers (Table 1) were labelled using biotin (for P720) and digoxigenin (for P170 and P427) PCR labeling mix (Roche Molecular Biochemicals). For P332 and P132, the oligonucleotide probes were synthesized with 5' end-labelled biotin (BIO) and 6-carboxyfluorescein (6-FAM), respectively (Syntol, Ltd., Moscow) (Table1).

The detection was performed using FITC conjugated to antidigoxigenin for P170 and P427 and Cy3 conjugated to streptavidin (Roche) for P720 and P332; the chromosomes were counterstained with DAPI. Signals in all variants were visualized using

Table 1. Designed primers for tandem repeats and oligonucleotide sequence used as probes (for P332 and P132).

Repeat	Primers / oligonucleotide probe
P720	F: 5'-AGCCACGTCATCAACTTTCA-3'
	R: 5'-TGTCCAGTTTGTACGCGAAG-3'
P170	F: 5'-TCCTTGGAAGAATCTAGTCGTCA-3'
	R: 5'-TCGGTTTTGCGCAGTGTTAA-3'
P427	F:5'-CGCCTCGACTCGCGTTACCC-3'
	R:5'-GCCGAGACGAGCACGTGACA-3'
P332	F: 5'-GCTCTTCACTCGGTAGGATTT-3'
	R: 5'-TCCCGTACTCGCCTAAGT-3'
	BIO-5'-CGAGTGAGAGGATTGCTCTTCACTCGGTAGATTTTT-3'
P132	F:5'-TTTTACACTAGAGTTGAACTTGCTC-3'
	R:5'-TGTAAAATTATTTGAACTAGGCTAT-3'
	6-FAM-5'-TTTTACACTAGAGTTGAACTTGCTCTATAGGCTAGTAC-3'

an AxioZeiss Imager V1 (Carl-Zeiss, Oberkochen, Germany) fluorescence microscope with Cy3 or FITC filter. The results were recorded with an AxioCam MRm Zeiss camera (Carl-Zeiss, Oberkochen, Germany) and contrasted using AxioVision. Reprobing of the slides was performed according to Shibata and Hizume (2015) with modifications. At least four slides were prepared for each probe and at least ten chromosome spreads per slide were examined for reproducibility of the probe signals.

Results

In order to develop cytogenetic markers for *Th. ponticum*, we chose five of the largest copy number repeats identified in the genome-wide sequence of *A. tauschii*: P720, P170, P427, P332, P132 (Kroupin et al. 2019). In order to determine the relative quantity of these repeats in the genome of *Th. ponticum*, we carried out the real-time quantitative polymerase chain reaction using primers. It was shown that repeats P720 and P427 had the largest copy number, P132 and P332 showed the average copy number, and the smallest copy number was found in P170 (Figure 1).

As a result of the FISH procedure, five studied repeats were localized to the chromosomes of *Th. ponticum* (Figure 2).

P720 was localized to all chromosomes and the signal was of varying intensity (Figure 2a, Suppl. material 1: Figure S1). The signal was localized to terminal (telomeric and subtelomeric) regions of all chromosomes at one or both arms. Additionally, five chromosomes demonstrated the pericentromeric localization of the P720 signal (indicated by asterisks in Figure 2a and Suppl. material 1: Figure S1a).

P427 produced strong reproducible signals at 16 chromosomes that were localized partially to the pericentromeric regions and partially to the terminal regions (indicated by asterisks in Figure 2b and Suppl. material 1: Figure S2), including one chromo-

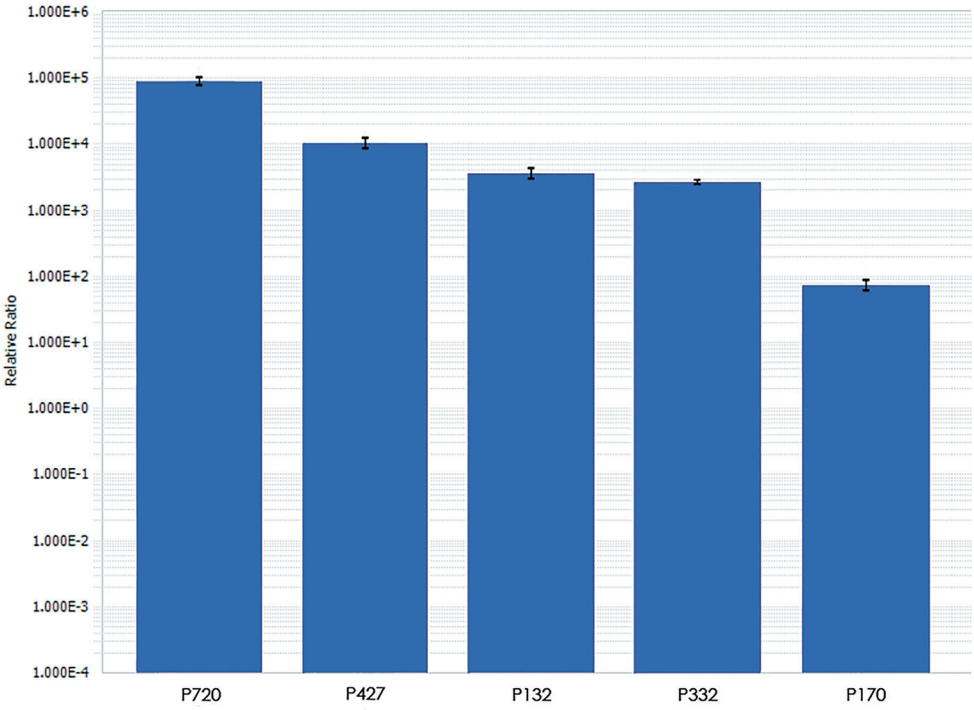

Figure 1. The decimal logarithm of the quantity of tandem repeats relative to the reference gene (VRN1) in *Th. ponticum* as revealed using qPCR. Error bar=standard deviation.

some with the pericentromeric and an interstitial signal at the long arm and the other chromosome with the pericentromeric and interstitial signals at both arms (chromosome a and chromosome b, respectively, Figure 2b and Suppl. material 1: Figure S2). Additionally, we detected minor faint signals at up to 24 chromosomes; however, their number varied between chromosome spreads and slides.

P132 was localized to two chromosomes in the pericentromeric region (Figure 2c, Suppl. material 1: Figure S3). P332 showed pericentromeric localization at two chromosomes (Figure 2d, Suppl. material 1: Figure S4). P170 provided a clear signal on four chromosomes: at two chromosomes in the pericentromeric region and at two chromosomes in the interstitial region of the short arm (Figure 2e, Suppl. material 1: Figure S5). To find out whether the studied repeats are colocalized to the same chromosomes of *Th. ponticum* we performed reprobing multicolor FISH at the same chromosome spreads (Figure 3, for the individual probe localization at this chromosome spread see Suppl. material 1: Figures S1–S5).

As a result of reprobing, we revealed the following groups of chromosomes: 9 chromosomes with both subtelomeric P427 and P720 signals at the same arm (Figure 3a, indicated by asterisks); 4 chromosomes with the subtelomeric P720 signal and pericentromeric P427 signals (Figure 3a, indicated by arrowheads); one chromosome with subtelomeric P720 signals at both arms and the pericentromeric and interstitial P427

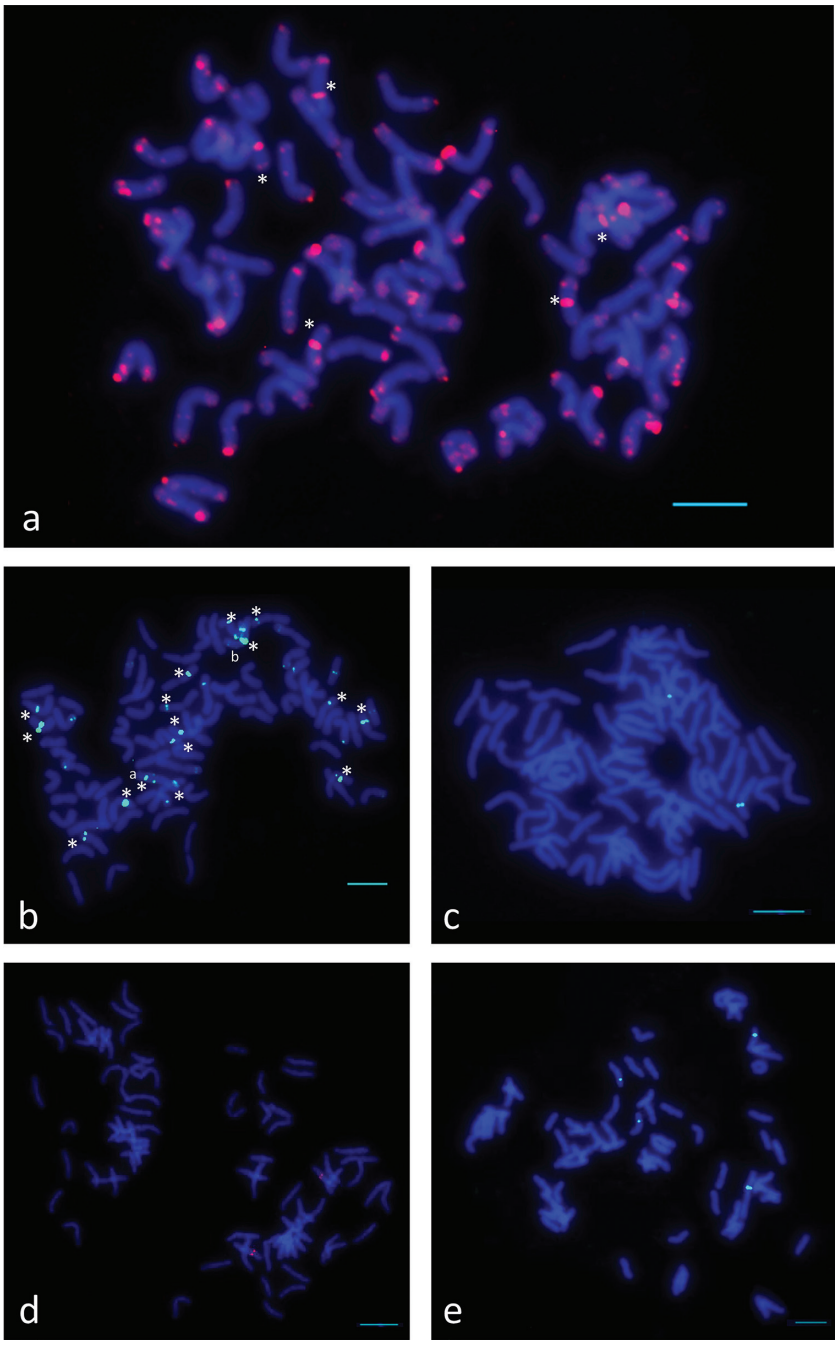

Figure 2. Fluorescence *in situ* hybridization in *Th. ponticum* using the following probes **a** P720 (red, asterisks show chromosomes with pericentromeric localization of P720) **b** P427 (green, asterisks show chromosomes with strong signal of P427, a and b show chromosomes with interstitial localization of P427) **c** P132 (green) **d** P332 (red) **e** P170 (green). P720, P427, and P132 are PCR products labeled with biotin (P720) and digoxigenin (P427 and P132), P332 and P170 are oligonucleotide probes labeled with biotin (P332) and 6-carboxyfluorescein (P170). Scale bar: 10μm.

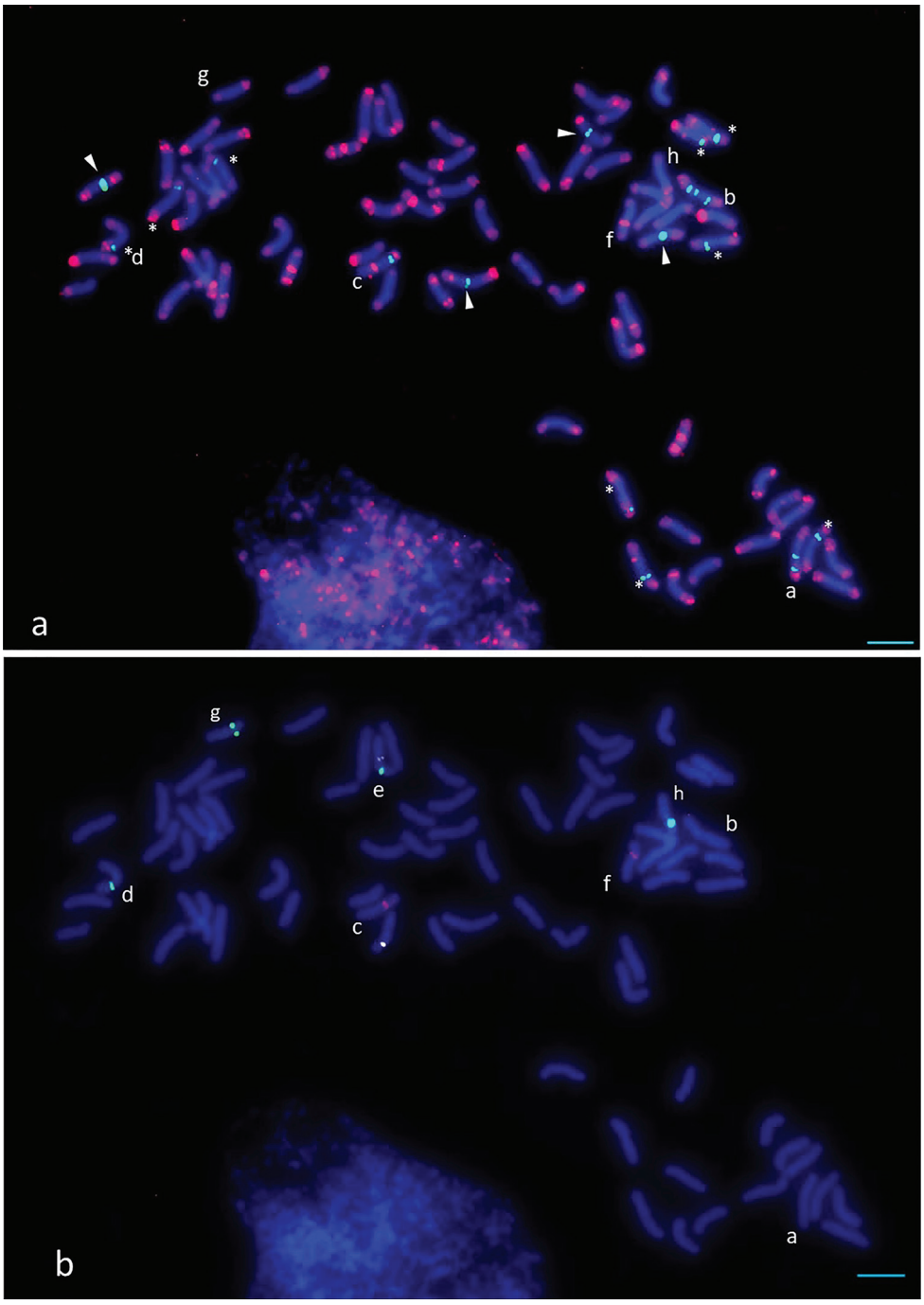

Figure 3. Fluorescence *in situ* hybridization in *Th. ponticum* using the reprobing multicolor FISH technique **a** P720 (red), P427 (green) **b** P332 (red), P132 (white, pseudocolor), P170 (green). P720, P427, and P132 are PCR products labeled with biotin (P720) and digoxigenin (P427 and P132), P332 and P170 are oligonucleotide probes labeled with biotin (P332) and 6-carboxyfluorescein (P170). The designation of the asterisks, arrowheads and letters (a-f) is given in the text. Scale bar: 10μm.

signals at the short arm (Figure 3a, chromosome a); one chromosome with the subtelomeric P720 signals at both arms and the centromeric and interstitial P427 signals at both arms (Figure 3a, chromosome b); one chromosome with the pericentromeric and subtelomeric P720 signals at the long arm and the subtelomeric P427 signal (Figure 3a, chromosome c). P332 was localized to the chromosome with the pericentric and subtelomeric P720 and subtelomeric P427 signals (Figure 3, chromosome c), P170 was localized to the chromosome with the subtelomeric P720 and P427 signals (Figure 3, chromosome d), P132 and P170 were colocalized at the different arms of one and the same chromosome (Figure 3, chromosome e), P332 was localized to the chromosome with the pericentric and subtelomeric signals of P720 (Figure 3, chromosome f); two chromosomes carried both P170 and subtelomeric P720 signals (Figure 3, chromosomes g and h).

Discussion

The development of molecular cytogenetic markers is a long and routine process. Previously, we developed an algorithm allowing to select the most likely candidates for the role of chromosomal markers based on the genome-wide sequence using qPCR (Kroupin et al. 2019). In our study, we demonstrated the effectiveness of our approach for the development of new cytogenetic markers for *Th. ponticum* based on the five repeats of *A. tauschii* of the largest copy number.

According to the results of qPCR, P720 and P427 had the highest abundance in the genome of *Th. ponticum*, which we localized to all or most of the chromosomes as a result of FISH. P720 showed a comparable copy number in bread and durum wheat and rye, which may indicate its prevalence among Triticeae (Kroupin et al. 2019). Repeats with lower copy numbers P170, P332 and P132 were localized only to a few chromosomes of *Th. ponticum*.

P720 and P427 were localized both to the terminal and pericentromeric regions of all or most of the chromosomes of *Th. ponticum*, which may indicate the conservative nature of these repeats. We also localized P720 to both the pericentromeric and terminal regions on the chromosomes of A, B and D subgenomes of wheat and R of rye (Kroupin et al. 2019). Detection of subtelomeric sequences in centromeric and pericentromeric regions is found in plants, including such grass as rice (Lee et al. 2005, Bao et al. 2006), maize (Alfenito and Birchler 1993, Jin et al. 2005) and *Agropyron cristatum* (Linnaeus, 1753) Gaertner, 1770 (Said et al. 2018). This phenomenon may be related to chromosome fusion or other ancient chromosome rearrangements (Garrido-Ramos 2015, Murat et al. 2010). At the same time, P720 and P427 showed interstitial localization on some chromosomes. The availability of subtelomeric repeating sequences in the middle of the arm is not uncommon for grasses and may be associated with heterochromatinization of interstitial regions (Komuro et al. 2013, Badaeva et al. 2016, Garrido-Ramos 2015).

P720 produced a brighter signal on the D subgenome chromosomes on the chromosomes of bread wheat (Kroupin et al. 2019). The different signal intensity of P720

and P427 in the terminal regions might also be related to the polyploid nature of *Th. ponticum* and may be important for chromosome differentiation during meiosis because telomeres play a significant role in the formation of bivalents (Garrido-Ramos 2015, Loginova and Silkova 2018). The localization of the P720 and P427 signals in both the pericentromeric and terminal sites may also be explained by the fixation of an occasional chromosomal rearrangement, since it provided differentiation of these chromosomes during meiosis. The signals of varying intensity of tandemly organized repetitive DNA were described in other closely related species, for example, in *Thinopyrum intermedium* (Host, 1805) Barkworth & D.R. Dewey, 1985 in centromere (Divashuk et al. 2016) and chromosomes of *A. cristatum* in terminal regions (Han et al. 2016).

In our work, we have shown that P170 is localized to four chromosomes of *Th. ponticum*, while the repeat itself is mostly characteristic for D subgenome of bread wheat and is absent on chromosomes of A, B and R subgenomes (Kroupin et al. 2019). Such a common hybridization may be related to the proximity of these chromosomes to the D subgenome of bread wheat. Most of the chromatin introgressions with valuable genes of *Th. ponticum* occur in the chromosome of the D subgenome of *Triticum aestivum* Linnaeus, 1753, which may be related to its proximity to the genome of *Th. ponticum* (Chen et al. 2012). Since the PCR product obtained using primers developed for the repeat monomer and genomic DNA of the studied species was used for the FISH procedure, differences in the localization and intensity of the repeat signal on the chromosomes of *Th. ponticum* in the present study and bread wheat and hexaploid triticale in Kroupin et al. (2019) may be associated with different copy numbers of the repeats on chromosomes of different species (quantitative differences), as well as with differences in the sequence of monomers (qualitative differences).

P332, P170, and P132 were hybridized on several (from two to four) chromosomes of *Th. ponticum*. P170 was hybridized specifically on chromosomes of the D subgenome, and P332 was not identified in the R subgenome of rye (Kroupin et al. 2019). Such species specificity and hybridization on a small number of chromosomes of *Th. ponticum* allows us to consider these repeats as good candidates for chromosome-specific markers. FISH reprobing procedure enabled us to distinguish individual chromosomes on the basis of the combination of the developed probes. Chromosomes a-h (Figure 3) can be univocally identified in the studied accession of *Th. ponticum* using our cytogenetic markers and the probes can be applied for the comparison of different *Th. ponticum* chromosomes among accessions of *Th. ponticum* for population studies and may be useful in studies of wide hybrids of wheat in combination with the classical FISH probes of wheat.

We colocalized the developed probes using reprobing FISH and revealed that the chromosome set of *Th. ponticum* is imbalanced: chromosomes a-f (Figure 3) have no pairs and the pattern of the signal localization is unique for each of these chromosomes. P720 was localized to the pericentromeric region at five chromosomes while P427 produced an interstitial signal at the short arm of one chromosome and at both arms of the other chromosome. This may be a peculiarity of a given accession of *Th. ponticum* and may be a result of chromosomal rearrangements at meiosis because of homeological pairing between the chromosomes. Alternatively, such uneven distribu-

tion of the signals may be the result of ancient chromosomal rearrangements that have been fixed by the natural selection. The imbalanced chromosome constitution may not be an obstacle for propagation of a given *Th. ponticum* plant since it can be propagated both by sexual and vegetative means and a given chromosome combination may be advantageous in a particular environment.

In conclusion, using our algorithm, we selected five repeats, two highly abundant repeats with localization on all or most of the chromosomes, and three repeats with a lower copy number with localization on several individual chromosomes. The repeats we selected can be used as a tool for the comparative cytogenetics of Triticeae to study phylogenetics and evolutionary relationships between species.

Acknowledgements

The work is supported by Russian Science Foundation grant № 18-76-00035.

References

Alfenito MR, Birchler JA (1993) Molecular characterization of a maize B-chromosome centric sequence. Genetics 135(2): 589–597. https://doi.org/10.1093/oxfordjournals.jhered.a111297

Badaeva E, Ruban A, Zoshchuk S, Surzhikov S, Knüpffer H, Kilian B (2016) Molecular cytogenetic characterization of *Triticum timopheevii* chromosomes provides new insight on genome evolution of *T. zhukovskyi*. Plant Systematics and Evolution 302(8): 943–956. https://doi.org/10.1007/s00606-016-1309-3

Bao W, Zhang W, Yang Q, Zhang Y, Han B, Gu M, Xue Y, Cheng Z (2006) Diversity of centromeric repeats in two closely related wild rice species, *Oryza officinalis* and *Oryza rhizomatis*. Molecular Genetics and Genomics 275(5): 421–430. https://doi.org/10.1007/s00438-006-0103-2

Bernatzky R, Tanksley S (1986) Toward a saturated linkage map in tomato based on isozyme and random cDNA sequences. Genetics 112(4): 887–898.

Brasileiro-Vidal A, Cuadrado A, Brammer S, Zanatta A, Prestes A, Moraes-Fernandes M, Guerra M (2003) Chromosome characterization in *Thinopyrum ponticum* (Triticeae, Poaceae) using *in situ* hybridization with different DNA sequences. Genetics and Molecular Biology 26(4): 505–510. https://doi.org/10.1590/S1415-47572003000400014

Chen G, Zheng Q, Bao Y, Liu S, Wang H, Li X (2012) Molecular cytogenetic identification of a novel dwarf wheat line with introgressed *Thinopyrum ponticum* chromatin. Journal of Biosciences 37(1): 149–155. https://doi.org/10.1007/s12038-011-9175-1

Chen Q, Conner RL, Laroche A, Thomas JB (1998) Genome analysis of *Thinopyrum intermedium* and *Thinopyrum ponticum* using genomic *in situ* hybridization. Genome 41(4): 580–586. https://doi.org/10.1139/gen-41-4-580

Divashuk M, Khuat T, Kroupin P, Kirov I, Romanov D, Kiseleva A, Khrustaleva L, Alexeev D, Zelenin A, Klimushina M, Razumova O, Karlov G (2016) Variation in copy number of

Ty3/Gypsy centromeric retrotransposons in the genomes of *Thinopyrum intermedium* and its diploid progenitors. PLOS ONE 11(4): e0154241. https://doi.org/10.1371/journal.pone.0154241

Forte P, Virili M, Kuzmanović L, Moscetti I, Gennaro A, D'Ovidio R, Ceoloni C (2014) A novel assembly of *Thinopyrum ponticum* genes into the durum wheat genome: pyramiding *Fusarium* head blight resistance onto recombinant lines previously engineered for other beneficial traits from the same alien species. Molecular Breeding 34(4): 1701–1716. https://doi.org/10.1007/s11032-014-0175-3

Garrido-Ramos M (2015) Satellite DNA in plants: More than just rubbish. Cytogenetic and Genome Research 146(2): 153–170. https://doi.org/10.1159/000437008

Gazza L, Galassi E, Ciccoritti R, Cacciatori P, Pogna N (2016) Qualitative traits of perennial wheat lines derived from different *Thinopyrum* species. Genetic Resources and Crop Evolution 63(2): 209–219. https://doi.org/10.1007/s10722-015-0240-8

Han H, Liu W, Lu Y, Zhang J, Yang X, Li X, Hu Z, Li L (2016) Isolation and application of P genome-specific DNA sequences of *Agropyron* Gaertn. in Triticeae. Planta 245(2): 425–437. https://doi.org/10.1007/s00425-016-2616-1

He F, Xing P, Bao Y, Ren M, Liu S, Wang Y, Li X, Wang H (2017) Chromosome pairing in hybrid progeny between *Triticum aestivum* and *Elytrigia elongata*. Frontiers in Plant Science 8. https://doi.org/10.3389/fpls.2017.02161

Jin WW, Lamb JC, Vega JM, Dawe RK, Birchler JA, Jiang J (2005).Molecular and functional dissection of the maize B chromosome centromere. Plant Cell 17(5): 1412–1423. https://doi.org/10.1105/tpc.104.030643

Kocheshkova A, Kroupin P, Bazhenov M, Karlov G, Pochtovyy A, Upelniek V, Belov V, Divashuk M (2017) Pre-harvest sprouting resistance and haplotype variation of *ThVp*-1 gene in the collection of wheat-wheatgrass hybrids. PLOS ONE 12(11): e0188049. https://doi.org/10.1371/journal.pone.0188049

Komuro S, Endo R, Shikata K, Kato A (2013) Genomic and chromosomal distribution patterns of various repeated DNA sequences in wheat revealed by a fluorescence *in situ* hybridization procedure. Genome 56(3): 131–137. https://doi.org/10.1139/gen-2013-0003

Kroupin P, Divashuk M, Belov V, Glukhova L, Aleksandrov O, Karlov G (2011) Comparative molecular cytogenetic characterization of partial wheat-wheatgrass hybrids. Russian Journal of Genetics 47(4): 432–437. https://doi.org/10.1134/s1022795411040077

Kroupin P, Kuznetsova V, Romanov D, Kocheshkova A, Karlov G, Dang T, Khuat T, Kirov I, Alexandrov O, Polkhovskiy A, Razumova O, Divashuk M (2019) Pipeline for the rapid development of cytogenetic markers using genomic data of related species. Genes 10(2): 113. https://doi.org/10.3390/genes10020113

Lang T, Li G, Yu Z, Ma J, Chen Q, Yang E, Yang Z (2019) Genome-wide distribution of novel Ta-3A1 mini-satellite repeats and its use for chromosome identification in wheat and related species. Agronomy 9(2): 60. https://doi.org/10.3390/agronomy9020060

Lee H, Zhang W, Langdon T, Jin W, Yan H, Cheng Z, Jiang J (2005) From the cover: Chromatin immunoprecipitation cloning reveals rapid evolutionary patterns of centromeric DNA in *Oryza* species. Proceedings of the National Academy of Sciences 102(33): 11793–11798. https://doi.org/10.1073/pnas.0503863102

Li D, Zhang X (2002) Physical localization of the 18S-5·8S-26S rDNA and sequence analysis of ITS regions in *Thinopyrum ponticum* (Poaceae: Triticeae): Implications for concerted evolution. Annals of Botany 90(4): 445–452. https://doi.org/10.1093/aob/mcf213

Li H, Wang X (2009) *Thinopyrum ponticum* and *T. intermedium*: the promising source of resistance to fungal and viral diseases of wheat. Journal of Genetics and Genomics 36(9): 557–565. https://doi.org/10.1016/S1673-8527(08)60147-2

Liu L, Luo Q, Li H, Li B, Li Zheng Q (2018a) Physical mapping of the blue-grained gene from *Thinopyrum ponticum* chromosome 4Ag and development of blue-grain-related molecular markers and a FISH probe based on SLAF-seq technology. Theoretical and Applied Genetics 131(11): 2359–2370. https://doi.org/10.1007/s00122-018-3158-7

Liu L, Luo Q, Teng W, Li B, Li H, Li Y, Li Z, Zheng Q (2018b) Development of *Thinopyrum ponticum*-specific molecular markers and FISH probes based on SLAF-seq technology. Planta 247(5): 1099–1108. https://doi.org/10.1007/s00425-018-2845-6

Loginova D, Silkova O (2018) The genome of bread wheat *Triticum aestivum* L.: unique structural and functional properties. Russian Journal of Genetics 54(4): 403–414. https://doi.org/10.1134/s1022795418040105

Mago R, Zhang P, Xia X, Zhang J, Hoxha S, Lagudah E, Graner A, Dundas I (2018) Transfer of stem rust resistance gene SrB from *Thinopyrum ponticum* into wheat and development of a closely linked PCR-based marker. Theoretical and Applied Genetics 132(2): 371–382. https://doi.org/10.1007/s00122-018-3224-1

Mo Q, Wang C, Chen C, Wang Y, Zhang H, Liu X, Ji W (2017) Molecular cytogenetic identification of a wheat-*Thinopyrum ponticum* substitution line with stripe rust resistance. Cereal Research Communications 45(4): 564–573. https://doi.org/10.1556/0806.45.2017.037

Murat F, Xu J, Tannier E, Abrouk M, Guilhot N, Pont C, Messing J, Salse J (2010) Ancestral grass karyotype reconstruction unravels new mechanisms of genome shuffling as a source of plant evolution. Genome Research 20(11): 1545–1557. https://doi.org/10.1101/gr.109744.110

Pei Y, Cui Y, Zhang Y, Wang H, Bao Y, Li X (2018) Molecular cytogenetic identification of three rust-resistant wheat-*Thinopyrum ponticum* partial amphiploids. Molecular Cytogenetics 11(1): 27. https://doi.org/10.1186/s13039-018-0378-0

Pozniak C, Knox R, Clarke F, Clarke J (2006) Identification of QTL and association of a phytoene synthase gene with endosperm colour in durum wheat. Theoretical and Applied Genetics 114(3): 525–537. https://doi.org/10.1007/s00122-006-0453-5

Said M, Hřibová E, Danilova T, Karafiátová M, Čížková J, Friebe B, Doležel J, Gill B, Vrána J (2018) The *Agropyron cristatum* karyotype, chromosome structure and cross-genome homoeology as revealed by fluorescence *in situ* hybridization with tandem repeats and wheat single-gene probes. Theoretical and Applied Genetics 131(10): 2213–2227. https://doi.org/10.1007/s00122-018-3148-9

Salina EA, Adonina IG (2018) Cytogenetics in the study of chromosomal rearrangement during wheat evolution and breeding. In: Larramendy ML (Ed.) Cytogenetics. London. https://www.intechopen.com/online-first/cytogenetics-in-the-study-of-chromosomal-rearrangement-during-wheat-evolution-and-breeding/

Sepsi A, Molnár I, Szalay D, Molnár-Láng M (2008) Characterization of a leaf rust-resistant wheat–*Thinopyrum ponticum* partial amphiploid BE-1, using sequential multicolor GISH and FISH. Theoretical and Applied Genetics 116(6): 825–834. https://doi.org/10.1007/s00122-008-0716-4

Shibata F, Hizume M (2015) Multi-color fluorescence *in situ* hybridization. Cytologia 80(4): 385–392. https://doi.org/10.1508/cytologia.80.385

Tsitsin NV (1978) Perennial Wheat. Nauka, Moscow, 287 pp.

Yaakov B, Meyer K, Ben-David S, Kashkush K (2013) Copy number variation of transposable elements in *Triticum–Aegilops* genus suggests evolutionary and revolutionary dynamics following allopolyploidization. Plant Cell Reports 32(10): 1615–1624. https://doi.org/10.1007/s00299-013-1472-8

Yao H, Tang CG, Zhao J, Zheng Q, Li B, Hao CY, Li ZS, Zhang XY (2016) Isolation of *Thinopyrum ponticum* genome specific repetitive sequences and their application for effective detection of alien segments in wheat. Scientia Agricultura Sinica 49(19):3683–3693. https://doi.org/10.3864/j.issn.0578-1752.2016.19.002

Zhu C, Wang Y, Chen C, Wang C, Zhang A, Peng N, Wang Y, Zhang H, Liu X, Ji W (2017) Molecular cytogenetic identification of a wheat – *Thinopyrum ponticum* substitution line with stripe rust resistance. Genome 60(1): 860–867. https://doi.org/10.1139/gen-2017-0099

Supplementary material 1

Figures S1–S5

Authors: Pavel Yu. Kroupin, Victoria M. Kuznetsova, Ekaterina A. Nikitina, Yury Ts. Martirosyan, Gennady I. Karlov, Mikhail G. Divashuk

Data type: Adobe Acrobat Document (.pdf)

Explanation note: Supplementary Figure 1. Fluorescence *in situ* hybridization in *Th. ponticum* using P720 as a probe (red, PCR product labeled with biotin). Supplementary Figure 2. Fluorescence *in situ* hybridization in *Th. ponticum* using P427 as a probe (green, PCR product labeled with digoxigenin). Supplementary Figure 3. Fluorescence *in situ* hybridization in *Th. ponticum* using P132 as a probe (white pseudocolor, PCR product labeled with digoxigenin). Supplementary Figure 4. Fluorescence *in situ* hybridization in *Th. ponticum* using P332 as a probe (red, oligonucleotide labeled with biotin).

Link: https://doi.org/10.3897/CompCytogen.v13i3.36112.suppl1

CompCytogen 13(3): 245–263 (2019)
doi: 10.3897/CompCytogen.v13i3.35775
http://compcytogen.pensoft.net

RESEARCH ARTICLE

COMPARATIVE Cytogenetics
A peer-reviewed open-access journal
International Journal of Plant & Animal Cytogenetics, Karyosystematics, and Molecular Systematics

Karyotype structure and NOR activity in Brazilian *Smilax* Linnaeus, 1753 species (Smilacaceae)

Daniel Pizzaia[1], Vanessa M. Oliveira-Maekawa[2], Aline R. Martins[3], Mateus Mondin[1], Margarida L.R. Aguiar-Perecin[1]

1 *Department of Genetics, Luiz de Queiroz College of Agriculture, ESALQ, University of São Paulo, Avenida Pádua Dias, 11, 13418-900 Piracicaba, SP, Brazil* **2** *Department of Plant Biology, The University of Campinas, UNICAMP, Barão Geraldo, 13083-970, Campinas, SP, Brazil* **3** *Department of Biological Sciences, Luiz de Queiroz College of Agriculture, ESALQ, University of São Paulo, Avenida Pádua Dias,11 13418-900, Piracicaba, SP, Brazil*

Corresponding author: *Margarida L. R. Aguiar-Perecin* (mlrapere@usp.br)

Academic editor: *Puneet Kumar* | Received 13 May 2019 | Accepted 5 July 2019 | Published 22 August 2019

http://zoobank.org/E41B30A6-8807-4166-B535-AD8EDF587EB6

Citation: Pizzaia D, Oliveira-Maekawa VM, Martins AR, Mondin M, Aguiar-Perecin MLR (2019) Karyotype structure and NOR activity in Brazilian *Smilax* Linnaeus, 1753 species (Smilacaceae). Comparative Cytogenetics 13(3): 245–263. https://doi.org/10.3897/CompCytogen.v13i3.35775

Abstract

The genus *Smilax* Linnaeus, 1753 (Smilacaceae) is a large genus of dioecious plants distributed in tropical, subtropical and temperate regions. Some *Smilax* species have medicinal importance and their identification is important for the control of raw material used in the manufacture of phytotherapeutical products. The karyotypes of seven Brazilian *Smilax* species were investigated. Mitotic metaphases of roots from young plants were analysed in Feulgen-stained preparations. The karyotypes were asymmetric and modal with 2n = 2x = 32 chromosomes gradually decreasing in size. In *S. goyazana* A De Candolle & C De Candolle, 1878, a polyploid species, 2n = 4x = 64. In all the species, the large and medium-sized chromosomes were subtelocentric and submetacentric and the small chromosomes were submetacentric or metacentric. Their karyotypes were quite similar, with differences in the arm ratio of some chromosomes. *S. fluminensis* Steudel, 1841 differed from the other species by having a large metacentric chromosome 1. These findings suggest that evolution occurred without drastic changes in the chromosomal structure in the species analyzed. Terminal secondary constrictions were visualized on the short arm of some chromosomes, but they were detected only in one homologue of each pair. Due to the terminal location and the degree of chromosome condensation, secondary constrictions were not visualized in some species. The nucleolus organizer regions (NORs) were mapped by silver-staining and fluorescent *in situ* hybridization (FISH) in *S. rufescens* Grisebach, 1842 and *S. fluminensis*. Silver-staining and FISH signals were colocalized on the short arms of

six chromosomes in *S. rufescens* and four chromosomes in *S. fluminensis*. In FISH preparations, one of the largest chromosomes had the secondary constrictions highly decondensed in some cells. This finding and the heteromorphism observed in Feulgen-stained chromosomes suggest that differential rRNA gene expression between homologous rDNA loci can occur in some cells, resulting in different degrees of ribosomal chromatin decondensation. The presence of a heteromorphic chromosome pair in *S. rufescens*, *S. polyantha* Grisebach, 1842 and *S. goyazana* suggests a chromosomal sex determination in these dioecious species.

Keywords
Smilax, karyotype, chromosomal evolution, nucleolus organizer region (NOR), Silver-staining, FISH, 45S rDNA

Introduction

The genus *Smilax* Linnaeus, 1753 (Smilacaceae) is a large genus of dioecious plants distributed in tropical, subtropical and temperate regions. The genus has approximately 300 species, and their classification has been controversial (see Mangaly 1968). This genus had been assigned to the family Liliaceae, but for the past 20 to 30 years, botanists have accepted Smilacaceae as a distinct family belonging to the order Liliales according to APG III (The Angiosperm Phylogeny Group 2009). The genus *Smilax* comprises the largest number of species within the Smilacaceae family, of which 32 species occur in Brazil (Andreata 1995, 2009).

Some *Smilax* species have medicinal importance. Roots have been used as antisyphilitic, anti-inflammatory and antimicrobial remedies or as antioxidant agents (Andreata 1995, de Souza et al. 2004, Cox et al. 2005). The unequivocal characterization of *Smilax* species with potential medicinal applications is highly important, but some problems in the taxonomic identification of some species have been reported. The genus has high variability in morphology, and morphological features were described for species in Brazil (Andreata 2009), North America (Mangaly 1968) and Asia (Koyama 1960, Fu et al. 1995). Leaf morphology has been emphasized as an important feature for species identification by Mangaly (1968) and Andreata (2009). The possible evolution of inflorescences in *Smilax* and *Heterosmilax* Kunth, 1850 was considered (Kong et al. 2007). Reports on the morphoanatomy of vegetative organs (Martins and Appezzato-da-Gloria 2006, Martins et al. 2010, 2012) and molecular phylogeny (Sun et al. 2015) have also contributed to species systematic.

The characterization of karyotypes in higher plants has evolutionary and taxonomic significance. Some studies on *Smilax* cytogenetics have reported chromosome numbers and karyotype characterization. Chromosome numbers of n = 16 were described for most species, but n = 13 and n = 15 were also recorded (Speese 1939, Mangaly 1968, Mehra and Sachdeva 1976, Vijayavalli and Mathew 1989, Fu and Hong 1990, Fu et al. 1993, 1995, Huang et al. 1997, Kong et al., 2007, Pizzaia et al. 2013; Sun et al. 2015). Some polyploids (n= 32, 48 and 64) have been found in Asian species (Vijayavalli and Mathew 1989, Fu and Hong 1990, Fu et al. 1993, 1995, Huang et al. 1997, Kong et al. 2007, Sun et al. 2015). The karyotypes of the species analyzed were asymmetric and modal, with most chromosomes being submetacentric and subtelo-

centric and all of them gradually decreasing in size (Vijayavalli and Mathew 1989, Fu and Hong 1990, Fu et al. 1993, 1995, Kong et al. 2007, Pizzaia et al. 2013). *Smilax* species are dioecious and heteromorphic chromosomes have been detected in some species, and are thought to be sexual chromosomes (Mangaly 1968, Vijayavalli and Mathew 1989, Fu et al.1995, Pizzaia et al. 2013). Secondary constrictions and satellites were detected in few species (Vijayavalli and Mathew 1989, Fu et al. 1995 and Pizzaia et al. 2013).

Pizzaia et al. (2013) described for the first time the nucleolus organizer regions of a *Smilax* species (*S. rufescens*), which were mapped by silver staining (Ag-NOR) and fluorescent *in situ* hybridization (FISH) of 45S rDNA probes. Silver signals colocalized with rDNA sites were observed on the short arms of six chromosomes.

In the present study, we investigated the karyotype characteristics of seven species of Brazilian species of *Smilax* using conventional techniques. We compared the positions of 45S rDNA sites of *S. rufescens* with the sites in *S. fluminensis*. Procedures to germinate wild-collected seeds to obtain plants providing roots for cytogenetic research were also developed. We aimed to analyze aspects of karyotype evolution in these species and to contribute to their taxonomic treatment.

Material and methods

Seeds from wild plants collected from southern, southeastern, northeastern and western central Brazil were used (Table 1). The plants are dioecious, vines or herbaceous vines, or rarely, subshrubs or shrubs such as *S. goyazana* and *S. brasilienesis* Sprengel, 1825 (Andreata 1995). The plants were identified by Dr. R.H.P Andreata (Santa Ursula University, Brazil) and were incorporated into the ESA herbarium (ESALQ, USP).

Experiments to germinate seeds to obtain plants were evaluated as reported by Pizzaia et al. (2013). Briefly, the seeds were germinated in plastic boxes containing *Sphagnum* moss, at 27 °C. The seedlings were transferred to plastic pots containing vegetable soil + vermiculite and maintained under screenhouse conditions with the temperature varying from 20 °C to 32 °C. The sex of the young plants was not known.

Roots excised from young plants were pretreated with 8-hydroxyquinoline combined with cycloheximide, a protein synthesis inhibitor that induces chromosome condensation. Some treatments were evaluated, and in most cases, two treatments were used: combinations of 300 mg/L 8-hydroxyquinoline with 1.25 mg/L or 20 mg/L cycloheximide at 28 °C for 3 h and 2.5 h, respectively. The roots were then fixed in 3:1 ethanol:acetic acid and kept at 4 °C. The roots were Feulgen-stained as previously described (Bertão and Aguiar-Perecin 2002). For karyotype analysis, chromosomes of at least five metaphase spreads were measured. Chromosomes were identified according to their absolute length (μm), relative length (expressed as percentage of the haploid set), arm ratio (large arm/short arm) and chromosome types were designated according to Levan et al. (1964). The ratio of the largest chromosome/smallest chromosome was also described. The classification of the karyotypes according to their asymmetry (Stebbins, 1971) was adopted. The evaluation of the relative chromosome length in

Table 1. Origin of collection, chromosome number, chromosome and haploid set length (μm) and ratio of the largest/smallest chromosomes of the *Smilax* species.

Species	Origin†	2n	Chromosome length		
			Range (μm)	Ratio (largest/smallest)	Haploid set (μm)
S. rufescens Grisebach, 1842	Ilha do Cardoso (SP)	32	5.62–1.84	3.05	54.24
S. fluminensis Steudel, 1841	Uruana (GO)	32	6.41–1.33	4.82	43.47
	Itirapina (SP)	32	6.48–1.31	4.95	43.32
S. polyantha Grisebach, 1842	Botucatu (SP)	32	5.85–1.92	3.05	44.09
	Mogi Guaçu (SP)	32	5.36–1.94	2.80	41.03
S. brasiliensis Sprengel, 1825	Itapagipe (MG)	32	5.04–1.77	2.85	38.02
S. campestris Grisebach, 1842	Caçapava do Sul (RS)	32	6.20–1.95	3.18	43.44
S. cissoides Martius ex Grisebach, 1842	Feira de Santana (BA)	32	5.51–2.00	2.75	40.17
S. goyazana A. de Candolle & C de Candolle, 1878	Brasilia (DF)	64	4.85–1.61	3.01	79.25

†In brackets states of Brazil: SP (São Paulo), GO (Goias), MG (Minas Gerais), BA (Bahia), DF (Distrito Federal, Brasília).

the tetraploid *S. goyazana* was carried out by estimating the percentage of the haploid set/2. The diploid-tetraploid comparisons were therefore based on one genome for the expression of the relative chromosome lengths.

Active NORs were detected in metaphase chromosomes of *S. rufescens* and *S. fluminensis*, by employing the silver-staining technique according to Stack et al. (1991) with minor modifications as previously reported (Pizzaia et al. 2013). Briefly, roots fixed in 3:1 etanol:acetic acid for 24 h were used to make squash preparations. The slides were heated for 2 h at 60 °C, incubated for 8 min in 2X SSC at the same temperature, washed with distilled water (3–5 min) and air-dried. Then, 50 μl 100% silver nitrate solution was added to the preparation, which was then covered with a nylon coverslip and incubated at 60 °C for 10 min on a Petri dish with moist filter paper. Coverslips were removed in tap water, and the slides were washed in distilled water, air-dried and mounted in Entellan (Merck, Germany).

Fluorescent *in situ* hybridization was used to detect 45S rDNA sites as previously described (Mondin et al. 2007). Metaphases of *S. rufescens* and *S. fluminensis* were investigated. Briefly, the probe used was the 9.1-kb maize 45S rDNA repeating unit labelled with biotin 14-dATP by nick translation (Bionick Labelling System, Invitrogen, USA). Biotin was detected with mouse anti-biotin followed by rabbit anti-mouse and swine anti-rabbit antibodies, both conjugated with TRITC (DAKO, Denmark). The probe (5 ng/μl) was added to the hybridization mixture and denatured by heating at 95 °C for 10 min. Hybridization was carried out at 37 °C for 20 h. Post-hybridization steps followed the protocol described by Mondin et al. (2007). The slides were counterstained with 1 μg/ml DAPI in Vectashield (Vector, USA).

All preparations were examined with a Zeiss Axiophot-2-epifluorescence microscope with appropriate filters. The images were acquired by a CCD camera using the IKAROS software to analyze the Feulgen-stained metaphases and the ISIS software for the FISH images (Meta-Systems, Germany). Silver-stained chromosomes were photographed using the Fujicolor Superia 100 film (Fuji Photo Film, Brazil). All images were processed with Adobe Photoshop 6.0.

Results

Karyotype anyses

The experiments to germinate seeds from wild plants were successful for obtaining plants and roots with high index of mitosis. The pretreatments used also provided metaphases suitable for karyotype analysis.

All of the species analyzed had 2n = 2x = 32, except the tetraploid *S. goyazana* with 2n = 4x = 64. The karyotypes were asymmetric and modal with the chromosomes gradually decreasing in size, as shown in Fig. 1. The lengths of the haploid set and of the largest and smallest chromosomes (μm), as well as their ratio, are included in Table 1. The values of relative chromosome length, arm ratio, chromosome type, and Stebbins karyotype classification are given in Table 2. The karyotypes of these species are described for the first time, except for *S. rufescens* (Pizzaia et al. 2013), included here for comparison. The analysis of the karyotypes showed the following characteristics.

S. rufescens Grisebach, 1842

This species with 2n = 2x = 32 showed a karyotype with 7 pairs of st-type, 6 pairs of sm-type and 2 pairs of m-type chromosomes, and the heteromorphic pair 10 with sm- and m-type chromosomes with similar sizes, probably sex chromosomes. The size of the chromosomes varied from 1.84 to 5.62 μm with a largest/smallest ratio of 3.05 and the Stebbins karyotype classifications was 3B. The total haploid length was 54.24 μm. Secondary constrictions were detected on the short arms of chromosomes 7, 11 and 14 in some metaphases. These constrictions were visible only in one homologue of each chromosome pair. (Fig. 1A; Tables 1, 2). As it was unclear if satellites were visible, the detected structures were considered as secondary constrictions (Pizzaia et al. 2013).

S. fluminensis Steudel, 1841

Specimens collected from Uruana (GO) and Itirapina (SP) were analyzed. Both specimens had 2n= 2x = 32. The karyotypes were quite similar with slight differences in the arm ratio of chromosomes 7, 8 and 15. The plants from Uruana showed a karyotype with 4 pairs of st-type, 10 pairs of sm-type and 2 pairs with m-type chromosomes. The size of the chromosomes varied from 1.33 to 6.41 μm with a largest/ smallest ratio of 4.82 and the Stebbins karyotype classification was 3C. The total haploid length was 43.47 μm. Secondary constrictions were not detected (Fig. 1B, Tables 1, 2). The plants from Itirapina (SP) showed a karyotype with 5 pairs of st-type, 7 pairs of sm-type and 4 pairs of m-type chromosomes. The size of the chromosomes varied from 1.31 to 6.48 μm with a largest/ smallest ratio of 4.95 and the Stebbins karyotype classification was 3C. The total haploid length was 43.42 μm. A satellite and secondary constriction were detected on the short arm of chromosome 8 and were visible only in one homologue of the chromosome pair (Fig. 1C, Tables 1, 2).

Table 2. Karyological data of Smilax species including chromosome relative length, arm ratio, karyotype type.

	Chromosomes															
Species																
Relative length (%)	**1**	**2**	**3**	**4**	**5**	**6**	**7**	**8**	**9**	**10**	**11**	**12**	**13**	**14**	**15**	**16**
S. rufescens	10.37	9.64	8.70	8.23	7.55	7.08	6.36	6.03	5.82	5.06/5.06	4.75	4.57	4.35	4.09	3.87	3.41
S. fluminensis (Uruana)	15.08	11.32	9.25	8.84	8.26	6.50	5.87	5.59	5.11	4.81	4.03	4.04	3.95	3.77	3.53	3.33
S. fluminensis (Itirapina)	15.79	10.87	8.67	8.35	8.16	7.00	6.31	5.96	5.43	5.04	4.26	4.24	4.09	4.01	3.77	3.13
S. polyantha (Botucatu)	11.80	10.29	9.68	9.01	8.29	7.88	6.99	6.76	5.94	5.21	5.00	4.75	4.56	4.43	4.05	3.90
S. polyantha (Mogi Guaçu)	10.52	9.71	8.86	8.15	7.90	6.95	6.85	6.07	5.95	5.59	4.91/491	4.37	4.34	3.88	3.06	3.02
S. brasiliensis	11.82	10.50	10.00	9.24	8.74	8.17	7.61	6.94	6.44	5.41	5.19	4.89	4.89	4.80	4.65	4.17
S. campestris	11.06	9.32	8.54	8.18	7.47	7.25	6.70	6.40	5.65	5.32	4.63	4.14	4.14	3.85	3.81	3.47
S. cissoides	10.33	9.39	8.18	7.97	7.70	7.24	6.56	6.11	5.82	5.28	4.69	4.23	4.19	3.57	3.57	3.50
S. goyazana	5.51	5.51	5.00	4.50	4.48	4.38	4.29	4.28	3.79	3.69	3.64	3.59	3.45	3.28	3.18	3.09
	Chromosomes															
	17	**18**	**19**	**20**	**21**	**22**	**23**	**24**	**25**	**26**	**27**	**28**	**29**	**30**	**31**	**32**
S. goyazana (cont)	2.94	2.85	2.85	2.73	2.69	2.17	2.09	2.05	1.97	1.94	1.89/1.89	1.89	1.85	1.77	1.71	1.67

	Chromosomes																	
Arm ratio / Chromosome types	**1**	**2**	**3**	**4**	**5**	**6**	**7**	**8**	**9**	**10**	**11**	**12**	**13**	**14**	**15**	**16**	**Karyotypes**	**Stebbins karyotype classification**
S. rufescens	5.28	4.13	4.46	3.41	3.28	3.00	3.30	2.56	2.82	2.17/1.67	2.15	1.99	1.92	1.84	1.53	1.24	7st+6.5sm+2.5m	3B
	st	st	st	st	st	st	st	sm	sm	sm/m	sm	sm	sm	sm	m	m		
S. fluminensis (Uruana)	1.02	2.02	3.17	2.91	3.03	4.00	2.50	2.70	2.98	2.55	2.31	3.00	1.77	1.49	1.70	1.85	4st+10sm+2m	3C
	m	sm	st	sm	st	st	sm	sm	sm	sm	sm	st	sm	m	sm	sm		
S. fluminensis (Itirapina)	1.07	2.08	3.00	2.68	3.03	3.03	1.60	3.0	2.24	2.49	2.03	3.00	1.84	1.49	1.56	1.78	5st+7sm+4m	3C
	m	sm	st	sm	st	st	m	st	sm	sm	sm	st	sm	m	m	sm		
S. polyantha (Botucatu)	6.10	6.00	5.00	4.00	4.00	3.8	3.10	3.00	2.11	2.43	1.59	3.00	2.50	1.45	1.35	1.24	9st+3sm+4m	3B
	st	st	st	st	st	st	st	st	sm	sm	m	st	sm	m	m	m		
S. polyantha (Mogi Guaçu)	6.00	6.00	4.00	3.50	3.50	3.17	3.17	3.00	3.00	3.00	2.00/3.00	2.04	2.00	1.60	1.50	1.24	10.5st+2.5sm+3m	3B
	st	st	st	st	st	st	st	st	st	st	sm/st	sm	sm	m	m	m		
S. brasiliensis	6.00	5.10	4.00	3.90	3.38	3.17	3.00	2.72	2.54	2.74	3.00	1.89	2.00	1.78	1.47	1.50	8st+6sm+2m	3B
	st	st	st	st	st	st	st	sm	sm	sm	st	sm	sm	sm	m	m		
S. campestris	4.51	4.1	3.23	2.94	3.18	2.27	3.00	2.7	1.99	2.17	1.5	1.50	1.38	1.5	1.62	1.4	5st+5sm+6m	3B
	st	st	st	sm	st	sm	st	sm	sm	sm	m	m	m	m	m	m		
S. cissoides	4.60	4.54	3.00	3.82	2.79	3.44	2.4	3.00	3.00	2.00	2.00	1.70	1.87	2.00	1.49	1.50	7st+7sm+2m	3B
	st	st	st	st	sm	st	sm	st	st	sm	sm	sm	sm	sm	m	m		
S. goyazana	8.00	7.5	5.75	4.35	4.89	5.01	4.16	4.00	3.00	3.17	3.00	2.7	3.44	3.10	3.03	3.00	2t+15.5st+ 8.5sm+6m	3B
	t	t	st	st	st	st	st	st	st	st	st	sm	st	st	st	st		
	Chromosomes																	
	17	**18**	**19**	**20**	**21**	**22**	**23**	**24**	**25**	**26**	**27**	**28**	**29**	**30**	**31**	**32**		
S. goyazana (cont)	3.00	2.96	2.96	2.7	3.00	1.83	1.5	1.78	2.50	2.60	3.00/2.09	1.17	1.18	1.32	1.43	1.40		
	st	sm	sm	sm	st	sm	m	sm	sm	sm	st/sm	m	m	m	m	m		

t: telocentric, st: subtelocentric, sm: submetacentric, m: metacentric

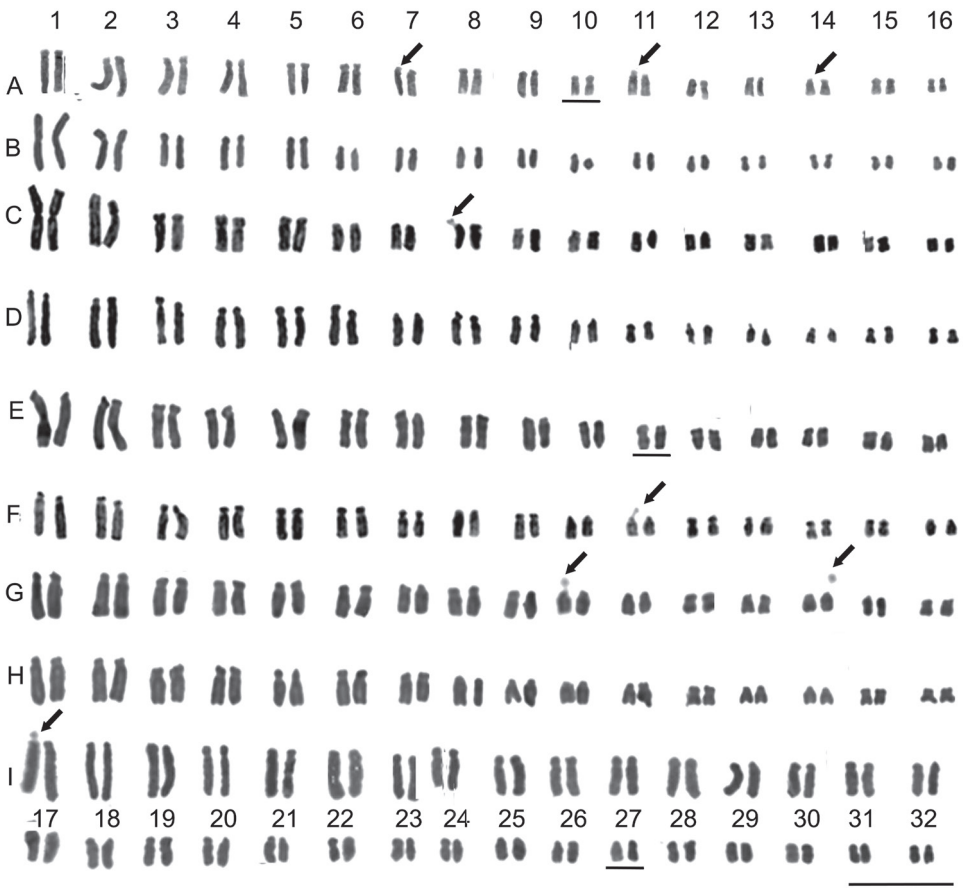

Figure 1. Karyotypes of *Smilax* species: Feulgen-stained metaphase chromosomes. **A** *S. rufescens* **B** *S. fluminensis* (Uruana access) **C** *S. fluminensis* (Itirapina access) **D** *S. polyantha* (Botucatu access) **E** *S. polyantha* (Mogi Guaçu access) **F** *S. brasiliensis* **G** *S. campestris* **H** *S. cissoides* **I** *S. goyazana*. Arrows indicate secondary constrictions and satellites. Note the heteromorphic pair 10 in *S. rufescens*, pair 11 in *S. polyantha* (Mogi Guaçu) and pair 27 in *S. goyazana*. Scale bar: 10 μm.

S. polyantha Grisebach, 1842

Specimens collected from Botucatu (SP) and Mogi Guaçu (SP) were analyzed. Both had 2n = 2x = 32. The karyotypes were quite similar with slight differences in the arm ratio of chromosomes 9, 10, 11 and 12. The plants from Botucatu showed a karyotype with 9 pairs of st-type, 3 pairs of sm-type and 4 pairs of m-type chromosomes. The size of chromosomes varied from 1.92 to 5.85 μm with a largest/smallest ratio of 3.05 and the Stebbins karyotype classification was 3B. The total haploid length was 44.09. Secondary constrictions were not detected (Fig. 1D, Tables 1, 2). The plants from Mogi Guaçu (SP) showed a karyotype with 10 pairs of st-type, 2 pairs of sm-type and 3 pairs of m-type chromosomes and the heteromorphic pair 11 with sm-type and

st-type chromosomes of similar sizes, probably sexual chromosomes. The size of the chromosomes varied from 1.94 to 5.36 μm with a largest/smallest ratio of 2.80 and the Stebbins karyotype classification was 3B. The total haploid length was 41.03 μm. Secondary constrictions were not detected (Fig. 1E, Tables 1, 2).

S. brasiliensis Sprengel, 1825

This species with 2n = 2x = 32 showed a karyotype with 8 pairs of st-type, 6 pairs of sm-type and 2 pairs of m-type chromosomes. The size of chromosomes varied from 1.77 to 5.04 μm with a largest/smallest ratio of 2.85 and the Stebbins karyotype classification was 3B. The total haploid length was 38.02 μm. A satellite and secondary constriction were observed on chromosome 11 and they were visible only in one homologue of the chromosome pair (Fig. 1F, Tables 1, 2).

S. campestris Grisebach, 1842

This species with 2n = 2x = 32 showed a karyotype with 5 pairs of st-type, 5 pairs of sm-type and 6 pairs of m-type chromosomes. The size of chromosomes varied from 1.95 to 6.20 μm with a largest/smallest ratio of 3.18 and the Stebbins karyotype classification was 3B. The total haploid length was 43.44 μm. Satellites and secondary constrictions were detected on the chromosomes 10 and 14, visible only in one homologue of each pair (Fig. 1G, Tables 1, 2).

S. cissoides Martius ex Grisebach, 1842

This species with 2n = 2x = 32 showed a karyotype with 7 pairs of st-type, 7 pairs of sm-type and 2 pairs of m-type chromosomes. The size of chromosomes varied from 2.00 to 5.51 μm with a largest/smallest ratio of 2.75 and the Stebbins karyotype classification was 3B. The total haploid length was 40.17 μm. Satellites were not detected (Fig. 1H, Tables 1, 2).

S. goyazana A de Candolle & C de Candolle, 1878

This polyploid species with 2n = 4x = 64 showed a karyotype with 2 pairs of t-type, 15 pairs with st-type, 8 pairs with sm-type, 6 pairs with m-type chromosomes and the heteromorphic pair 27 with st-type and sm-type chromosomes with similar sizes. The size of chromosomes varied from 1.61 μm to 4.85 with a largest/smallest ratio of 3.01 and the Stebbins karyotype classification was 3B. The total haploid length was 79.25 μm. A satellite and secondary constriction were detected on the largest and t-type chromosome 1, and it was visible only in one of the homologues (Fig. 1I, Tables 1, 2).

NOR-regions visualized by silver staining and FISH

As previously reported (Pizzaia et al. 2013), *in situ* hybridization detected sites of 45S rDNA in six chromosomes of *S. rufescens*. A larger pair of medium-sized chromosomes showed distended secondary constrictions with different lengths between the homologues (Fig. 2A). This pair must correspond to chromosome 7 shown in Fig. 1A. Metaphases with both homologues displaying similar lengths of stretched secondary constrictions were also visualized (not shown). Two pairs of the smallest chromosomes showed minor sites of ribosomal DNA, and they must correspond to pairs 11 and 14, as shown in Fig. 1A. Secondary constrictions were not detected in these small chromosomes in FISH preparations.

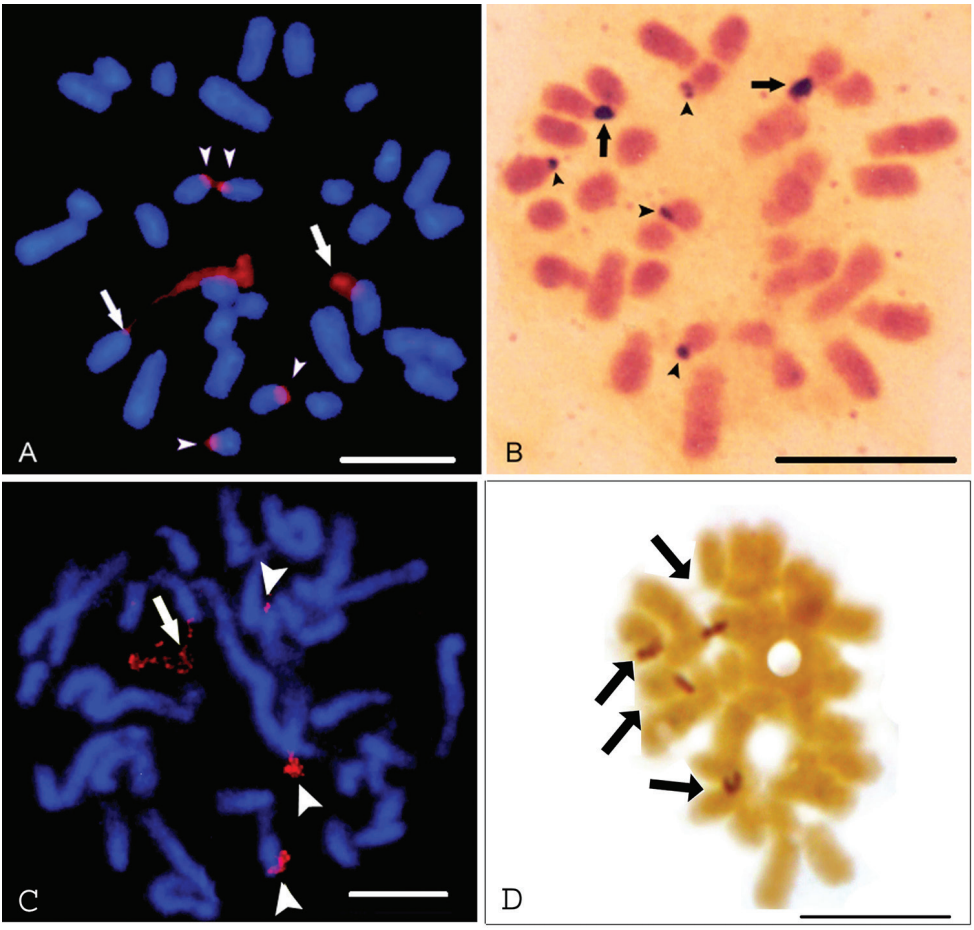

Figure 2. FISH signals of 45S rDNA (red) (**A, C**), silver staining (**B, D**) in *S. rufescens* (**A, B**) and *S. fluminensis* (**C, D**). Arrows in **A** and **C** indicate distended secondary constrictions, and arrowheads show condensed rDNA sites. Arrows in **B** and **D** indicate larger silver signals and arrowheads in B shows small sites. Scale bar: 10 μm.

In the silver-stained metaphases of *S. rufescens*, six chromosomes showed positive signals on the termini of the short arms (Fig. 2B), thereby giving evidence that the six sites of rDNA were active. Two chromosomes had larger signals, and minor silver-stained sites were observed in four chromosomes, as previously shown (Pizzaia et al. 2013).

In *S. fluminensis*, only four chromosomes showed 45S rDNA sites. In Fig 2C, which illustrates a prometaphase, a highly distended secondary constriction is seen in one medium-sized chromosome that must correspond to the satellited chromosome 8 visualized in Fig 1C. The other two chromosomes show secondary constrictions that are less distended. A small signal is observed in a smaller chromosome. One metaphase with two chromosomes showing highly distended secondary constrictions was also observed (not shown).

In the silver-stained metaphases of *S. fluminensis*, four chromosomes showed positive signals on the termini of short arms (Fig 2D). The signals had the same size.

Discussion

Karyotype analyses

All of the diploid species studied here had 2n = 2x = 32, except the polyploid *S. goyazana* with 2n = 4x= 64. Most diploid species from East Asia and India also have 2n = 2x = 32 (Vijayavalli and Mathew 1989, Fu and Hong 1990, Fu et al. 1993, 1995, Huang et al. 1997, Kong et al. 2007, Sun et al. 2015), while a survey of species from North America (USA) found most of the species with 2n = 2x = 26 and one species with 2n = 2x = 30 (Mangaly 1968). The chromosome number in polyploids is variable (2n = 64, 96, 128 (Vijayavalli and Mathew 1989, Fu and Hong 1990, Fu et al. 1993, 1995, Kong et al. 2007), all based on n = 16. In the present study, the tetraploid *S. goyazana* has 2n = 4x =64. In some species, populations with variable numbers of chromosomes were described, such as the *S. china* Linnaeus, 1753 complex, in which diploids (2n = 30, 32) and polyploids (2n = 64, 96) were described (see Sun et al. 2015). The species investigated in our study have n = 16, thereby giving additional evidence that this must be the basic number in the genus *Smilax*. The chromosome number of polyploids is also derived from the basic number x = 16.

The karyotypes of the species analyzed were asymmetric, and the absolute size of the chromosomes was rather similar, gradually decreasing in size, except in *S. fluminensis*, in which the metacentric chromosome 1 was larger than in the other species. This finding was clearly emphasized with the evaluation of the ratio between the largest and smallest chromosomes that varied from 2.75 to 3.18 in most species compared with the values of *S. fluminensis* that were larger (4.82–4.95). The relative chromosome lengths were also quite similar with clear differences concerning the relative lengths of chromosome 1 in most species (10.33 to 11.82) compared with *S. fluminensis* (15.08–15.79). In a general sense, these data were similar to those reported for species from East Asia

(Fu and Hong 1990, Fu et al. 1993, 1995, Kong et al. 2007). From this finding, we can conclude that chromosomal evolution in *Smilax* was not accompanied by large modifications in chromosome and haploid set size, as well as large chromosomal rearrangements in the species with 2n = 32.

The presence of a large metacentric chromosome 1 in the karyotype of *S. fluminensis* is a special feature that is unusual in *Smilax* species. Fu et al. (1995) described the karyotype of *S. mirtillus* A de Candolle & C de Candlolle, 1878 with a second heteromorphic pair showing m- and sm-chromosomes as a special karyotype. Additionally, a heteromorphic subtelocentric pair 1 was found in two *Smilax* species by Fu et al. (1995). A size heteromorphism of the homologues of the satellited pair 7 was detected in male plants of *S. aspera* Linnaeus, 1753 by Vijayavalli and Mathew (1989). These authors assumed an XY (male) and XX (female) type of chromosome sex complex for this species. In our study, in *S. rufescens*, pair 10 was heteromorphic for their centromere positions, and the chromosomes were not NOR-bearing chromosomes. In *S. polyantha* (from Mogi-Guaçu) and *S. goyazana* we also detected heteromorphism related to centromere position in pairs 11 and 27, respectively. As we used young plants, we had no information on their sex, therefore we can speculate only that these heteromorphic pairs are sexual chromosomes. These findings give evidence that differentiated sexual chromosomes must be a characteristic of *Smilax* karyotypes, however more analyses are needed for deeper conclusions.

In general, the species analyzed had asymmetric karyotypes with chromosomes gradually decreasing in size and showing variability in centromere position. The classification of the karyotypes according to Stebbins (1971) showed that all the karyotypes were classified as 3B, except *S. fluminensis* that was 3C. Interestingly, most karyotypes of species 2n=32 from China, analyzed by Fu et al. (1993, 1995), also belong to class 3B, with few of them classified as 3C. In the present investigation, in most species, the largest and medium-sized chromosomes were subtelocentric and submetacentric. The smallest chromosomes were submetacentric and metacentric. For instance, *S. polyantha* (from Mogi Guaçu) had the highest number of subtelocentric chromosomes among the largest ones, and in *S. campestris*, the highest number of submetacentric and metacentric types was detected among the medium-sized and smallest chromosomes. The features observed suggest that during the evolution of these species, slight alterations occurred in the position of the centromeres, probably due to different accumulation of repetitive DNA in chromosome arms, as discussed below. Only *S. fluminensis* with a large metacentric chromosome 1 suffered a different type of chromosome rearrangement.

The genus *Smilax* has been assigned to the family Smilacaceae and to the order Liliales sensu APG III thus, it is a sister family of Liliaceae. Peruzzi et al. (2009) considered that the ancestral basic number for Liliaceae is x=8, based on the frequency of counts 2n=32 in *Smilax* and cytological data suggesting this genus to be paleopolyploid, according to Vijayavalli and Mathew (1989). Peruzzi et al (2009) reported that *Smilax* species have small mean genome size (9.16 pg) compared with some Liliaceae, such as the genera *Streptopus* Michaux, 1803 (3.43 pg), and *Prosartes* D Don, 1830 (5.08 pg), which also have a small mean genome size in contrast with the tribe Lilieae,

in which genera with large genomes were found: *Lilium* Linnaeus, 1753 (56.31 pg) *Fritillaria* Linnaeus, 1753 (44.49 pg), *Cardiocrinum* Lindley, 1846 (36.18 pg) and *Notholirion* Boissier, 1889 (27.82 pg).

Peruzzi et al. (2009) suggested that the ancestral Liliaceae species would have a small genome size and that evolution occurred in the direction of increasing size. In general, it is well known that in plants there is a positive correlation between genome size and the amount of repetitive DNA for both *in tandem* and dispersed repeats. For instance, in maize, the evolution from an ancestral plant occurred with an increase in the content of repetitive DNA. Expressive variation in genome size was observed among maize varieties (Laurie and Bennett 1985). The analysis of the inbred line B73 (reference genome) showed that 85% of the genome was composed of transposable elements, of which 75% belonged to LTR retrotransposon families (Schnable et al. 2009). The arm ratios of the knobless chromosomes 2 and 4 of the inbred line KYS compared with their homologues in the tropical JD lines were significantly different, possibly due to differences in their content of repetitive DNA (Mondin et al. 2014). From this scenario, we could infer that the differences in arm ratios observed among *Smilax* species analyzed in this study are due to different contents of repetitive DNA in their chromosome arms.

Significant differences in karyotype asymmetry are apparent within Liliales, in which two different aspects can be observed, such as variation in chromosome length and variation in centromere position. Variation in chromosome lengths such as the observed in *Smilax*, was observed in some Liliaceae genera with small genome sizes such as *Streptopus* and *Prosartes*, while in some genera, such as *Lilium* and *Fritillaria*, the asymmetry is mainly due to variation in the position of centromeres (two large metacentric chromosomes and subtelocentric and telocentric chromosomes with rather similar lengths (see Peruzzi et al. 2009).

Secondary constrictions were not described for the karyotypes of most *Smilax* species reported in the literature. Vijayavalli and Mathew (1989) detected satellites on the short arm of subtelocentric chromosomes in three species (*S. aspera*, *S. bracteata* Presl, 1827 and *S. zelanica* Linnaeus, 1753) and a secondary constriction on the long arm of chromosome 1 in *S. wightii* A de Candolle & C de Candolle, 1753 but did not detect secondary constrictions in the karyotypes of the cytotypes of the polyploid *S. ovalifolia* Roxburgh, 1832. Fu et al. (1995) reported the presence of secondary constrictions only on the long arm of two subtelocentric pairs (second and third) in *S. corbularia* Kunth, 1850 in a study involving nine species of *Smilax* and three species of *Heterosmilax*. In our study, we detected secondary constrictions on the short arms of subtelocentric chromosomes in *S. rufescens*, *S. fluminensis*, *S. brasiliensis*, *S. campestris* and the polyploid *S. goyazana* in conventionally stained preparations. All of these constrictions were located on medium-sized and small chromosomes, except for *S. goyazana* which has a large chromosome 1 bearing a secondary constriction and satellite. As discussed below, the 45S rDNA is located on the termini of the NOR-chromosome short arms thus, due to the degree of chromosome condensation, secondary constrictions might not be visualized in conventionally stained chromosomes.

NOR regions

In the present study, *in situ* hybridization of 45S rDNA probes showed six sites of ribosomal DNA in *S. rufescens* and four sites in *S. fluminensis*. In addition to differing from *S. rufescens* and the other species analyzed by the presence of a large metacentric chromosome 1, *S. fluminensis* has a different number of ribosomal DNA sites. The number of positive silver-staining signals was correlated with the FISH signals in both species. Terminal secondary constrictions were observed in three chromosome pairs of *S. rufescens*. As it was unclear if satellites were visible, the structures visualized were considered terminal secondary constrictions. In more condensed metaphases, only two chromosomes displayed secondary constrictions (Pizzaia et al. 2013). In the Itirapina access of *S. fluminensis*, only one chromosome exhibited a secondary constriction, and a satellite was observed. In Fig. 1C, the formation of a satellite is more conspicuous. Therefore, in the case of *S. fluminensis*, we find that due to the terminal position of the NOR region and the degree of chromosome condensation, secondary constrictions could not be detected in all chromosomes.

Secondary constrictions have been considered to be the organization pattern of active ribosomal chromatin on metaphase chromosomes. Silver-staining on secondary constriction allows the visualization of ribosomal genes that were transcribed in the previous interphase. It has been shown that silver binds to proteins that are components of the transcription machinery and remain at NOR regions throughout metaphase and anaphase (see revision in Caperta et al. 2002). The organization pattern of the rDNA site visualized by FISH in one metaphase chromosome pair in species such as *Secale cereale* Linnaeus, 1753 (Caperta et al 2002; 2007) and *Zea mays* Linnaeus, 1753 (Kato et al. 2004, Mondin et al. 2014) is a distended secondary constriction and a condensed block of proximal ribosomal chromatin, which is transcriptionally inactive. As the NOR region is localized on a subterminal position of the short chromosome arm in these species, a satellite stained by DAPI is visualized. In both *S. rufescens* and *S. fluminensis*, a condensed chromatin block was not visualized in the chromosome presenting a distended secondary constriction, and neither a DAPI-stained satellite was detected. This last observation provides evidence that the rDNA sites are localized at chromosome termini. Therefore, we suppose that the satellite observed in the Feulgen-stained metaphase of *S. fluminensis* shown in Fig. 1C would be a structure containing rDNA, as in species of *Passiflora* Linnaeus, 1753 in which ribosomal DNA was observed on secondary constrictions and satellites (Cuco et al. 2005).

Details on the structure and function of the NOR chromosomes, as well as the quantification of observed events were not the scope of this study, but the detection of some features allows some discussion. The presence of positive-silver staining signals corresponding with the number of rDNA sites revealed by FISH showed that all these loci were active in both species analyzed. However, in some Feulgen-stained metaphases of *S. rufescens* only two chromosomes bearing secondary constriction were observed (Pizzaia et al. 2013), whereas in the metaphase of *S. fluminensis* seen in Fig.

1B, secondary constrictions were not detected, and in Fig. 1C, only one was observed. As mentioned above, these findings are a consequence of the terminal position of the rDNA loci and the degree of chromosome condensation not allowing the visualization of the secondary constrictions. Additionally, in the FISH preparation of *S. rufescens* shown in Fig 2A, one largest NOR chromosome has a secondary constriction that is highly distended in comparison with its homologous. This chromosome would be more active than its homologue. This heteromorphism of the secondary constriction was observed in FISH preparations of *S. cereale*, giving evidence of differential expression of homologous rDNA loci (Caperta et al. 2002; 2007). This behavior was also supported by the observation of differences in the size of the silver-staining signals. In an experiment carried out to evaluate this event, metaphases showing heteromorphic secondary constriction were more frequent than the homomorphic ones, and the rDNA loci on homologous chromosomes had equivalent numbers of ribosomal cistrons (Caperta et al. 2002).

In the present study, heteromorphic secondary constrictions were detected in FISH preparations of *S. rufescens* and *S. fluminensis*, but metaphases with both homologues of the largest NOR chromosome pair displaying distended secondary constrictions were also observed (not shown). Therefore, we conclude that in these species, differential expression of rDNA loci occurs only in some cells. The observation of homologous NOR chromosomes showing differences in the presence of secondary constrictions in Feulgen-stained metaphases of *S. rufescens*, *S. fluminensis* and also in *S. campestris*, *S. cissoides* and *S. goyazana* suggests that differential expression of rDNA loci is frequent in the genus *Smilax*.

Interestingly, the treatment of roots of *S. cereale* with the methyltransferase inhibitor 5-azacytidine (5-AC) resulted in an increase of rRNA gene transcription and then in a reduction in the number of cells showing a significant difference in the size of silver-stained domains in the two NORs (Caperta et al. 2007). The authors concluded that ribosomal gene silencing was controlled by DNA methylation and that rRNA gene transcription, silver-staining and NOR chromatin decondensation were interrelated in *S. cereale*. Fig 2B shows two apparently non-homologous chromosomes of *S. rufescens* with larger silver-stained domains, suggesting the occurrence of differential rRNA expression. Fig 2D illustrates NOR chromosomes of *S. fluminensis* with silver-stained NORs of similar sizes. These observations provide evidence that differential rRNA gene expression, as well as equal expression occur in these species.

The differential expression between homologous NOR chromatin is a different phenomenon in relation to nucleolar dominance. Nucleolar dominance has been characterized as an epigenetic phenomenon that occurs in plant allopolyploids and hybrids, in which only one ancestral set of ribosomal genes retains the ability to organize the nucleolus, while the rDNA loci derived from the other progenitor are silenced. For instance, in *Atropa belladonna* Linnaeus, 1753 derived from a tetraploid and a diploid ancestor species, only four out of six rDNA sites are transcriptionally active, as revealed by silver-staining (Volkov et al. 2017). In *Quercus robur* Linnaeus, 1753, two

rDNA loci were observed, NOR-1 and NOR-2 (Bockor et al. 2014). Only NOR-1 showed decondensed chromatin in FISH preparations and positive silver signals. In interphases, NOR-2 was condensed and located away from the nucleolus, while the major locus (NOR-1) was associated with the nucleolus and exhibited different degrees of condensation. Treatment with 5-azacytidine increased the total level of RNA transcripts and decreased the degree of DNA methylation at NOR-2 site however, the chromatin condensation of this locus was not affected, suggesting that NOR-2 has lost the function of rRNA synthesis and nucleolus organization.

Conclusions

The karyotypes of seven Brazilian *Smilax* species investigated were asymmetric and modal with 2n = 2x = 32 chromosomes gradually decreasing in size. In *S. goyazana*, a polyploid species, 2n = 4x = 64. In all the species, the large and medium-sized chromosomes were subtelocentric and submetacentric and the small chromosomes were submetacentric or metacentric. Their karyotypes were quite similar, with slight differences in the arm ratio of some chromosomes and belong to class 2B according with Stebbins classification (1971). *S. fluminensis* differed from the other species by having a large metacentric chromosome 1 and belonging to class 3C. These findings suggest that evolution occurred without drastic changes in karyotype structure in the species analyzed, except *S. fluminenesis*. Terminal secondary constrictions were visualized on the short arm of some chromosomes, but they were detected only in one homologue of each pair. Due to the terminal location and the degree of condensation of the chromosomes, secondary constrictions were not visualized in some species. In *S. rufescens* and *S. fluminensis* all the rDNA loci were active as demonstrated by silver-staining signals colocalized with the FISH signals. We concluded that differential expression of rDNA loci occurs in these species based on the observation of a distended secondary constriction in the largest NOR chromosome visualized in FISH preparations of some cells in both species. Distended secondary constrictions were not observed in the smallest chromosomes, probably due to their small size and the degree of metaphase condensation. In this connection, it is interesting to note that the absence of secondary constriction on an active locus was observed in *Crotalaria juncea* Linnaeus, 1753, in which two silver-stained rDNA loci were observed, that is, one major locus showing secondary constriction and one minor locus in which a secondary constriction was not detected (Mondin et al. 2007). The largest silver signals were observed in two chromosomes in *S. rufescens*, while signals with the same size were observed in *S. fluminensis*, demonstrating, in this species, that differential expression of rRNA genes does not occur in some cells. Additionally, the observation of homologous NOR chromosomes with differences in the presence of secondary constrictions in Feulgen-stained metaphases of *S. rufescens*, *S. fluminensis*, and in *S. campestris*, *S. cissoides* and *S. goyazana* suggests that *Smilax* is an interesting genus for further studies on the activity of the NOR sites.

Acknowledgments

We acknowledge the support of the Fundação de Apoio à Pesquisa do Estado de São Paulo (FAPESP, Project BIOTA, #05/58964-9), of the Conselho Nacional de Desenvolvimento Científico e Tecnológico (CNPq), of Dr. Beatriz Appezzato-da-Glória (University of São Paulo) and Dr. Eliana R. Forni-Martins (The University of Campinas) for cooperation in this research, and Mrs. S. C. M. Molina for technical assistance.

References

Andreata RHP (1995) Revisão das espécies brasileiras do gênero *Smilax* Linnaeus (Smilacaceae). PhD Thesis, Instituto de Biociências, Universidade de São Paulo, São Paulo, 397 pp.

Andreata RHP (2009) A new species of *Smilax* and key to all species of Minas Gerais, Brasil. Systematic Botany 34: 28–31. https://doi.org/10.1600/036364409787602302

Bertão MR, Aguiar-Perecin MLR (2002) Maize somatic chromosome preparation: pretreatments and genotypes for obtention of high index of metaphase accumulation. Caryologia 55: 115–119. https://doi.org/10.1080/00087114.2002.10589266

Bockor VV, Barisic D, Horvat T, Maglica Z, Vojta A, Zoldos V (2014) Inhibition of DNA methylation alters chromatin organization, nuclear positioning and activity of 45S rDNA loci in cycling cells of *Q. robur*. PLoS ONE 9(8): e103954. https://doi.org/10.1371/journal.pone.0193954

Caperta AD, Neves N, Morais-Cecilio L, Malhó R, Viegas W (2002) Genome restructuring in rye affects the expression, organization and disposition of homologous rDNA loci. Journal of Cell Science 115: 2839–2846.

Caperta AD, Neves N, Viegas W, Pikaard CS, Preuss S (2007) Relationships between transcription, silver staining, and chromatin organization of nucleolar organizers in *Secale cereale.* Protoplasma 232: 55–59. https://doi.org/10.1007/s00709-007-0277-4

Cox SD, Jayasinghe KC, Markham JL (2005) Antioxidant activity in Australian native sarsaparilla (*Smilax glyciphylla*). Journal of Ethnopharmacology 101: 162–168. https://doi.org/10.1016/j.jep.2005.04.005

Cuco SM, Vieira MLC, Mondin M, Aguiar-Perecin MLR (2005) Comparative karyotype analysis of three *Passiflora* L. species and cytogenetic characterization of somatic hybrids. Caryologia 58: 220–228. https://doi.org/10.1080/00087114.2005.10589454

De Souza GC, Haas AP, von Poser GL, Schapoval EE et al. (2004) Ethnopharmacological studies of antimicrobial remedies in the south of Brazil. Journal of Ethnopharmacology 90: 135–143. https://doi.org/10.1016/j.jep.2003.09.039

Fu C-X, Hong D-Y (1990) A chromosomal study on 7 species of *Smilax* L. Acta Phytotaxonomica Sinica 28: 211–222.

Fu C-X, Shen C-D, Zhong G-Q, Hong D-Y (1993) Variation and evolution of the karyotype on Smilax II. Karyotypic analysis of seven species from southern China. Cathaya 5: 151–166.

Fu C-X, Shen C-D, Huang, A-J, Hong D-Y (1995) Variation and evolution of the karyotype in *Smilax* and *Heterosmilax* (Smilacaceae) III. Analyses of karyotypes and evolution from twelve taxa in southern China. Cathaya 7: 105–124.

Huang A, Shen C, Fu C (1997) The chromosome numbers of 13 species in *Smilax* L. Journal of Wuhan Botanical Research. 15: 279–280.

Kato A, Lamb JC, Birchler JA (2004) Chromosome painting using repetitive DNA sequences as probes for somatic chromosome identification in maize. Proceedings of the National Academy of Sciences U.S.A. 101: 13554–13559. https://doi.org/10.1073/pnas.0403659101

Kong H-H, Wang A-L, Lee J, Fu C-X (2007) Studies of systematic evolution and karyotypic variation in *Smilax* and *Heterosmilax* (Smilacaceae). Acta Phytotaxonomica Sinica 45: 257–273. https://doi.org/10.1360/aps050125

Koyama T (1960) Materials toward a monograph of the genus *Smilax*. Quarterly Journal of the Taiwan Museum 13: 1–61.

Laurie DA, Bennett MD (1985) Nuclear DNA content in the genera *Zea* and *Sorghum*: intergeneric, interspecific and intraspecific variation. Heredity 55: 307–313. https://doi.org/10.1038/hdy.1985.112

Levan A, Fredga A, Sanderberg AA (1964) Nomenclature for centromeric position on chromosomes. Hereditas 52: 201–220. https://doi.org/10.1111/j.1601-5223.1964.tb01953.x

Mangaly JK (1968) A cytotaxonomic study of the herbaceous species of *Smilax* section *Coprosmanthus*. Rhodora 70: 55–82.

Martins AR, Appezzato-da-Glória (2006) Morfoanatomia dos órgãos vegetativos de *Smilax polyantha* Griseb. (Smilacaceae). Revista Brasileira de Botânica 29: 555–567. https://doi.org/10.1590/S0100-84042006000400005

Martins, AR, Pütz N, Soares AS, Bombo Appezzato-da-Glória B (2010) New approaches to underground systems in Brazilian *Smilax* species (Smilacaceae). The Journal of the Torrey Botanical Society 137: 220–235. https://doi.org/10.3159/10-RA-024R.1

Martins AR, Soares AS, Bombo, AB, Fidelis A, Novembre ADLC, Appezzato-da-Glória B (2012) Germination and seedling morphology of four South American *Smilax* (Smilacaceae). Revista de Biología Tropical 60: 495–504. https://doi.org/10.15517/rbt.v60i1.2784

Mehra PN, Sachdeva SK (1976) Cytological observations on some W. Himalayan monocots II. Smilacaceae, Liliaceae and Trilliaceae. Cytologia 41: 5–22. https://doi.org/10.1508/cytologia.41.5

Mondin M, Santos-Serejo JA, Aguiar-Perecin MLR (2007) Karyotype characterization of *Crotalaria juncea* (L.) by chromosome banding and physical mapping of 18S-5.8S-26S and 5S rRNA gene sites. Genetics and Molecular Biology 30: 65–72. https://doi.org/10.1590/S1415-47572007000100013

Mondin M, Santos-Serejo JA, Bertão MR, Laborda P, Pizzaia D, Aguiar-Perecin MLR (2014) Karyotype variability in tropical maize sister inbred lines and hybrids compared with KYS standard line. Frontiers in Plant Science 5: 544. https://doi.org/10.3389/fpls.2014.00544

Peruzzi L, Leitch IJ, Caparelli KF (2009) Chromosome diversity and evolution in Liliaceae. Annals of Botany 103: 459–475. https://doi.org/10.1093/aob/mcn230

Pizzaia D, Oliveira VM, Martins AR, Appezzato-da-Gloria B, Forni-Martins E, Aguiar-Perecin MLR (2013) Karyotype characterization reveals active 45S rDNA sites located on chro-

mosome termini in *Smilax rufescens* (Smilacaceae). Genetics and Molecular Research 12: 1303–1310. https://doi.org/10.4238/2013.April.25.1

Schnable PS, Ware D, Fulton RS, Stein JC et al. (2009) The B73 maize genome: complexity, diversity, and dynamics. Science 326: 1112–1115. https://doi.org/10.1126/science.1178534

Stack S, Herickhoff L, Sherman J, Anderson L (1991) Staining plant cells with silver. I. The salt-nylon technique. Biotechnic & Histochemistry 1: 69–78. https://doi.org/10.3109/10520299109110553

Speese BM (1939) Mitosis in leaves of *Smilax*. American Journal of Botany 26: 852–855. https://doi.org/10.1002/j.1537-2197.1939.tb09367.x

Stebbins GL (1971) Chromosomal evolution in higher plants. Edward Arnold Ltd, London, 216 pp.

Sun Z-S, Wang Y-H, Zhao Y-P, Fu C-X (2015) Molecular, chromosomal and morphological characters reveal a new diploid species in the *Smilax china* complex (Smilacaceae). Phytotaxa 212: 199–212. https://doi.org/10.11646/phytotaxa.212.3.2

The Angiosperm Phylogeny Group (2009) An update of the Angiosperm Phylogeny Group classification for the orders and families of flowering plants: APG III. Botanical Journal of the Linnean Society 161: 105–121. https://doi.org/10.1111/j.1095-8339.2009.00996.x

Vijayavalli B, Mathew PM (1989) Karyomorphology of five South Indian species of *Smilax* Linn. Cytologia 54: 65–72. https://doi.org/10.1508/cytologia.54.65

Volkov RA, Panchuk II, Borisjuk N, Hosiawa-Baranska M, Maluszynska J, Hemleben V (2017) Evolutional dynamics of 45S and 5S ribosomal DNA in ancient allohexaploid *Atropa belladonna*. BMC Plant Biology 17: 21–35. https://doi.org/10.1186/s12870-017-0978-6

CompCytogen 13(3): 265–275 (2019)
doi: 10.3897/CompCytogen.v13i3.36449
http://compcytogen.pensoft.net

SHORT COMMUNICATION

COMPARATIVE Cytogenetics
A peer-reviewed open-access journal
International Journal of Plant & Animal Cytogenetics, Karyosystematics, and Molecular Systematics

Banded karyotype of Nelore cattle (*Bos taurus indicus* Linnaeus, 1758)

Andréia Pires Amancio[1,2], Sabrina Sara Moreira Duarte[2,3], Rafael Carneiro Silva[2], Alex Silva da Cruz[2], Danilo Conrado Silva[2], Claudio Carlos da Silva[1,2,4,5], Aparecido Divino da Cruz[1,2,3,4]

1 *PhD Program in Biotechnology and Biodiversity, Federal University of Goiás, Rede Centro Oeste de Pós-Graduação de Pesquisa e Inovação, Rua 235, n. 40, Setor Leste Universitário, Goiânia, GO 74605-050, Brazil* **2** *Replicon Research Group, Genetics Master's Program, School of Agrarian and Biological Sciences, Pontifical Catholic University of Goiás, Rua 235, n. 40, Setor Leste Universitário, Goiânia, GO 74605-050, Brazil* **3** *Genetics and Molecular Biology Master's and PhD Program, Federal University of Goias, Avenida Esperança, s/n., Campus Samambaia, Goiânia, GO 74690-900, Brazil* **4** *Human Cytogenetics and Molecular Genetics Laboratory, Health Secretary of Goias State Goiânia, GO, Brazil* **5** *State University of Goiás, Campus Eseffego, Goiânia, GO, Brazil*

Corresponding author: *Andréia Pires Amancio* (andreiaamancio5@gmail.com)

Academic editor: *Nina Bulatova* | Received 23 May2019 | Accepted 4 August 2019 | Published 29 August 2019

http://zoobank.org/2A818874-4B15-49D7-A689-BF50ECF518BE

Citation: Amancio AP, Duarte SSM, Silva RC, da Cruz AS, Silva DC, da Silva CC, da Cruz AD (2019) Banded karyotype of Nelore cattle (*Bos taurus indicus* Linnaeus, 1758). Comparative Cytogenetics 13(3): 265–275. https://doi.org/10.3897/CompCytogen.v13i3.36449

Abstract

Chromosome banding techniques were applied and standardized to obtain karyotype characteristics for the first time in Brazil of Nelore cattle – *Bos taurus indicus* Linnaeus, 1758 – (bovine subspecies most prominent in Brazilian livestock). Blood samples were collected from the animals of the School of Agrarian and Biological Sciences of the Pontifical Catholic University of Goiás, two males and two females of pure breed. These samples were submitted to the cell culture method to study metaphase chromosomes. Chromosome banding techniques (C, G and NOR) revealed the karyotype architecture of Nelore cattle common with that of other breeds of zebu cattle formerly karyotyped. The diploid chromosome number was invariably normal, 2n = 60. C-banding revealed C-positive heterochromatin in centromeric regions almost in all chromosomes. G-banding presented the expected band pattern in the respective chromosome pairs in correspondence with the established chromosomal patterns for the species. Ag-staining for nucleolus organizer regions (AgNOR) was identified on the telomeric end of the long arm in 7 autosomal chromosomes. In this study we found more regions in chromosomes with staining than presented in the literature for the *Bos indicus* group (BIN). These NOR regions were repeated on the same chromosomes for the 4 animals studied.

Keywords
AgNOR; Brazil breeds; Cytogenetics; Karyotype; Zebu

Introduction

Nelore is an important bovine breed and well noted in Brazil for its meat production, body size and sturdiness. However, the meat industry has demanded products of higher quality. Thus, in the last 5 years, specifically with respect to meat production, the cross between Angus (taurine) and Nelore (zebu) breeds has been growing in Brazil. Indiscriminate crossing of Nelore cattle may result in a dilution of the breed and a decline in their number which may result in complete genetic extinction. Consequently, the conservation of the original breed is necessary (Reddy et al. 2016).

Despite this trend in the market, Nelore still comprises up to 80% of the national cattle of bovine breeds raised for meat, mostly due to its combination of productivity and adaptability to the tropics (Júnior et al. 2016). The states of Mato Grosso, Mato Grosso do Sul, and Goiás, a region known as Central Brazil, hold 43% of the country bovine cattle composed of Nelore breed (IBGE 2017).

Cytogenetic studies are highly useful for genetic characterization and for effective conservation of the species seriously at risk of extinction (Bharti et al. 2017). Genotype-based selection could be a powerful tool to assist farmers on making decisions regarding phenotype/genotype correlations and their interaction with the environment when managing their herds (Paulino et al. 2014).

Despite the extensive genomic investigation in cattle, not so many novelties are reported about bovine chromosomes that could be an excellent and inexpensive tool to provide important pieces of information useful for animal characterization, herd management, and evolutionary studies of breeds (David et al. 2014). The application of cytogenetic techniques has led to a simple cytological determination of the two main subspecies used in formation of domestic cattle breeds – *Bos taurus taurus* Linnaeus, 1758, Y(BTA) is submetacentric, and *Bos taurus indicus* Linnaeus, 1758, Y(BIN) is acrocentric (Halnan and Watson1982). In their karyotypes, the X chromosome is always the only morphologically distinguishable chromosome among monotonously acrocentric metaphases, being large and submetacentric (Raudsepp and Chowdhary 2016).

For correct identification of individual chromosomes, several banding techniques were developed, broadly divided into two categories: those that produce bands along the entire chromosome (Q, G, and R) and those that mark specific regions of each chromosome (C, T, or NOR) (Miranda and Mattevi 2011). Among other breeds of BIN cytogenetically studied, Nelore cattle in Brazil are still not so exploited, due to the difficulty to standardize and update the cytogentic techniques commonly used to study chromosomes, for example, the time necessary to culture cell and preparation of slides with material for banding techniques.

We are presenting in this work the necessary characterization of Nelore's chromosomes using G-, C-, and NOR-branding methodologies.

Material and methods

Biological samples were collected from four animals (2 male, 2 female), products industrial breeding Nelore, belonging to the study station of the Faculty of Agrarian of Biological Sciences / Pontifical Catholic University of Goiás. The herd maintained at lots of 28 m² of pasture and fed with fodder twice a day. Both males were 28 months old, weighing about 430kg. Both females were 35 months old, weighing about 480 kg. Blood samples of about 3ml of peripheral blood from the external jugular vein of each animal were kept in vaccum tubes containing heparin to prevent blood clotting and cooled on ice until arriving at the laboratory. Conventional cytological techniques were applied adapted to local and laboratory conditions of peripheral blood culturing and chromosome preparation (Verma and Babu 1995; David et al. 2014; Rosetto 2015).

Cell culture and cytological preparation

Cell culture was performed from 1ml of blood sample transferred into RPMI 1640 (Gibco RPMI 1640 Medium) (4ml), enriched with FBS (Fetal Bovine Serum, Gibco (1ml), PHA (Phytohemagglutinin, Gibco) and antibiotics (Penicillin G sodium salt, Sigma-Aldrich) (100U/μL). The cell suspension was stored in an incubator at 38 °C under 5% of carbon dioxide (CO_2) for 71 hours. After this time, 75μl of colchicine (Colcemid, Gibco) was added and incubation continued for an additional 30 minutes. Subsequently, samples were transferred to a 15ml conical tube and centrifuged for 10 minutes at 1000rpm, and then the supernatant was discarded (leaving about 1ml of material in the tube). A total of 10ml of hypotonic solution (KCl at 0.075 M) was added into the tube and incubated for 35 minutes at 38 °C, 5% CO_2. The cells were then fixed with Carnoy's solution (3 parts of methanol to 1 part of acetic acid), fixation was performed for 10 minutes at room temperature and immediately centrifuged for 10 minutes at 1000rpm. The cell pellet was fixed by three successive washes with the fixative, until the material became clear. Fixed cells were maintained in a suspension with 5ml of fixative in the refrigerator until the time of chromosomal analysis.

C-banding

The cell suspension was dropped on a microscope slide over a water-bath steaming at 60 °C. Slides were previously cleaned and degreased to guarantee adequate spreading of metaphases. Metaphase spreads were aged in the refrigerator for 2 days. Subsequently, the slides were soaked in 0.2N HCl solution for 10 min, rinsed in distilled water. DNA denaturation was carried out in a solution of 5% barium hydroxide for 15 min at 37 °C, slides were rinsed in distilled water at room temperature. After drying, the slides were stained with 10% Giemsa's solution for 5 minutes (KaryoMAX Giemsa Stain Solution).

G-banding

For the GTG banding, slides with the metaphase spreads were stored at room temperature for 7 days. After aging, slides were treated in 0.025% trypsin solution (Gibco) diluted in 4mL of PBS at 37 °C for 6–7 seconds. Afterwards, slides were stained in 5% Giemsa's solution for 5 minutes (KaryoMAX Giemsa Stain Solution).

NOR banding

Ag-staining of NORs (Nucleolus Organizer Regions) was carried out after aging the slides for 2 days in a refrigerator. Subsequently, 2 drops of 50% silver nitrate (AgNO3, Sigma-Aldrich) and 2 drops of 2% gelatin diluted in 1% formic acid were added to the material and covered by a glass coverslip. The slide was then placed into a humid chamber at 65 °C protected from light for a time ranging from 3 to 5 minutes until the slide surface showed a copper-like color.

Analysis of metaphases and chromosomal measurement

Metaphases were captured using white light microscopy with the aid of a karyotyping station consisting of a microscope Axioplan 2 Imaging (Carl Zeiss, Alemanha) with motorized platinum controlled by Metafer 3.4.0 software (Metasystems Corporation, Germany). Captured images were analyzed using IKAROS (Metasystems Corporation, Germany).

Twenty metaphases of each animal were analyzed. The lengths of chromosomes in micrometers were measured in mitotic metaphase of male and female cells. Karyotype symmetry/asymmetry index (S/AI), the mean length of short arm (Ls), length of long arm (Ll), total length of arm (LT), arm ratio (AR-long/short chromosome), centromeric index (CI) and type of chromosome and formula were estimated according to Eroğlu (2015).

All chromosomes measurements were translated by computation using software IKAROS (Metasystems Corporation, Germany), after pairing each pair of homologs in G- banded karyotype. Homologs were paired for all four animals, according to sex, and the final chromosome measurement corresponded to arithmetic mean of individual estimation for each chromosome.

Results and discussion

The study of Brazilian Nelore cattle adds to the list of the zebu (*B. t. indicus*) breeds so far karylogically investigated. The diploid number in all 4 studied animals was found to be 60, consisting of 29 pairs of autosomes and one pair of sex chromosomes – the kar-

yotype constitution, common to domestic cows of taurine/*B. taurus* and zeburine/*B. indicus* origin and established in all former reports (Wurster and Benirschke 1968; Evans et al. 1973; Mayr and Gruber 1986).

The Brazilian Nelore line originated from Ongole, a predominant breed in India (Oliveira et al. 2002). Our results were similar to those of Bharti and collaborators (2017) characterized the Ongole cattle with 29 acrocentric autosomal chromosomes and the sexual pairs, chromosome X as large submetacentric and chromosome Y as small acrocentric, thus suggesting common chromosome architecture of the Nelore cattle with that of other recognized breeds of BIN.

The measures for autosomes did not vary between male and female. Therefore, here we show the corresponding figures for the males in order to show all autosomal and both heteromorphic sex chromosome for the studied subspecies. All chromosomes measurements were represented in Table 1.

The chromosome pairs indicate evidence of interchromosomal asymmetry. S/AI for Nelore karyotype was 2.97 and 2.98 for female and male animals, respectively, classified its karyotype between symmetric and asymmetric, most likely due to the presence of the X chromosomes. The karyotype formulae were also different for male and female Nelore cows, corresponding, respectively, to 1SM+59A and 2SM+58A. For additional discussion about the importance to know the values of the karyotype symmetry/asymmetry in higher animals, readers are strongly advised to read the work of Eroğlu (2015).

With respect to sex chromosomes in Nelore, in our results the ratio between X and Y chromosomes was 2.45 indicating a remarkable in level of allosomic heteromorphism, a common observation among animals harboring XY sex determination mechanism, leading to an evolutionary stronger reproductive isolation (Lima 2014).

Chromosome X is relatively a few larger than chromosome 1, the largest acrocentric chromosome in the bovine karyotype. X/1 proportion is close to one (1,1μm). On the other hand, Y chromosome is close in size to autosomal chromosomes 24 (BIN), with an average size of 29,5μm then compared to the smallest acrocentric chromosome 29 (BIN), Y/29 proportion was found to be 1,3. Due to its acrocentric morphology and its small size, the Y chromosome of Nelore can easily be confused with several other small autosomal chromosomes that are also acrocentric. Here we report difficulty in the identification of Y(BIN) when relying only on Giemsa staining, just as reported by Melo (2009).

However, C-, GTG-, and NOR-banding provided a better morphological characterization of all chromosomes, including Y chromosome in Nelore, facilitating the proper differentiation of autosomal and sexual chromosomes for the breed.

In our case, Y is acrocentric, as in the first descriptions of the zebu karyotype (Halnan and Watson 1982.) This decision was made based on arm ratio and centromeric index (CI) for all Y chromosomes measured. Acrocentric chromosomes generally show an extend satellite and visually may suggest the shape of submetacentric chromosomes.

C-banding demonstrated dark bands (C-positive) on all centromeric region of autosomes, analyzed in the bovine material which showed well-defined heterochromatin

Table 1. The average measurements and arm ratio of the entire chromosome complement for male *Bos taurus indicus* Linnaeus, 1758, after homologs were paired up following GTG- banding.

Chromosome pair	Total length (µm)	Long arm (µm)	Short arm (µm)	Arm ritio (long/short)	Centromeric index	Chromosome type
1	67,9	61,7	6,2	9,952	9,131	A
2*	60,9	54,3	6,6	8,227	10,837	A
3*	57,8	51,8	6	8,633	10,381	A
4*	56,7	50,8	5,9	8,610	10,406	A
5	53,5	48,4	5,1	9,490	9,533	A
6	52,6	46,9	5,7	8,228	10,837	A
7	49,9	44,6	5,3	8,415	10,621	A
8	50,5	45,1	5	8,352	10,693	A
9	49,5	44,4	5,1	8,706	10,303	A
10	47,4	42,2	5,2	8,115	10,970	A
11*	45,6	40,6	5,0	8,120	10,965	A
12	42,2	37	5,2	7,115	12,322	A
13	38,7	33,1	5,6	5,911	14,470	A
14	40,3	35	5,3	6,604	13,151	A
15	38,5	33,5	5,0	6,700	12,987	A
16	38,6	33	5,6	5,893	14,508	A
17	37,8	32,2	5,6	5,750	14,815	A
18	35,6	30,2	5,4	5,593	15,169	A
19	33,5	28	5,5	5,091	16,418	A
20	32,3	26,4	6	4,475	18,266	A
21	31,7	26,5	5,2	5,096	16,404	A
22	32,2	26,9	5,3	5,075	16,460	A
23	31	26,1	4,9	5,327	15,806	A
24	29,5	24,2	5,3	4,566	17,966	A
25*	28,2	23	5,2	4,423	18,440	A
26	26,5	21,3	5,2	4,096	19,623	A
27	26,6	21,5	5,1	4,216	19,173	A
28*	25,3	20,2	5,1	3,961	20,158	A
29	22,6	18	4,6	3,913	20,354	A
X	66,6	44,2	22,4	1,973	33,634	SM
y	29,4	23,7	5,7	4,2	19,388	A

Note: A: acrocentric; SM: submetacentric.
*Nucleolus organizer chromosomes.

blocks. Stranzinger et al. (2007), studied the polymorphism of chromosome Y in various breeds of cattle (*Bos taurus*) in Switzerland, showed the C-negative X chromosome and C-positive Y chromosome from C-banding. However, in the animals in this study no dark bands (light or C-negative) were identified on the X and Y chromosomes (Figure 1).

The GTG banding provides alternated light and dark bands on the chromosomes, the distribution of these bands is different for each chromosome, facilitating the identification of the homologous pairs. Pinheiro et al. (1984) analyzed the BIN and BTA bovine chromosomes by G bands and found that the pattern of bands presented by the chromosomes was identical and that the difference between these animals was evidently genic.

Thus, in the GTG banding analysis the haploid set of Nelore cattle consists of 29 autosomes and 1 sexual pair including X and Y chromosome. The pair composition

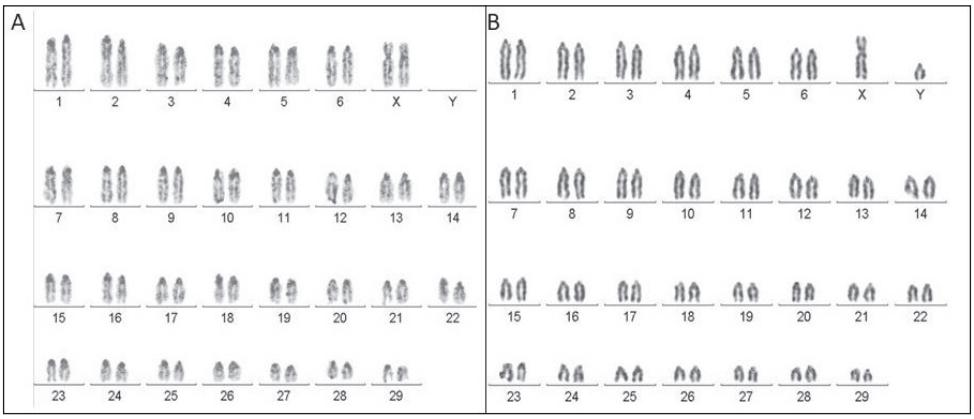

Figure 1. C-banded bovine chromosomes of Nelore breed. **A** female (XX) **B** male (XY).

presented in Figure 2 follows the nomenclature of the standard GTG-banded cattle karyotype (Di Berardino et al. 2001). In addition, the GTG banding can serve as a guide for the diagnosis and association of possible chromosomal alterations, being considered a differential technique for the characterization of species at chromosome levels (Rosetto 2015).

In spite of the diverse qualities that the GTG- banding provides, it requires an extended time of 7 days for preparation of the slides, along with the obtaining of metaphases in good condition for the analysis of the chromosomes.

The NOR technique, initially described by Mayr and Gruber (1986), revealed 5 pairs of the zebu (*B. indicus*) chromosomes 2, 3, 4, 11 and 28 with the nucleolar organizer regions located on the long arms. That was considered an important discovery in the conserved regions in the genus *Bos* Linnaeus, 1758 and may vary within species BTA and BIN. There are genomic controversies in the literature regarding the location of the nucleolar organizer regions in the *Bos taurus* species, some breeds presented six pairs of NORs in chromosomes 2, 3, 4, 11, 25 and 28, whereas others presented 5 pairs in chromosomes 2, 3, 4, 11 and 25 respectively (Melo 2009).

The seven nucleolus organizing regions (NORs) were located on the autosomal chromosomes of cattle Nelore. The four animals that made up the sample group in this study presented the NORs in the same chromosomal pairs, which are the autosomal pairs 2, 3, 4, 11, 22, 25 and 28 shown in figure 3. In contrast, Mayr and Gruber (1986) indicated that NORs of the cattle BIN appear on eight positions of the long arm of the pair autosomes 2, 3, 4 and 28.

Jantarat and colleagues (2009) performed the banding in C, G and NOR Thai's native cattle (*Bos taurus indicus*) and the results were compared to our study. There was a difference in the result of the NOR technique, the Thai's native cattle presented NOR in three pairs of autosomal chromosomes whereas for the studied Nelore breed, seven pairs of chromosomes presented the silver placement in the telomeric region.

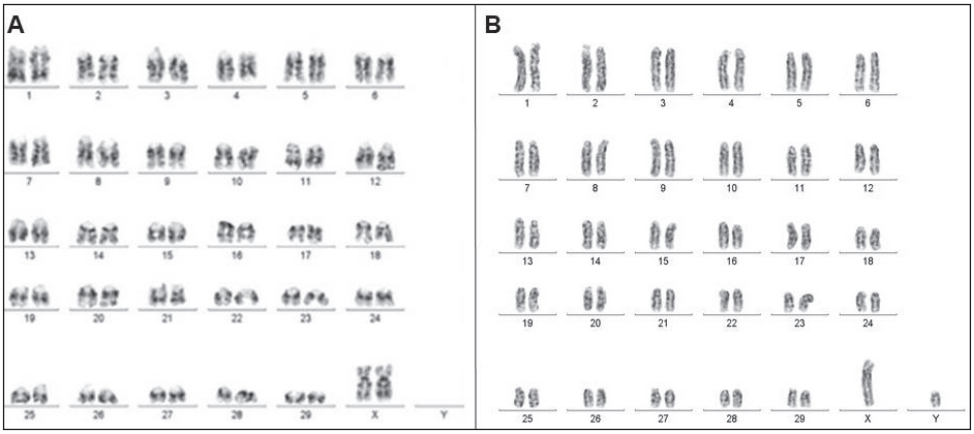

Figure 2. GTG-banding profile for the pairing of the chromosomes of the Nelore karyotype. **A** female (XX) **B** male (XY).

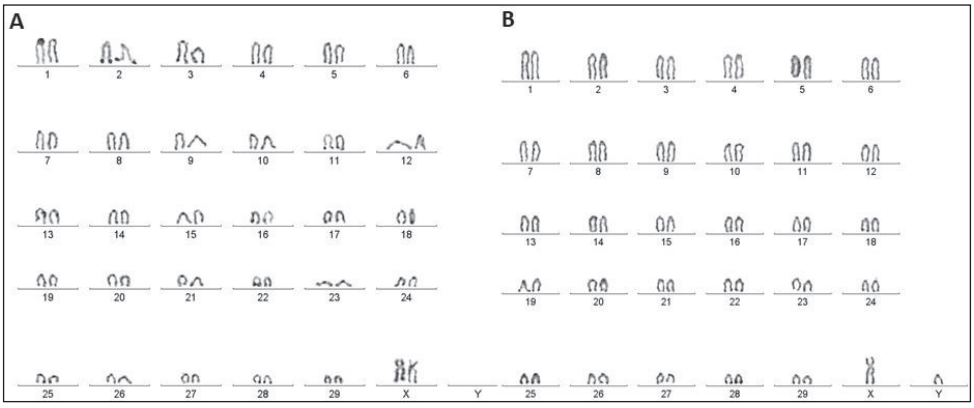

Figure 3. The nucleolus organizer regions on the long arm of the pairs of autosomal chromosomes 2, 3, 4, 11, 22, 25, and 28 by NOR-banding technique in female and male respectively. **A** female (XX) **B** male (XY).

Conclusion

About 80% of the Brazilian herd is composed of zebu breeds (*Bos t. indicus*), animals with more rusticity and easy adaptation to the predominant environment in the country (Amaral et al. 2012). Among these breeds, Nelore stands out the beef cattle with the greatest expansion in the central-west region. Therefore, it is important to study the cytogenetics of this group, being the most used chromosome banding techniques (CRPBZ 2015).

There was no cytogenetic characterization by banding techniques (C-, GTG- and NOR) for the Nelore Brazilian breed. For the animals of this study, the C banding made possible an exact identification of the acrocentric chromosomes. The technique GTG-banding provided the correct characterization of the pairs homologues, espe-

cially the autosomal chromosomes of cattle that are all acrocentric. In particular, the in this study it was possible to identify nucleolus organizing regions in other chromosomes, different from what was already known for subspecies *Bos t. indicus*.

The variation in the composition of the chromosomes that make up the national herds, especially those in this study, can be explained by the many preceding intersections and inbreeding. This management practice is commonly used to increase the herd of animals with favorable traits. Therefore, our observation can be in correspondence to the work of Carneiro et al. (2007) which refers to genetic diversity and genealogical control of the Nelore breed.

In addition to the banding techniques excellent for studies of morphology and chromosome classification, instead of new cytogenetic methodologies, such as Fluorescent In Situ Hybridization (FISH) and High Resolution Banding, can be used to understand chromosomal rearrangements and to clarify phenomena that may be related to the integrity of bovine genetic material (Luna 2012, De Lorenzi et al. 2017).

Acknowledgments

The authors are grateful to the School of Agrarian and Biological Sciences of the Pontifical Catholic University of Goiás (PUC-Goiás) for authorizing the collection of bovine samples. We are also grateful for both Replicon Research Group of Pontifical Catholic University of Goias and Human Cytogenetics and Molecular Genetics Laboratory of Health Secretary of Goias State for logistical support for the execution of this study. The study was funded by the Coordenadoria de Aperfeiçoamento de Ensino Superior (CAPES) and from the Fundação de Amparo à Pesquisa do Estato de Goiás (FAPEG).

References

Amaral G, Carvalho F, Capanema L, Carvalho CA (2012) Panorama da pecuária sustentável. BNDS Setorial 36: 249–288.

Bharti A, Panduranga Reddy P, Gnana Prakash M, Sakaram D (2017) Cytogenetic characterization of ongole cattle. International Journal of Advanced Biological Research 7(3): 574–577.

Carneiro TX, Gonçalves EC, Schneider MPC, Silva A (2007) Diversidade genética e eficiência de DNA microssatélite para o controle genealógico da raça Nelore. Arquivo Brasileiro de Medicida Veterinária e Zootecnica 59(5): 1257–1262. https://doi.org/10.1590/S0102-09352007000500024

CRPBZ – Centro de Referencia da Pecuária Brasileira – ZEBU. Zebuinocultura 2015. http://www.zebu.org.br/Home/Secao/9331 [accessed: 10 May 2019]

David JAO, Aguiar LL, Mainardi VF (2014) Aplicações da citogenética em ciência animal. Deminicis BB, Martins CB (Eds) Caufes. 1ª Tópicos Especiais em Ciência Animal III. Alegre, Espirito Santo, Brasil, 222–228.

De Lorenzi L, Iannuzzi A, Rossi E, Bonacina S, Parma P (2017) Centromere Repositioning in Cattle (*Bos taurus*) Chromosome 17. Cytogenetic and Genome Research 151: 191–197. https://doi.org/10.1159/000473781

Di Berardino D, Iannuzzi L (1981) Chromosome banding homologies in swamp and murrah buffalo. Journal of Heredity 72: 183–188. https://doi.org/10.1093/oxfordjournals.jhered.a109469

Di Berardino D, Di Meo GP, Gallagher DS, Hayes H, Iannuzzi L (2001) ISCNDB2000 International system for chromosome nomenclature of domestic bovids. Cytogenetics and Cell Genetics, 92: 283–299. https://doi.org/10.1159/000056917

Eroğlu H (2015) Which chromosomes are subtelocentric or acrocentric? A new karyotype symmetry/asymmetry index. Caryologia 68: 1–7. https://doi.org/10.1080/00087114.2015.1032614

Evans HJ, Buckland RA, Sumner AT (1973) Chromosome homology and heterochromatin in goat, sheep and ox studied by banding techniques. Chromosoma (Berlin) 42: 383–402. https://doi.org/10.1007/BF00399407

Halnan CRE, Watson JI (1982) Y chromosome variants in cattle *Bos taurus* and *Bos indicus*. Annales de génétique et de sélection animale, INRA Editions 14(1): 1–16. https://doi.org/10.1186/1297-9686-14-1-1

IBGE – Instituto Brasileiro de Geografia e Estatística. Diretoria de Pesquisas, Coordenação de Agropecuária, Pesquisa da Pecuária Nacional 2017. http://www.ibge.gov.br [accessed: 20 January acessado 2019]

Júnior CPB, Borges LS, de Sousa PHAA, de Oliveira MRA, Cavalcante DH, de Andrade TV, Barros CD, Sousa Júnior SC (2016) Melhoramento Genético em Bovinos de Corte (*Bos indicus*) Efeitos ambientais, melhoramento genético animal, pecuária de corte, peso ao desmame. Nutri Time 13(1): 4558–4564.

Lima TG (2014) Higher levels of sex chromosome heteromorphism ate associated with markedly stronger reproductive isolation. Nature Communications 5(4743). https://doi.org/10.1038/ncomms5743

Luna HS (2012) Citogenética clássica aplicada ao monitoramento de germoplasma bovino. Revista Brasileira de Reprodução Animal, Belo Horizonte, Minas Gerais, (Brasil) 36(2): 84–93.

Mayr B, Gruber K (1986) Nucleolus organizer regions and heterochromatin in the zebu (*Bos indicus* L.). Theoretical and Applied Genetics 73: 832–835. https://doi.org/10.1007/BF00289387

Melo TC (2009) Avaliação de aberrações cromossômicas em bovinos (*Bos taurus taurus*) infectados pelo papilomavírus bovino. Ph.D. Dissertation, Universidade Federal de Pernanbuco, Recife, Brasil.

Miranda JA, Mattevi MS (2011) Técnicas de bandeamento e coloração cromossômica. Maluf SW, Riegel M Ed Artmed. Citogenética Humana, (Brasil) 63–69.

Oliveira JHR, Magnabosco CU, Borges AMSM (2002) Nelore: base genética e evolução seletiva no Brasil. Documentos/Embrapa Cerrados (INFOTECA-SE), Planaltina, Distrito Federal (Brasil) 49: 54 pp.

Oliveira Júnior GA, Perez BC, Ferraz JBS (2017) Genomics applied to puberty in beef cattle (*Bos indicus*). Revista Brasileira Reprodução Animal, Belo Horizonte, Minas Gerais (Brasil) 41(1): 264–269.

Paulino MF, Detmann E, Silva GA, Almeida MA, Márquez CED, Moreno SPD, Moura HF, Cardenas GE, Lima CAJ, Martins SL, Manso RM, Ortega MER, Lopes AS, Carvalho VV (2014) Bovinocultura otimizada. 9a Simpósio internacional de produção de gado de corte, Universidade Federal de Viçosa, Viçosa, Minas Gerais (Brasil), 139–164.

Pinheiro LEL, Ferrari I, Ferraz JBS, Almeida JR (1984) Heteromorfismo cromossômico na raça caracu. Revista Brasileira de Reprodução Animal, Belo Horizonte 8 (1): 17–20.

Raudsepp T, Chowdhary BP (2016) Chromosome Aberrations and Fertility Disorders in Domestic Animals. Annual Review of Animal Biosciences, 4: 15–43. https://doi.org/10.1146/annurev-animal-021815-111239

Reddy PRK, Reddy AN, Ramadevi A, Kumar DS (2016) Nutritional significance of indigenous cow milk with regard to A2 beta casein – An overview. International Journal of Science, Environment and Technology 5(5) 3376–3380.

Rosetto CFR (2015) Avaliação do bandeamento cromossômico por digestão enzimática e tratamento com solução tampão citratado. Ph.D. Dissertation, Universidade Estadual Paulista Júlio de Mesquita Filho, Faculdade de Medicina de Botucatu, São Paulo.

Jantarat S, Tanomtong A, Kakampuy W, Kaewsri S, Buranarom K (2009) Standardized karyotype and idiogram of Thai's native cattle, *Bos indicus* (Artiodactyla, Bovidae) by convention staining, G-banding, C-banding and NOR-banding techniques. Thai Journal of Genetics 2(2): 164–174. https://doi.org/10.14456/tjg.2009.15

Stranzinger GF, Steiger D, Kneubuhler J, Hagger C (2007) Y chromosome polymorphism in various breeds of cattle (*Bos taurus*) in Switzerland. Journal of Applied Genetics 48: 241–245. https://doi.org/10.1007/BF03195218

Verma RS, Babu A (1995) Human chromosomes principles and techiniques. 2nd edn. McGraw-Hill, New York, 419 pp.

Wurster DH, Benirschke K (1968) Chromosome studies in the superfamily Bovoidae. Chromosoma (Berlin) 25: 152–171. https://doi.org/10.1007/BF00327175

CompCytogen 13(3): 277–281 (2019)
doi: 10.3897/CompCytogen.v13i3.36581
http://compcytogen.pensoft.net

RESEARCH ARTICLE

COMPARATIVE Cytogenetics
A peer-reviewed open-access journal
International Journal of Plant & Animal Cytogenetics, Karyosystematics, and Molecular Systematics

A cytogenetic analysis in two species of Cassidinae (Coleoptera, Chrysomelidae)

Eduard Petitpierre[1]

1 *Dept. Biologia, Universitat de les Illes Balears, 07122 Palma de Mallorca, Spain*

Corresponding author: *Eduard Petitpierre* (eduard.petitpierre@uib.es)

Academic editor: *Dorota Lachowska* | Received 28 May 2019 | Accepted 28 June 2019 | Published 3 September 2019

http://zoobank.org/78062B46-BE11-48D7-A5FD-C8A8131DAD71

Citation: Petitpierre E (2019) A cytogenetic analysis in two species of Cassidinae (Coleoptera, Chrysomelidae). Comparative Cytogenetics 13(3): 277–281. https://doi.org/10.3897/CompCytogen.v13i3.36581

Abstract

Two species of Cassidinae have been chromosomally analyzed, *Cassida humeralis* Kraatz, 1874 from France, with 2n = 18, 8 + Xy_p meioformula and *Anacassis fuscata* (Klug, 1829) from Uruguay, with 2n = 30, 14 + Xy meioformula. The karyotype of the former is composed of similar meta/submetacentric autosomes, a small X-chromosome and a tiny y-chromosome, as many other *Cassida* and tribe Cassidini species, whereas that of the latter has four pairs of acro/telocentric autosomes at least and the remaining meta/submetacentrics including the X-chromosome and a tiny y-chromosome, which points out to its probable apomorphic origin by centric fissions, as found in some other species of the tribe Mesomphaliini.

Keywords

Coleoptera, Chrysomelidae, Cassidinae, *Cassida humeralis*, *Anacassis fuscata*, karyotypes

Introduction

The leaf beetles of subfamily Cassidinae are a very large group with some 6,000 species distributed in 43 tribes (Chaboo 2007). Nearly 130 species have been chromosomally analysed mostly from the Palaearctic, Neotropical and Oriental regions (Petitpierre et al. 1988, Petitpierre et al. 1998; De Julio et al. 2010; Lopes et al. 2015; Lopes et al. 2017). Although the range of chromosome numbers is very large, from 2n = 12 to 2n (♂) = 51, roughly 40% of their species show 2n = 18 chromosomes (De Julio et al. 2010). Moreover, the sex-chromosome system in males is the "parachute type" Xy_p, as

found in nearly 95% of Cassidinae (De Julio et al. 2010) and in most beetles of the suborder Polyphaga (Smith and Virkki 1978). The present paper is a small contribution to the cytogenetics of Cassidinae and a brief discussion on its chromosomal evolution.

Material and methods

Two species of Cassidinae, each from two individuals, have been chromosomally surveyed: *Cassida humeralis* Kraatz, 1874, from Revens (Gard, France) and *Anacassis fuscata* (Klug, 1829) from Sauce (Canelones, Uruguay). The male adult individuals were anaesthetized with ethyl acetate before dissecting their testes with insect pins and using then the methods of chromosome treatments reported by Petitpierre et al. (1998), for obtaining chromosome spreads which were conventionally stained with Giemsa. Finally, the slides were examined and photographed with a Zeiss Axioskop photomicroscope.

Results

Cassida humeralis provided spermatogonial metaphases with 2n = 18 chromosomes, all the autosomes showing similar sizes and metacentric shapes except one pair of submetacentrics, whereas the X sex-chromosome was a clearly smaller metacentric with

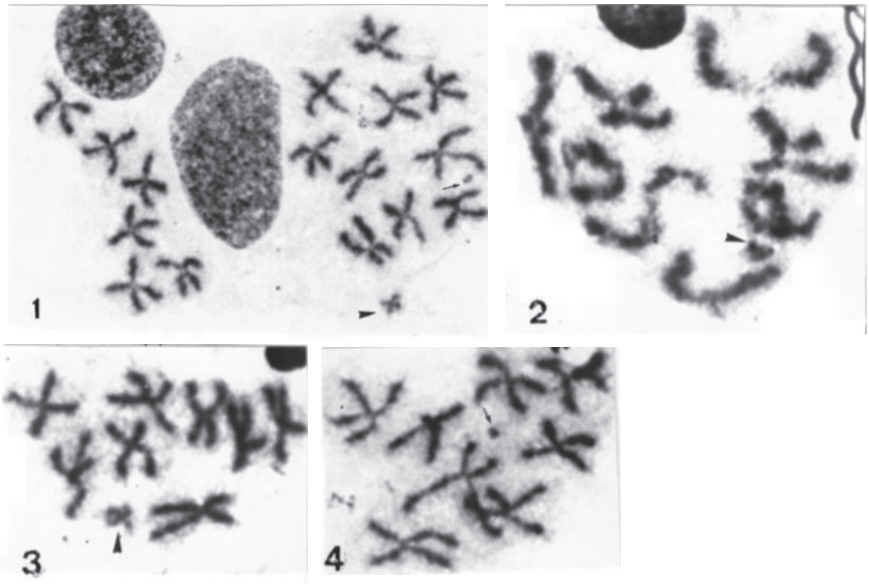

Figures 1–4. *Cassida humeralis*: **1** spermatogonial metaphase with 2n = 18 meta/submetacentric chromosomes, the small X-chromosome is arrowheaded and the tiny y-chromosome pointed by an arrow **2** meiotic diakinesis with a 8 + Xyp meioformula, the Xyp is arrowheaded **3** meiotic metaphase II of X-chromosome (arrowheaded) class with nine chromosomes **4** meiotic metaphase II of y-chromosome (arrowed) class with nine chromosomes.

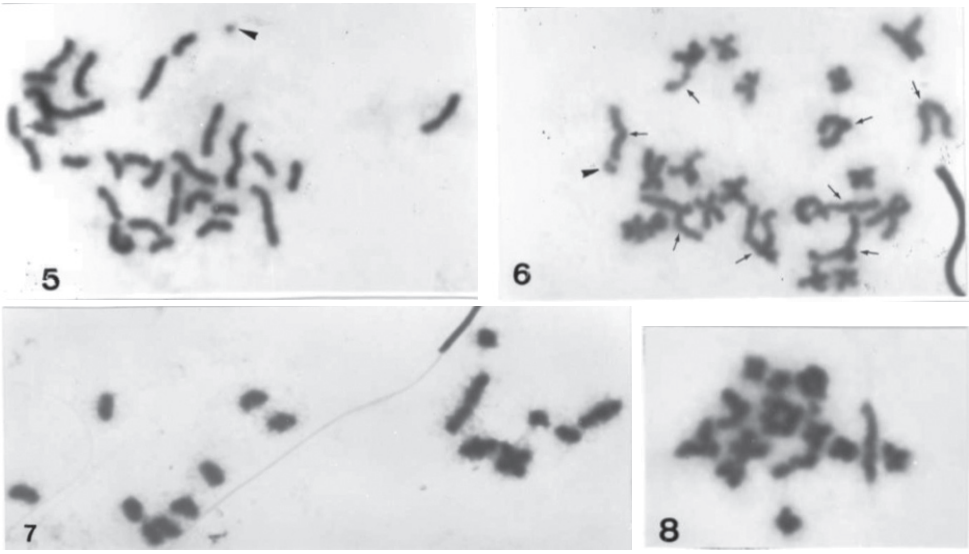

Figures 5–8. *Anacassis fuscata*. **5** spermatogonial metaphase with 2n = 30 chromosomes **6** spermatogonial metaphase showing at least four acro/telocentric autosome pairs indicated by arrows **7** meiotic metaphase I with a 14 + Xy meioformula **8** meiotic metaphase II of X-chromosome class with fifteen chromosomes.

regard to all autosomes and the y-chromosome a tiny element (Fig. 1). The meiotic metaphase I displayed an 8 + Xy_p formula, with rings of two chiasmata, cross and rod-shaped one-chiasma autosomal bivalents in variable numbers and the Xy_p sex-chromosome system (Fig. 2). The meiotic metaphases II showed as expected the two classes, with 8 + X and 8 + y haploid chromosome numbers, respectively (Figs 3, 4).

Anacassis fuscata had spermatogonial metaphases with 2n = 30 chromosomes of mostly medium and small sizes (Fig. 5), at least four pairs of them acro/telocentrics and the remaining meta- or submetacentrics including the X-chromosome, and a tiny y-chromosome (Fig. 6). The meiotic metaphase I displayed a 14 + Xy meiformula (Fig. 7), and a metaphase II showed 14 + X haploid chromosomes (Fig. 8).

Discussion and conclusions

The karyotype of *Cassida humeralis* has 2n = 18 chromosomes as in 23 (69.7%) of the 33 cytogenetically known species of the genus *Cassida*, and in 40 (65.6%) among the total of 61 checked species of the tribe Cassidini, including species of further fourteen genera (Petitpierre et al. 1998; De Julio et al. 2010; Lopes et al. 2016, 2017). The prevalent metacentric shape of most autosomes in *C. humeralis* is also in agreement with those found in five other species of the same genus and in other genera of Cassidini tribe as well as a small metacentric X-chromosome and a tiny Y-chromosome (Petitpierre 1977; Petitpierre et al. 1998; De Julio et al. 2010). De Julio et al. (2010) assumed that a meioformula of 9 + Xy_p (2n = 20), the probable most ancestral for coleopterans of the suborder Polyphaga (Smith and Virkki

1978; Dutrillaux and Dutrillaux 2009), might also be the ancestral for the subfamily Cassidinae, but although this is present in three species of *Cassida* and in three further ones of different genera in the tribe Cassidini too (De Julio et al. 2010), it seems clear that it could not be the basal one. Moreover, the range of diploid numbers in the tribe Cassidini is quite large from 2n = 16 in *Glyphocassis trilineata* (Hope, 1831) to 2n = 42 in *Agroiconota inedita* (Boheman, 1855), but all out of one checked species in this tribe show the Xy_p sex chromosome system in males, although a few of them are polymorphic for an additional y_p chromosome (De Julio et al. 2010).

The high chromosome number, 2n = 30, of *Anacassis fuscata*, is in agreement with others found in the Neotropical tribe Mesomphaliini (= Stolaini), whose range in numbers goes from 2n = 22 to 2n(♂) = 51, in 24 checked species of six genera, where ten species of them had diploid numbers ≥ 30 chromosomes (De Julio et al. 2010; Lopes et al. 2016, 2017). *Anacassis fuscata* shows at least four acro/telocentric autosome pairs which points out to their possible origin from meta- or submetacentric autosomes by centric fissions, as it is found in other species of the tribe Mesomphaliini (De Julio et al. 2010), and a tiny y-chromosome, but the X-chromosome was not distinguished. Nevertheless, *Anacassis fuscata* displays a simple sex-chromosome system Xy (probably Xy_p) in males, as occurs in species of other genera of this tribe, namely of *Chelymorpha* Chevrolat, 1837 , *Cyrtonota* Chevrolat, 1837, *Mesomphalia* Hope, 1839, *Paraselenis* Spaeth, 1913 and *Stolas* Billberg, 1820 (De Julio et al. 2010; Lopes et al. 2016, 2017), contrary to the highly complex sex-chromosome systems described in most species and chromosomal races of *Botanochara*, which are undoubtedly derived from the former simple one Xy_p by chromosomal rearrangements (De Julio et al. 2010; Lopes et al. 2017). Thus, the tribe Mesomphaliini is strikingly apomorphous from cytogenetic grounds, both due to the high diploid chromosome numbers and the highly complex sex-chromosome systems of a fair number of its species.

Eventually, the possible most ancestral karyotype for the whole Cassidinae s. lat. subfamily, that is including the ancient subfamilies of Cassidinae s. str. (tortoise beetles) and Hispinae (leaf-mining beetles), may be that of 2n = 18 (Xy_p) chromosomes, because it is prevalent in two of the three tribes with at least five or more examined species of Cassidinae s. str., and in three of the six so far checked tribes belonging to the ancient subfamily Hispinae. However, in order to secure the basal karyotype of Cassidinae s. lat., many more species, most of all in this latter group of the ancient subfamily Hispinae, would be necessary to confirm this point of view.

Acknowledgements

Mr. Bernard Bordy (Le Val-Saint-Eloi, Haute-Saône, France) and Dr. Rodrigo Ponce de León (Univ. de la República, Montevideo, Uruguay) are highly indebted for supplying samples of *Cassida humeralis* and for his help in capturing those of *Anacassis fuscata*, respectively.

References

Chaboo CS (2007) Biology and phylogeny of the Cassidinae sensu lato (tortoise and leaf-mining beetles) (Coleoptera: Chrysomelidae). Bulletin of the American Museum of Natural History, 305: 1–250. https://doi.org/10.1206/0003-0090(2007)305[1:BAPOTC]2.0.CO;2

De Julio M, Fernandes FR, Costa C, Almeida MC, Cella DM (2010) Mechanisms of karyotype differentiation in Cassidinae sensu lato (Coleoptera, Polyphaga, Chrysomelidae) based on seven species of Brazilian fauna and an overview of the cytogenetic data. Micron 41: 26–38. https://doi.org/10.1016/j.micron.2009.07.013

Dutrillaux AM, Dutrillaux B (2009) Sex chromosome rearrangements in Polyphaga beetles. Sexual Development 3: 43–54. https://doi.org/10.1159/000200081

Lopes AT, Fernandes FR, Schneider MC (2016) Comparative cytogenetic analysis in 13 tortoise beetles (Coleoptera: Chrysomelidae: Cassidinae) from Brazil. European Journal of Entomology 113: 352–363. https://doi.org/10.14411/eje.2016.046

Lopes AT, Fernandes FR, Schneider MC (2017) Chromosome mapping of 28S ribosomal genes in 11 species of Cassidinae (Coleoptera. Chrysomelidae). European Journal of Entomology 114: 546–553. https://doi.org/10.14411/eje.2017.069

Petitpierre E (1977) A chromosome survey of five species of Cassidinae (Coleoptera, Chrysomelidae). Cytobios 18: 135–142.

Petitpierre E, Segarra C, Yadav JS, Virkki N (1988) Chromosome numbers and meioformulae of Chrysomelidae. In: Jolivet P, Petitpierre E, Hsiao TH (Eds) Biology of Chrysomelidae. Kluwer Academic Publishers, Dordrecht, 161–186. https://doi.org/10.1007/978-94-009-3105-3_10

Petitpierre E, Carreras I, Gómez-Zurita J (1998) Cytogenetic analysis of European Cassida (Coleoptera, Chrysomelidae). Hereditas 128: 1–8. https://doi.org/10.1111/j.1601-5223.1998.00001.x

Smith SG, Virkki N (1978) Animal Cytogenetics vol. 3, Insecta 5, Berlin, 366 pp.

CompCytogen 13(3): 283–295 (2019)
doi: 10.3897/CompCytogen.v13i3.36676
http://compcytogen.pensoft.net

RESEARCH ARTICLE

COMPARATIVE Cytogenetics
A peer-reviewed open-access journal
International Journal of Plant & Animal Cytogenetics, Karyosystematics, and Molecular Systematics

New evidence for the presence of the telomere motif $(TTAGG)_n$ in the family Reduviidae and its absence in the families Nabidae and Miridae (Hemiptera, Cimicomorpha)

Snejana Grozeva[1], Boris A. Anokhin[2], Nikolay Simov[3], Valentina G. Kuznetsova[2]

1 *Cytotaxonomy and Evolution Research Group, Institute of Biodiversity and Ecosystem Research, Bulgarian Academy of Sciences, Sofia 1000, 1 Tsar Osvoboditel, Bulgaria* **2** *Department of Karyosystematics, Zoological Institute, Russian Academy of Sciences, St. Petersburg 199034, Universitetskaya nab., 1, Russia* **3** *National Museum of Natural History, Bulgarian Academy of Sciences, Sofia 1000, 1 Tsar Osvoboditel, Bulgaria*

Corresponding author: *Snejana Grozeva* (sngrov@gmail.com)

Academic editor: *M. José Bressa* | Received 31 May 2019 | Accepted 29 August 2019 | Published 20 September 2019

http://zoobank.org/9305DF0F-0D1D-44FE-B72F-FD235ADE796C

Citation: Grozeva S, Anokhin BA, Simov N, Kuznetsova VG (2019) New evidence for the presence of the telomere motif $(TTAGG)_n$ in the family Reduviidae and its absence in the families Nabidae and Miridae (Hemiptera, Cimicomorpha). Comparative Cytogenetics 13(3): 283–295. https://doi.org/10.3897/CompCytogen.v13i3.36676

Abstract

Male karyotype and meiosis in four true bug species belonging to the families Reduviidae, Nabidae, and Miridae (Cimicomorpha) were studied for the first time using Giemsa staining and FISH with 18S ribosomal DNA and telomeric $(TTAGG)_n$ probes. We found that *Rhynocoris punctiventris* (Herrich-Schäffer, 1846) and *R. iracundus* (Poda, 1761) (Reduviidae: Harpactorinae) had 2n = 28 (24 + $X_1X_2X_3Y$), whereas *Nabis sareptanus* Dohrn, 1862 (Nabidae) and *Horistus orientalis* (Gmelin, 1790) (Miridae) had 2n = 34 (32 + XY) and 2n = 32 (30 + XY), respectively. FISH for 18S rDNA revealed hybridization signals on a sex chromosome, the X or the Y, in *H. orientalis*, on both X and Y chromosomes in *N. sareptanus*, and on two of the four sex chromosomes, Y and one of the Xs, in both species of *Rhynocoris* Hahn, 1834. The results of FISH with telomeric probes support with confidence the absence of the "insect" telomere motif $(TTAGG)_n$ in the families Nabidae and Miridae and its presence in both species of genus *Rhynocoris* of the Reduviidae, considered as a basal family of Cimicomorpha. Increasing evidence reinforces the hypothesis of the loss of the canonical "insect" telomere motif $(TTAGG)_n$ by at least four cimicomorphan families, Nabidae, Miridae, Tingidae, and Cimicidae, for which data are currently available.

Keywords

Heteroptera, *Rhynocoris punctiventris*, *R. iracundus*, *Nabis sareptanus*, *Horistus orientalis*, TTAGG-FISH

Introduction

The true bugs (Hemiptera: Heteroptera), with almost 45,000 described species distributed into 91 families and seven infraorders (Henry 2017), are one of the largest and most diverse groups of non-holometabolous insects. Overall, 40 species, 27 genera and 10 families have been studied in respect to the telomere structure (Okazaki et al. 1993, Sahara et al. 1999, Grozeva et al. 2011, Golub et al. 2015, 2017, 2018, Pita et al. 2016, Chirino et al. 2017, Angus et al. 2017). The species studied belong to three largest infraorders, including a more basal infraorder Nepomorpha and the evolutionary derived sister infraorders Pentatomomorpha and Cimicomorpha. The "insect" telomere motif $(TTAGG)_n$ was found in all studied species of the families Belostomatidae (Kuznetsova et al. 2012, Chirino et al. 2017) and Nepidae (Angus et al. 2017) from the Nepomorpha. Likewise, this motif was reported for the suborder Coleorrhyncha, a sister group to the Heteroptera (Kuznetsova et al. 2015). These facts indicate that it is most likely the ancestral telomeric repeat sequence of the Heteroptera in general. In contrast, all studied species of the families Lygaeidae s.l., Pentatomidae, and Pyrrhocoridae from the Pentatomomorpha, as well as those of the families Nabidae, Tingidae, Cimicidae, and Miridae from the Cimicomorpha were shown to lack this motif (Okazaki et al. 1993, Sahara et al. 1999, Grozeva et al. 2011, Golub et al. 2015, 2017, 2018). Based on this evidence, a hypothesis was advanced that the ancestral telomeric repeat TTAGG was lost at the base of the clade Pentatomomorpha + Cimicomorpha (= the Geocorisae sensu Schuh et al. 2009) being secondarily replaced by another yet unknown motif or an alternative telomerase-independent mechanism of telomere maintenance (Frydrychová et al. 2004, Mason et al. 2016). However, a recent research of Pita et al. (2016) discovered the putative ancestral "insect" motif in the cimicomorphan family Reduviidae (the assassin bugs), namely in the comparatively young (24–38 Ma, after Hwang and Weirauch 2012) hematophagous subfamily Triatominae. Due to this finding, the validity of the above hypothesis was questioned. Moreover, the postulated lack of the $(TTAGG)_n$ detection, at least in the families of Cimicomorpha, was suggested to be "due to a methodological problem of the telomeric probe rather than a loss process during their evolution" (Pita et al. 2016).

Primarily to address this issue, we did a $(TTAGG)_n$ FISH experiment involving four species of the Cimicomorpha, which have not previously been studied in respect to telomere composition. These are *Nabis* (*Halonabis*) *sareptanus* Dohrn, 1862 from the family Nabidae; *Horistus orientalis* (Gmelin, 1790) from the family Miridae; *Rhynocoris punctiventris* (Herrich-Schäffer, 1846) and *R. iracundus* (Poda, 1761) from the family Reduviidae, the subfamily Harpactorinae. Specifically, we looked for a strong evidence of the absence of the $(TTAGG)_n$ telomere motif in Nabidae and Miridae as well as an additional evidence of the presence of this motif in the family Reduviidae.

In addition, we aimed to detect the 18S rDNA loci in the above species. Finally, we characterized, for the first time, the karyotype and meiotic pattern of spermatogenesis in each of the species under study.

Material and methods

Taxon sampling, fixation and slide preparation

The true bug specimens were collected in May-June 2018, in Bulgaria. The localities from which the bugs were collected and the number of males and mitotic/meiotic preparations studied are given in Table 1. The insects were brought to the lab and fixed alive in a fixative consisting of 3 parts of 95% ethanol and 1 part of glacial acetic acid. Chromosome preparations were made from the male gonads. The testes were extracted from the abdomen, placed on a slide in a drop of 45% acetic acid, and squashed. The coverslips were removed with a razor blade after freezing with dry ice, and the slides were, then, dehydrated in fresh fixative (3 : 1) and air dried.

Routine staining

For this staining, we followed the Schiff-Giemsa method described by Grozeva and Nokkala (1996).

Fluorescence in situ hybridization (FISH)

Probes for 18S rDNA and $(TTAGG)_n$ were prepared and FISH was performed according to Grozeva et al. (2015) with some modifications. For primer information, see Grozeva et al. (2011). The telomere probe $(TTAGG)_n$ was amplified by PCR and labelled with rhodamine-5-dUTP (GeneCraft, Köln, Germany). An initial denaturation period of 3 min at 94 °C was followed by 30 cycles of 45 s at 94 °C, annealing for 30 s at 50 °C and extension for 50 s at 72 °C, with a final extension step of 3 min at 72 °C. The 18S rDNA probe was amplified by PCR and labelled with biotin-11-dUTP (Fermentas, Vilnius, Lithuania) using genomic DNA of the true bug *Pyrrhocoris apterus* (Linnaeus, 1758). An initial denaturation period of 3 min at 94 °C was followed by 33 cycles of 30 s at 94 °C, annealing for 30 s at 50 °C and extension for 1.5 min at 72 °C, with a final extension step of 3 min at 72 °C. The chromosome preparations were treated with 100 μg/ml RNase A and 5 mg/ml pepsin solution to remove excess RNA and proteins. Chromosomes were denatured in the hybridization mixture containing labelled 18S rDNA and $(TTAGG)_n$ probes (80–100 ng per slide) with an addition of salmon sperm blocking reagent and then hybridized for 42 h at 37 °C. 18S rDNA probes were detected with NeutrAvidin-Fluorescein conjugate (Invitrogen, Karlsbad, CA, USA). The chromosomes were mounted in an antifade medium (ProLong Gold antifade reagent with DAPI, Invitrogen) and covered with a glass coverslip. The number of males involved in the study ranged from three to one (Table 1), and the number of preparations examined ranged from one (*Horistus orientalis*) to 11 (*Rhynocoris iracundus*) and the number of prophase/metaphase plates examined ranged from a few (*H. orientalis*) to several dozen (*N. sareptanus* and *Rhynocoris* spp).

Table 1. Material studied.

Species	Locality	Date of collection	Number of males/ preparations analysed by Shiff-Giemsa staining	Number of males/ preparations analysed by FISH
Rhynocoris punctiventris (Herrich-Schäffer, 1846)	Bulgaria, Kresna Gorge 41.762378N, 23.169228E	23 May 2018	1/6	1/3
Rhynocoris iracundus (Poda, 1761)		23 May 2018	3/11	2/5
Horistus orientalis (Gmelin, 1790)		23 May 2018	1/1	1/2
Nabis (*Halonabis*) *sareptanus* Dohrn, 1862	Bulgaria, Pomorie Lake 42.565609N, 27.630627E	07 June 2018	3/5	1/1

As a control for the efficacy of our $(TTAGG)_n$ FISH experiments, we used chromosome preparations from *Scarlupella discolor* (Germar, 1821) (Hemiptera: Auchenorrhyncha) known to be $(TTAGG)_n$ -positive (Maryańska-Nadachowska et al. 2016).

Microscopy and imaging

The routinely stained preparations were analysed under a light microscope (Axio Scope A1 – Carl Zeiss Microscope) at 100× magnification and documented with a ProgRes MF Cool, Jenoptic (Jena, Germany). FISH images were taken using a Leica DM 6000 B microscope with a 100× objective, Leica DFC 345 FX camera, and Leica Application Suite 3.7 software with an Image Overlay module (Leica Microsystems, Wetzlar, Germany). The filter sets applied were A, L5 and N21 (Leica Microsystems). The specimens from which the chromosome preparations have been obtained are stored at the Institute of Biodiversity and Ecosystem Research, BAS (Sofia, Bulgaria).

Results and discussion

Family Reduviidae
Subfamily Harpactorinae
Tribe Harpactorini

Rhynocoris punctiventris, 2n ♂ = 28 (24A + $X_1X_2X_3Y$), Figs 1, 3, 4, 6b, 7
R. iracundus, 2n ♂ = 28 (24A + $X_1X_2X_3Y$), Figs 2, 5, 6a

Both species were found to have 28 chromosomes at spermatogonial metaphases (Figs 1, 5), and 12 autosomal bivalents and 4 univalent sex chromosomes at spermatocyte metaphases I (MI) (Figs 3, 6a, b). Such a chromosomal complement has been reported for all so far studied species of the genus *Rhynocoris* Hahn, 1834 and also for half the studied species of the tribe Harpactorini (see for review: Tiepo et al. 2016). The autosomes of spermatogonial metaphases and in turn both bivalents (MI) and univalent autosomes (MII) in meiosis are of a more or less similar size. Among the four sex chromosomes, the largest is considered as the Y and the others as X_1, X_2, and X_3 that

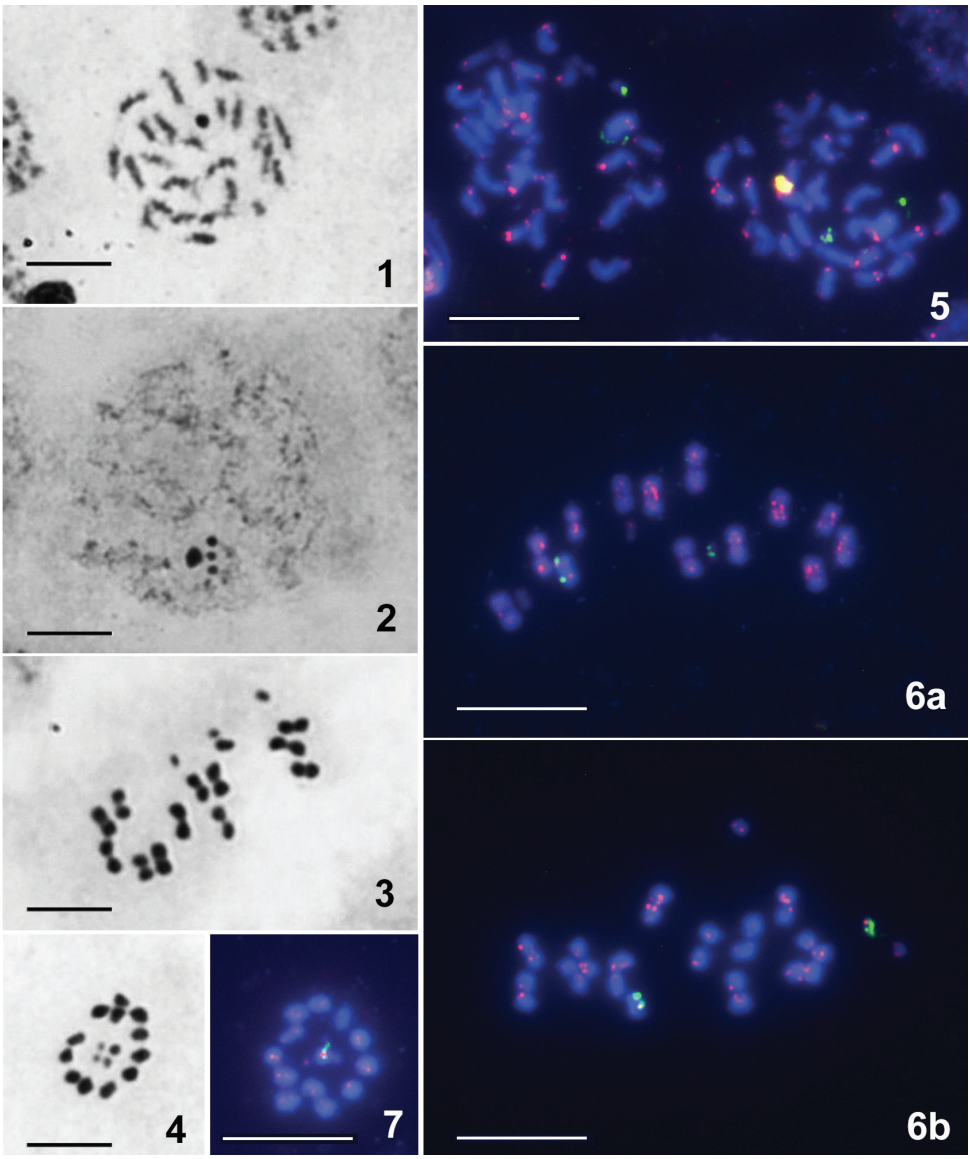

Figures 1–7. *Rhynocoris punctiventris* (**1, 3, 4, 6b, 7**) and *R. iracundus* (**2, 5, 6a**), 2n (♂) = 28 (24A + $X_1X_2X_3Y$). Routine staining (**1–4**), FISH with 18S rDNA (green) and telomeric $(TTAGG)_n$ (pink) probes (**5–7**). **1, 5** spermatogonial metaphase **2** early condensation stage with four sex chromosome bodies **3, 6a, b** metaphase I (MI) **4, 7** metaphase II (MII) with four sex chromosomes located in the center of the ring formed by autosomes. Hybridization signals of the $(TTAGG)_n$ probe are seen at the ends of chromosomes, and the signals of 18S rDNA FISH are seen on the Y chromosome and on one of the X chromosomes in both species (**5–7**). Scale bars: 10 μm.

could have originated through the fission processes of the original X chromosome of an ancestor with a simple system XY. Although we studied no females and have thus no direct confirmation of such interpretation of sex chromosome system in these two

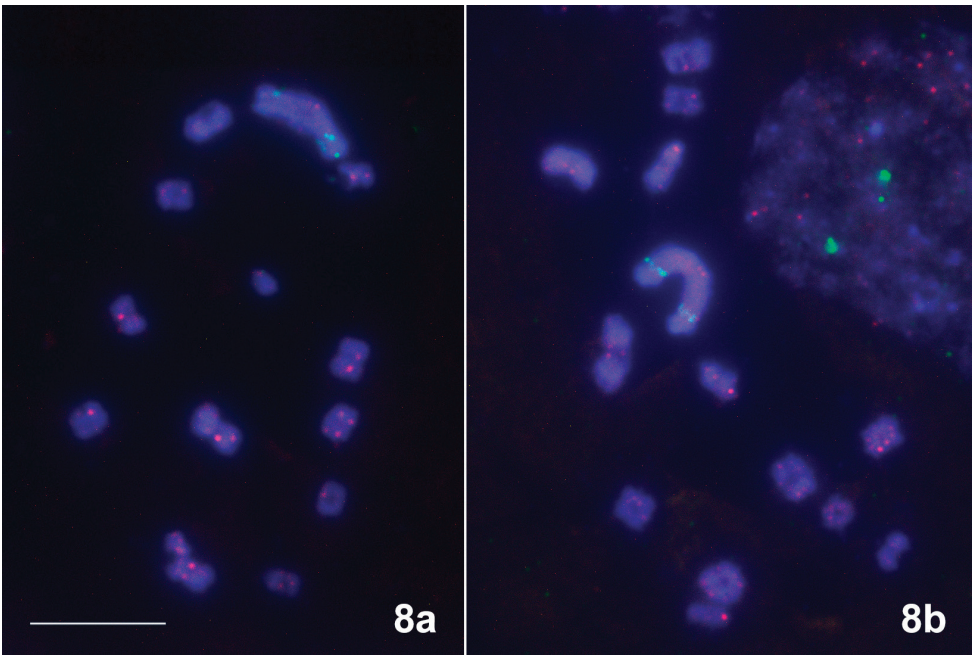

Figure 8. *Scarlupella discolor*. FISH with 18S rDNA (green) and telomeric $(TTAGG)_n$ (pink) probes. Hybridization signals of the $(TTAGG)_n$ probe are seen at the ends of chromosomes. Scale bar: 10 μm.

species, it is likely, as it represents the prevalent pattern reported for their close relatives (Tiepo et al. 2016). Three X chromosomes are of similar size and the smallest chromosomes of the complement. At condensation stage of meiosis, the four sex chromosome bodies were observed (Fig. 2). The analysis of MI and MII plates confirmed that the sex chromosomes followed the conventional in the Heteroptera (Ueshima 1979) post-reductional mode of separation of the sex chromosomes, i.e., they divide in the first division and segregate in the second division. As with other reduviid species (see e.g. Poggio 2007, Tiepo et al. 2016), at MII the autosomes are arranged to form a ring, with sex chromosomes being positioned inside the ring as a pseudo-tetravalent without having a visible connection between them (Figs 4, 7).

Figures 5 to 7 present the results of the application of FISH with $(TTAGG)_n$ and 18S rDNA probes to mitotic and meiotic chromosomes of *R. iracundus* (Figs 5, 6a) and *R. punctiventris* (Figs 6b, 7). Hybridization signals of the telomeric probe are clearly seen on the ends of chromosomes of both species indicating that their telomeres contain the canonical insect telomeric TTAGG tandem repeat. However not all chromosome ends show bright hybridization signals. The same variation in both the number and/or the intensity of signals has repeatedly been described in other true bug species (Pita et al. 2016, Angus et al. 2017, Chirino et al. 2017). Moreover, it was also observed at MI plates from *Scarlupella discolor* (Auchenorrhyncha) used here as a positive control for the $(TTAGG)_n$ probe in all our FISH experiments (Fig. 8a, b). Such

variation may be due to differences in the length of target TTAGG sequences (Chirino et al. 2017) or uneven access of the probe to the chromosomes (Pita et al. 2016). In all the figures presented, 18S rDNA FISH signals are seen on sex chromosomes, the Y and one of the X chromosomes. The condensation of sex chromosomes at MI made it impossible to determine the precise location of rDNA sites on them. At MI, these chromosomes are split into the sister chromatids and consequently show each twin hybridization signals of both telomeric and rDNA probes (Figs 6a, b). A similar pattern of the rDNA distribution was previously reported for *Cosmoclopius nigroannulatus* (Stål, 1860), another Harpactorini species with the same karyotype 2n = 24A + $X_1X_2X_3Y$ (Bardella et al. 2014).

Family Nabidae
Subfamily Nabinae
Tribe Nabini

Nabis (*Halonabis*) *sareptanus*, 2n ♂ = 34 (32A + XY), Figs 9–14

The chromosome complement of males studied here agrees with that reported earlier for males of this species originating from the Republic of Kazakhstan (Kuznetsova and Maryańska-Nadachowska 2000). However, the cited paper provided neither descriptions nor illustrations of karyotype and meiosis. According to our observations of different stages of meiosis, the autosomes of this species more or less gradually decrease in size; the X far exceeds in size the largest autosome, whereas the Y is one of the medium-sized elements of the complement (Figs 9–14). At the condensation stage, there are 16 autosomal bivalents and 2 univalent sex chromosomes, which are positively heteropycnotic and associate to one another via a nucleolus (Fig. 9). The first division is reductional for the autosomes and equational for the sex chromosomes (sex chromosome post-reduction). Figures 9 and 14 present late condensation stages with 16 autosomal bivalents and univalent chromosomes X and Y, which split into the sister chromatids each. As in other nabid species (Nokkala and Nokkala 1984, Kuznetsova and Maryańska-Nadachowska 2000), the homologues of every bivalent align in parallel without chiasmata between them (Figs 10, 14), i.e. meiosis is achiasmate of the so-called *alignment* type (Nokkala and Nokkala 1984). During the second division, sex chromosomes show "distance pairing" at MII (Fig. 11) and move to different poles at anaphase II (Fig. 12).

FISH with the $(TTAGG)_n$ probe revealed no signals on chromosomal spreads of *N. sareptanus* (Figs 13, 14) suggesting thus that its telomeres lack the "insect" telomere motif $(TTAGG)_n$. The hybridization signals of the 18S rDNA probe, as expected because of the association of the nucleolus with the sex chromosomes (see above), were present on both X and Y sex chromosomes (Figs 13, 14). This is the first evidence of the rDNA location in the family Nabidae.

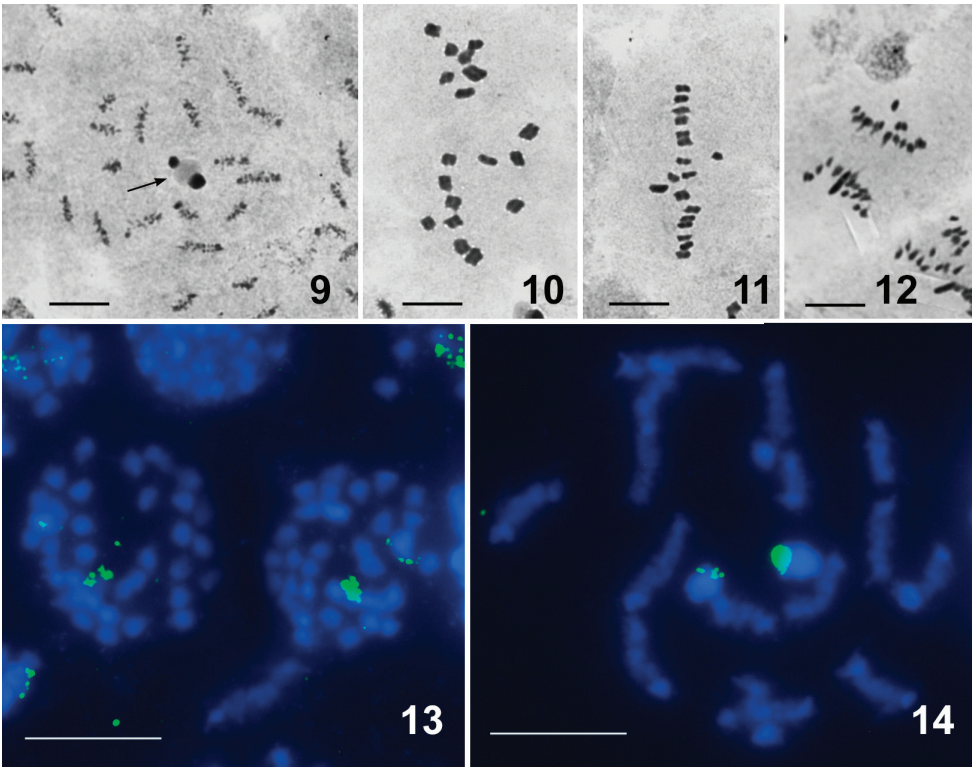

Figures 9–14. *Nabis* (*Halonabis*) *sareptanus*, 2n (♂) = 34 (32A + XY). Routine staining (**9–12**), FISH with 18S rDNA (green) and telomeric $(TTAGG)_n$ (pink) probes. (**13, 14**); **9, 14** condensation stage (**9** at the early condensation stage, 2 univalent sex chromosomes are positively heteropycnotic and associate to one another via a nucleolus; arrowed) **10** MI **11** MII **12** anaphase II (AII) **13** spermatogonial metaphase. There are no hybridization signals of the $(TTAGG)_n$ probe; the signals of the 18S rDNA probe are seen on both X and Y chromosomes (**13, 14**). Scale bars: 10 μm.

Family Miridae
Subfamily Mirinae
Tribe Mirini

Horistus orientalis, 2n ♂ = 32 (30A + XY), Fig. 15

Fifteen bivalents of autosomes and a pseudo-bivalent composed of the X and Y sex chromosomes are present at early MI (Fig. 15a, b). No chiasmata are present in the bivalents; however, one or occasionally two tenacious threads, the so-called *collochores*, hold the homologues together. This pattern, known as the *collochore* type of achiasmate meiosis (Nokkala and Nokkala 1986) was described in all hitherto studied representatives of the family Miridae (for references see Kuznetsova et al. 2011).

FISH with the $(TTAGG)_n$ probe revealed no signals on chromosomal spreads of *H. orientalis* suggesting thus that its telomeres lack, as in *N. sareptanus*, the "insect" tel-

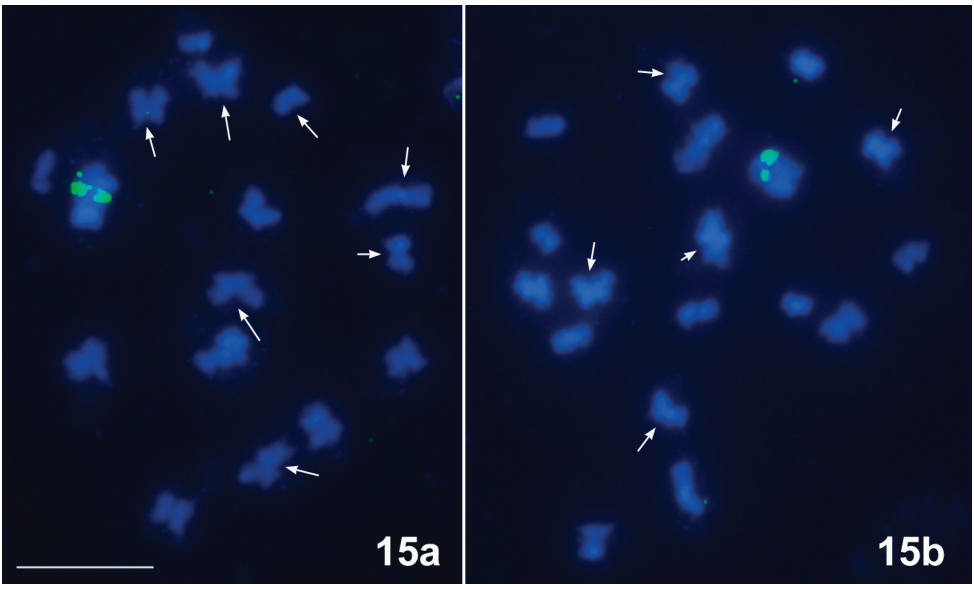

Figure 15. *Horistus orientalis*, 2n (♂) = 32 (30A + XY). FISH with 18S rDNA (green) and telomeric $(TTAGG)_n$ (pink) probes. Early MI – bivalents with one or occasionally two tenacious threads, the so-called *collochores* (arrowed). There are no hybridization signals of the $(TTAGG)_n$ probe; the signals of the 18S rDNA probe are seen on the XY sex chromosome pseudo-bivalent. Scale bar: 10 μm.

omere motif $(TTAGG)_n$. The twin hybridization signals of the 18S rDNA probe were seen on the XY sex chromosome pseudo-bivalent; however, we failed to understand whether they were present on the X or on the Y chromosome. In two another species of the family Miridae studied previously in this respect, *Deraeocoris rutilus* (Herrich-Schaeffer, 1838) and *D. ruber* Linnaeus, 1758, both with an XY sex chromosome system, rDNA clusters were shown to be located on the X chromosome and on both X and Y chromosomes, respectively (Grozeva et al. 2011).

Conclusion

The major result of our work is a compelling support for the absence of the canonical "insect" telomeric TTAGG tandem repeat in the families Nabidae and Miridae (Table 2). It now seems clear that prior notions of these families as groups lacking the insect telomere motif $(TTAGG)_n$ (Frydrychová et al. 2004, Grozeva et al. 2011) are correct. As mentioned in the Introduction, this motif was also not discovered in two another cimicomorphan families, namely, Cimicidae and Tingidae (Grozeva et al. 2004, Golub et al. 2015, 2017, 2018) and in all so far studied species of the sister to the Cimicomorpha infraorder Pentatomomorpha (in the families Lygaeidae s.l., Pyrrhocoridae, and Pentatomidae) (Frydrychová et al. 2004, Grozeva et al. 2011). Mason et al. (2016) have suggested a single loss event of the TTAGG telomeric

Table 2. Karyotypes and results of FISH mapping of telomere $(TTAGG)_n$ motif and 18S rDNA loci.

Taxon	2n ♂	Presence / absence of $(TTAGG)_n$ motif	Location of 18S rDNA loci
Family Reduviidae			
Rhynocoris punctiventris	28 (24A + $X_1X_2X_3Y$)	Present	Y and one of the X chromosomes
Rhynocoris iracundus	28 (24A + $X_1X_2X_3Y$)	Present	Y and one of the X chromosomes
Family Miridae			
Horistus orientalis	32 (30A + XY)	Absent	One of the sex chromosomes (unidentified)
Family Nabidae			
Nabis (*Halonabis*) *sareptanus*	34 (32A + XY)	Absent	Both X and Y chromosomes

repeat before the Cimicomorpha and Pentatomomorpha divergence, and after their separation from the Nepomorpha. The discovery of this motif in the supposedly monophyletic family Reduviidae, both in the second largest subfamily Triatominae (Pita et al. 2016) and in the largest subfamily Harpactorinae (present study), allows diverse speculations.

With approximately 6,800 described species in 25 subfamilies, the assassin bugs represent one of the largest families within the order Hemiptera. Phylogeny and relationships within and between subfamilies of the Reduviidae are far from being resolved (Hwang and Weirauch 2012). According to most available phylogenies, Reduvioidea (Reduviidae + Pachynomidae) are monophyletic and a sister group to the rest Cimicomorpha (Schuh et al. 2009, Weirauch and Schuh 2011). We can therefore assume a scenario where an ancestor of Cimicomorpha + Pentatomomorpha possessed the ancestral in Insecta (Frydrychová et al. 2004) and most likely initial in the Heteroptera (Kuznetsova et al. 2012) motif $(TTAGG)_n$, that retained in the Reduviidae but was then repeatedly lost by other families of the Geocorisae. Similarly, the huge insect orders Coleoptera and Hymenoptera include both TTAGG-positive and TTAGG-negative species, which was interpreted as the multiple loss of the initial telomeric sequence during their evolution (Frydrychová and Marec 2002, Gokhman et al. 2014, Menezes et al. 2017). To be sure, there remains much work toward elucidating the problem and testing the above hypothesis. Future telomere TTAGG-FISH analyses should focus on including additional species and higher-level taxa of the Heteroptera.

Acknowledgements

We thank Dr. Iliya Gyonov who collected *Scarlupella discolor* for this study. The present study was supported by the research project no. AAAA-A19-119020790106-0, by the research grant from the Russian Foundation for Basic Research no 17-04-00828, and by the program of Presidium RAS "Biodiversity of Natural Systems" (Genofunds of living nature and their conservation).

References

Angus RB, Jeangirard C, Stoianova D, Grozeva S, Kuznetsova VG (2017) A chromosomal analysis of *Nepa cinerea* Linnaeus, 1758 and *Ranatra linearis* (Linnaeus, 1758) (Heteroptera, Nepidae). Comparative Cytogenetics 11: 641–657. https://doi.org/10.3897/CompCytogen.v11i4.14928

Bardella VB, Gil-Santana HR, Panzera F, Vanzela ALL (2014) Karyotype diversity among predators of Reduviidae (Heteroptera). Comparative Cytogenetics 8(4): 351–367. https://doi.org/10.3897/CompCytogen.v8i4.8430

Chirino MG, Dalíková M, Marec F, Bressa MJ (2017) Chromosomal distribution of interstitial telomeric sequences as signs of evolution through chromosome fusion in six species of the giant water bugs (Hemiptera, *Belostoma*). Ecology and Evolution 7: 5227–5235. https://doi.org/10.1002/ece3.3098

Frydrychová R, Grossmann P, Trubač P, Vítková M, Marec F (2004) Phylogenetic distribution of TTAGG telomeric repeats in insects. Genome 47: 163–178. https://doi.org/10.1139/g03-100

Frydrychová R, Marec F (2002) Repeated loss of TTAGG telomere repeats in evolution of beetles (Coleoptera). Genetica 115: 179–187. https://doi.org/10.1023/A:1020175912128

Golub NV, Golub VB, Kuznetsova VG (2015) Variability of 18rDNA loci in four lace bug species (Hemiptera, Tingidae) with the same chromosome number. Comparative Cytogenetics 9: 513–522. https://doi.org/10.3897/CompCytogen.v9i4.5376

Golub NV, Golub VB, Kuznetsova VG (2017) Distribution of the major rDNA loci among four hemipteran species of the family Tingidae (Heteroptera, Cimicomorpha). Folia Biologica (Kraków) 65: 155–158. https://doi.org/10.3409/fb65_3.155

Golub NV, Golub VB, Kuznetsova VG (2018) New data on karyotypes of lace bugs (Tingidae, Cimicomorpha, Hemiptera) with analysis of the 18S rDNA clusters distribution. Comparative Cytogenetics 12: 515–528. https://doi.org/10.3897/CompCytogen.v12i4.30431

Gokhman VE, Anokhin BA, Kuznetsova VG (2014) Distribution of 18S rDNA sites and absence of the canonical TTAGG insect telomeric repeat in parasitoid Hymenoptera. Genetica 142: 317–322. https://doi.org/10.1007/s10709-014-9776-3

Grozeva S, Nokkala S (1996) Chromosomes and their meiotic behavior in two families of the primitive infraorder Dipsocoromorpha (Heteroptera). Hereditas 125: 31–36. https://doi.org/10.1111/j.1601-5223.1996.t01-1-00031.x

Grozeva S, Anokhin BA, Kuznetsova VG (2015) Recent advances in cytogenetics of bed bugs: FISH mapping of the 18S rDNA and TTAGG telomeric loci in *Cimex lectularius* Fabricius, 1803 (Hemiptera, Heteroptera, Cimicidae) Chapter 8. In: Sharakhov IV (Ed.) Protocols for chromosome mapping of arthropod genomes (1st ed.). CRC press (Taylor & Francis Group), 283–322.

Grozeva S, Kuznetsova VG, Anokhin BA (2011) Karyotypes, male meiosis and comparative FISH mapping of 18S ribosomal DNA and telomeric (TTAGG) repeat in eight species of true bugs (Hemiptera, Heteroptera). Comparative Cytogenetics 5(4): 355–374. https://doi.org/10.3897/compcytogen.v5i4.2307

Henry TJ (2017) Biodiversity of Heteroptera. In: Foottit RG, Adler PH (Eds) Insect biodiversity: science and society (2nd ed.). Oxford: Blackwell Publishing, 279–336. https://doi.org/10.1002/9781118945568.ch10

Hwang WS, Weirauch C (2012) Evolutionary history of assassin bugs (Insecta: Hemiptera: Reduviidae): insights from divergence dating and ancestral state reconstruction. PLoS ONE 7:e45523. https://doi.org/10.1371/journal.pone.0045523

Kuznetsova VG, Maryańska-Nadachowska A (2000) Autosomal polyploidy and male meiotic pattern in the bug family Nabidae (Heteroptera). Journal of Zoological Systematics and Evolutionary Research 38: 87–94. https://doi.org/10.1046/j.1439-0469.2000.382131.x

Kuznetsova VG, Grozeva SM, Anokhin BA (2012) The first finding of $(TTAGG)_n$ telomeric repeat in chromosomes of true bugs (Heteroptera, Belostomatidae). Comparative Cytogenetics 6: 341–346. https://doi.org/10.3897/compcytogen.v6i4.4058

Kuznetsova VG, Grozeva SM, Hartung V, Anokhin BA (2015) First evidence for $(TTAGG)_n$ telomeric sequence and sex chromosome post-reduction in Coleorrhyncha (Insecta, Hemiptera). Comparative Cytogenetics 9: 523–532. https://doi.org/10.3897/CompCytogen.v9i4.5609

Kuznetsova V, Grozeva S, Nokkala S, Nokkala C (2011) Cytogenetics of the true bug infraorder Cimicomorpha (Hemiptera, Heteroptera): a review. Zookeys 154: 31–70. https://doi.org/10.3897/zookeys.154.1953

Maryańska-Nadachowska A, Anokhin BA, Gnezdilov VM, Kuznetsova VG (2016) Karyotype stability in the family Issidae (Hemiptera, Auchenorrhyncha) revealed by chromosome techniques and FISH with telomeric $(TTAGG)_n$ and 18S rDNA probes. Comparative Cytogenetics 10(3): 347–369. https://doi.org/10.3897/CompCytogen.v10i3.9672

Mason JM, Randall TA, Capkova Frydrychova R (2016) Telomerase lost? Chromosoma 125: 65–73. https://doi.org/10.1007/s00412-015-0528-7

Menezes RST, Bardella VB, Cabral-de-Mello DC, Lucena DAA, Almeida EAB (2017) Are the TTAGG and TTAGGG telomeric repeats phylogenetically conserved in aculeate Hymenoptera? The Science of Nature 104(9–10): 85. https://doi.org/10.1007/s00114-017-1507-z

Nokkala S, Nokkala C (1984) Achiasmatic male meiosis in the Heteropteran genus *Nabis* (Nabidae, Hemiptera). Hereditas 101: 31–35. https://doi.org/10.1111/j.1601-5223.1984.tb00445.x

Nokkala S, Nokkala C (1986) Achiasmatic male meiosis of collochore type in the heteropteran family Miridae. Hereditas 105: 193–197. https://doi.org/10.1111/j.1601-5223.1986.tb00661.x

Okazaki S, Tsuchida K, Maekawa H, Ishikawa H, Fujiwara H (1993) Identification of a pentanucleotide telomeric sequence $(TTAGG)_n$, in the silkworm *Bombyx mori* and in other insects. Molecular and Cellular Biology 13: 1424–1432. https://doi.org/10.1128/MCB.13.3.1424

Pita S, Panzera F, Mora P, Vela J, Palomeque T, Lorite P (2016) The presence of the ancestral insect telomeric motif in kissing bugs (Triatominae) rules out the hypothesis of its loss in evolutionarily advanced Heteroptera (Cimicomorpha). Comparative Cytogenetics 10: 427–437. https://doi.org/10.3897/compcytogen.v10i3.9960

Poggio MG, Bressa MJ, Papeschi AG (2007) Karyotype evolution in Reduviidae (Insecta: Heteroptera) with special reference to Stenopodainae and Harpactorinae. Comparative Cytogenetics 1: 159–168. https://doi.org/10.3897/compcytogen.v5i1.1143

Sahara K, Marec F, Traut W (1999) TTAGG telomeric repeats in chromosomes of some insects and other arthropods. Chromosome Research 7: 449–460. https://doi.org/10.1023/A:1009297729547

Schuh RT, Weirauch Ch, Weeler WC (2009) Phylogenetic relationships within the Cimicomorpha (Hemiptera: Heteroptera): a total-evidence analysis. Systematic Entomology 34: 15–48. https://doi.org/10.1111/j.1365-3113.2008.00436.x

Tiepo AN, Pezenti LF, Lopes TBF, da Silva CRM, Dionisio JF, Fernandes JAM, Da Rosa R (2016) Analysis of the karyotype structure in *Ricolla quadrispinosa* (Linneus, 1767): inferences about the chromosomal evolution of the tribes of Harpactorinae (Heteroptera, Reduviidae). Comparative Cytogenetics 10(4): 719–729. https://doi.org/10.3897/CompCytogen.v10i4.10392

Ueshima N (1979) Hemiptera II: Heteroptera. In: John B (Ed.) Animal Cytogenetics 3. Insecta 6. Gebrüder Bornträger, Berlin, Stuttgart, 113 pp.

Weirauch Ch, Schuh RT (2011) Systematics and Evolution of Heteroptera: 25 Years of Progress. Annual Review of Entomology 56: 487–510. https://doi.org/10.1146/annurev-ento-120709-144833

CompCytogen 13(3): 297–309 (2019)
doi: 10.3897/CompCytogen.v13i3.35524
http://compcytogen.pensoft.net

RESEARCH ARTICLE

COMPARATIVE Cytogenetics
A peer-reviewed open-access journal
International Journal of Plant & Animal Cytogenetics, Karyosystematics, and Molecular Systematics

Chromosome spreading of the (TTAGGG)n repeats in the *Pipa carvalhoi* Miranda-Ribeiro, 1937 (Pipidae, Anura) karyotype

Michelle Louise Zattera[1], Luana Lima[2], Iraine Duarte[1], Deborah Yasmin de Sousa[1], Olívia Gabriela dos Santos Araújo[3], Thiago Gazoni[3], Tamí Mott[2], Shirlei Maria Recco-Pimentel[4], Daniel Pacheco Bruschi[1]

1 *Programa de Pós-Graduação em Genética, Departamento de Genética, Universidade Federal do Paraná (UFPR), Centro Politécnico, Jardim das Américas, 81531-990,Curitiba, Paraná State, Brazil* **2** *Instituto de Ciências Biológicas e da Saúde, Universidade Federal do Alagoas (UFAL), Avenida Louriva Melo Mota S/N, 57072-900, Maceió, Alagoas State, Brazil* **3** *Departamento de Biologia, Instituto de Biociências, Universidade Estadual Paulista (UNESP) – Câmpus Rio Claro, Avenida 24 A 1515, Bela Vista, 13506-900, Rio Claro, São Paulo State, Brazil* **4** *Instituto de Biologia, Departamento de Biologia Estrutural e Funcional, Universidade Estadual de Campinas (UNICAMP), Avenida Bertrand Russel S/N, Barão Geraldo, 13083-865, Campinas, São Paulo State, Brazil*

Corresponding author: *Daniel Pacheco Bruschi* (danielpachecobruschi@gmail.com)

Academic editor: *T. Capriglione* | Received 17 April 2019 | Accepted 10 September 2019 | Published 14 October 2019

http://zoobank.org/171B617B-2024-40C0-B41A-C072343D9489

Citation: Zattera ML, Lima L, Duarte I, Sousa DY, Santos Araújo OG, Gazoni T, Mott T, Recco-Pimentel SM, Bruschi DP (2019) Chromosome spreading of the (TTAGGG)n repeats in the *Pipa carvalhoi* Miranda-Ribeiro, 1937 (Pipidae, Anura) karyotype. Comparative Cytogenetics 13(3): 297–309. https://doi.org/10.3897/CompCytogen.v13i3.35524

Abstract

Pipidae is a clade of Anura that diverged relatively early from other frogs in the phylogeny of the group. Pipids have a unique combination of morphological features, some of which appear to represent a mix of adaptations to aquatic life and plesiomorphic characters of Anura. The present study describes the karyotype of *Pipa carvalhoi* Miranda-Ribeiro, 1937, including morphology, heterochromatin distribution, and location of the NOR site. The diploid number of *P. carvalhoi* is 2n=20, including three metacentric pairs (1, 4, 8), two submetacentric (2 and 7), three subtelocentric (3, 5, 6), and two telocentric pairs (9 and 10). C-banding detected centromeric blocks of heterochromatin in all chromosome pairs and the NOR detected in chromosome pair 9, as confirmed by FISH using the rDNA 28S probe. The telomeric probes indicated the presence of interstitial telomeric sequences (ITSs), primarily in the centromeric region of the chromosomes, frequently associated with heterochromatin, suggesting that these repeats are a significant component of this region. The findings of the present study provide important insights for the understanding of the mechanisms of chromosomal evolution in the genus *Pipa*, and the diversification of the Pipidae as a whole.

Keywords
Pipidae, chromosome banding, interstitial telomeric sequences, rearrangements, chromosome evolution

Introduction

Chromosome studies provide important insights into the diversification of karyotypes and represent an effective approach for the identification of homologies among species (Targueta et al. 2018). This approach provides a systematic understanding of the rearrangements of the genome that have occurred during the evolutionary history of the target group.

Pipids are a clade of anurans that diverged relatively early from other frogs in the phylogeny of the group (Pyron and Wiens 2011). Pipids have a unique combination of morphological features, some of which appear to represent a mix of adaptations to aquatic life and plesiomorphic characters of Anura (Cannatella and Trueb 1988, Cannatella 2015, Araújo et al. 2017). The frogs of the family Pipidae dwell in freshwater environments and have behavioral and physiological features that are unique in anuran amphibians, making this group an excellent model for evolutionary studies (Cannatella and Trueb 1988, Cannatella and De Sá 1993, Pough et al. 2001). The family currently includes four genera: *Hymenochirus* Boulenger, 1896 (4 species), *Pseudohymenochirus* Chabanaud, 1920 (1 species), *Xenopus* Wagler, 1827 (29 species), and *Pipa* Laurenti, 1768 (7 species), which are distributed in sub-Saharan Africa and South America (Frost 2019).

However, based on molecular phylogenetic inferences and presumed ancestral diploid numbers, some authors have distinguished a fifth lineage, *Silurana*, which includes all the species derived from an ancestor with 2n = 20 (Evans et al. 2004, Pyron and Wiens 2011), from *Xenopus*, which has an ancestral diploid number of 2n = 18. Evans et al. (2015) suggested that *Xenopus* should be divided into two subgenera, *Xenopus* and *Silurana*. Other authors consider *Xenopus* and *Silurana* a monophyletic clade, without the necessity of separation of subfamilies or genera between them (e.g., De Sá and Hillis 1990, Cannatella and De Sá 1993, Graf et al. 1996), in this work we will consider them as a single group, *Xenopus tropicalis* group (Frost 2019).

Pipa is the only non-African representative of the Pipidae, and evidences from a number of different sources indicates that this South American lineage is derived from an ancestor closely related to the extant members of the genus *Hymenochirus*. Pipidae was widely distributed in Gondwana and after its splintering, those lineages had distributions associated with the Afro-Tropical (*Hymenochirus*, *Pseudhymenochirus* and *Xenopus*) and Neotropical Regions (*Pipa*). The historical isolation resulted in the diversification of the ancestral lineage of the genus *Pipa*, which is found in South America, as far north as Panama (Trueb et al. 2005, Frost 2019).

The genus currently contains seven species: *P. arrabali* Izecksohn, 1976, *P. aspera* Mueller, 1924, *P. carvalhoi* Miranda-Ribeiro, 1937, *P. myersi* Trueb, 1984, *P. parva* Ruthven & Gaige, 1923, *P. pipa* (Linnaeus, 1758), and *P. snethlageae* Muller, 1914 (Frost 2019). In most cases, the only cytogenetic information available for the pipid

species is the diploid number. The *Xenopus* + *Silurana* lineages (*sensu* Evans et al. 2015), the sister group of *Pipa*, have the largest number of karyotyped species, including recurrent cases of polyploidy, with the chromosomal number being used as a criterion for the description of new species (Evans et al. 2015). The karyotypes of *Hymenochirus boettgeri* (Tornier, 1896) and *Pseudohymenochirus merlini* Chabanaud, 1920 (a monotypic genus) were described recently, filling gaps in the chromosomal history of the Pipidae (Mezzasalma et al. 2015). In the case of *Pipa* the available cytogenetic data are limited to the diploid numbers for *P. parva* (2n = 30) and *P. pipa*, with 2n = 22 (Wickbom 1950, Morescalchi 1968, Morescalchi et al. 1970). *Pipa carvalhoi* present a diploid number of 20 chromosomes; however, this information was only determined based on an ideogram published by Mezzasalma et al. (2015), which was inferred based on the data of an unpublished degree thesis (Pfeuffer-Friederich 1980).

As no data whatsoever are available for the other five *Pipa* species, further studies will be essential for the understanding of the genomic rearrangements that have occurred during the adaptive radiation of this lineage in South America. Here, we describe the karyotype of *P. carvalhoi*, including the position of the NORs and the distribution pattern of the heterochromatin. We also documented the intrachromosomal spread of the telomeric (TTAGGG)n motifs and discuss these findings in the context of the phylogenetic scenario of the family Pipidae.

Material and methods

Samples

We analyzed three specimens of *Pipa carvalhoi* collected in Buerarema (three male), Bahia state, Brazil, and three from Buíque (two male + one juvenile), Pernambuco state, Brazil. The collection of specimens was authorized by SISBIO/Instituto Chico Mendes de Conservação da Biodiversidade through protocol number 55481-1. The specimens were deposited in the "Célio Fernando Baptista Haddad" Amphibian Collection (CFBH), on the Rio Claro campus of São Paulo State University (UNESP) and in Natural History Museum in Universidade Federal de Alagoas (MHN-UFAL).

Staining procedures

The chromosomal preparations were obtained from intestinal and testicular cells treated with 2% colchicine for 4 hours, using techniques modified from King and Rofe (1976) and Schmid (1978). The mitotic metaphases were stained with 10% Giemsa for karyotyping. The heterochromatic regions were identified by C-banding, using the technique described by Sumner (1972) and C-banding + DAPI. We detected the NORs using the Ag-NOR method (Howell and Black 1980). The chromosomes were ranked and classified according to the scheme of Green and Sessions (1991).

Fluorescence *in situ* hybridization

Loci of 28S rDNA were detected fluorescence *in situ* hybridization (FISH). We used the 28S fragment isolated by Bruschi et al. (2012) to detect the rDNA genes. This probe was PCR-labeled with digoxigenin and hybridized following the protocol of Viegas-Péquignot (1992). Finally, the vertebrate telomeric (TTAGGG)n sequence probe was obtained by PCR amplification and labeling, based on Ijdo et al. (1991).

Results

The diploid number of the *P. carvalhoi* karyotype was 2n = 20 chromosomes (Fig. 1). The karyotype contains three metacentric pairs (1, 3, 8), two submetacentric (2 and 7), three subtelocentric (4, 5, 6), and two telocentric pairs, 9 and 10 (Fig. 1). The same karyotype was recorded in both populations.

The C-banding technique detected centromeric blocks of heterochromatin in all chromosome pairs. Interstitial heterochromatin blocks were also detected in the long arms of pair 5 (Fig. 1B). Pericentromeric C-positive banding was observed in the long arm of pair 3, and in the short arm of the submetacentric pair 7 (Fig. 1B). The centromeric blocks of heterochromatin presented DAPI-positive signals in all the chromosomes, in addition to pericentromeric heterochromatin in pair 3 (Fig. 1C). The DAPI staining also revealed a conspicuous bright signal in the pericentromeric regions of both arms of pair 3 and 8. Neither of these features were revealed by the C-banding (Fig. 1C).

Under conventional Giemsa staining, a secondary constriction was observed in the subterminal regions of the homologs of pair 9, which coincides with the NOR site (in both populations), detected by the Ag-NOR method and confirmed by FISH using the rDNA 28S probe (Fig. 2A), and this region was DAPI-negative (Fig. 2B). The telomeric probe hybridized all the telomeres in the chromosomes of *P. carvalhoi*. Conspicuous signals of Interstitial Telomeric Sequences (ITSs) can be observed in the centromeric/pericentromeric region of the homologs of pairs 1, 2, 4, 5, 6, 7, and 8, and in the interstitial region of the long arm of chromosome pair 9. A secondary constriction was also observed in chromosome pair 8 (Fig. 2A, C).

Discussion

The chromosomal evolution of the pipids appears to have involved complex rearrangements, including recurrent polyploidization events and associated shifts in the diploid number (Table 1). In the present study, we redescribed the karyotype of *P. carvalhoi*, including the distribution of the heterochromatin and the NOR site. In the phylogenetic reconstructions of the superfamily Pipoidea proposed by Pyron and Wiens (2011) and Irisarri (2011), the 2n = 22 diploid number was identified as the plesiomorphic condi-

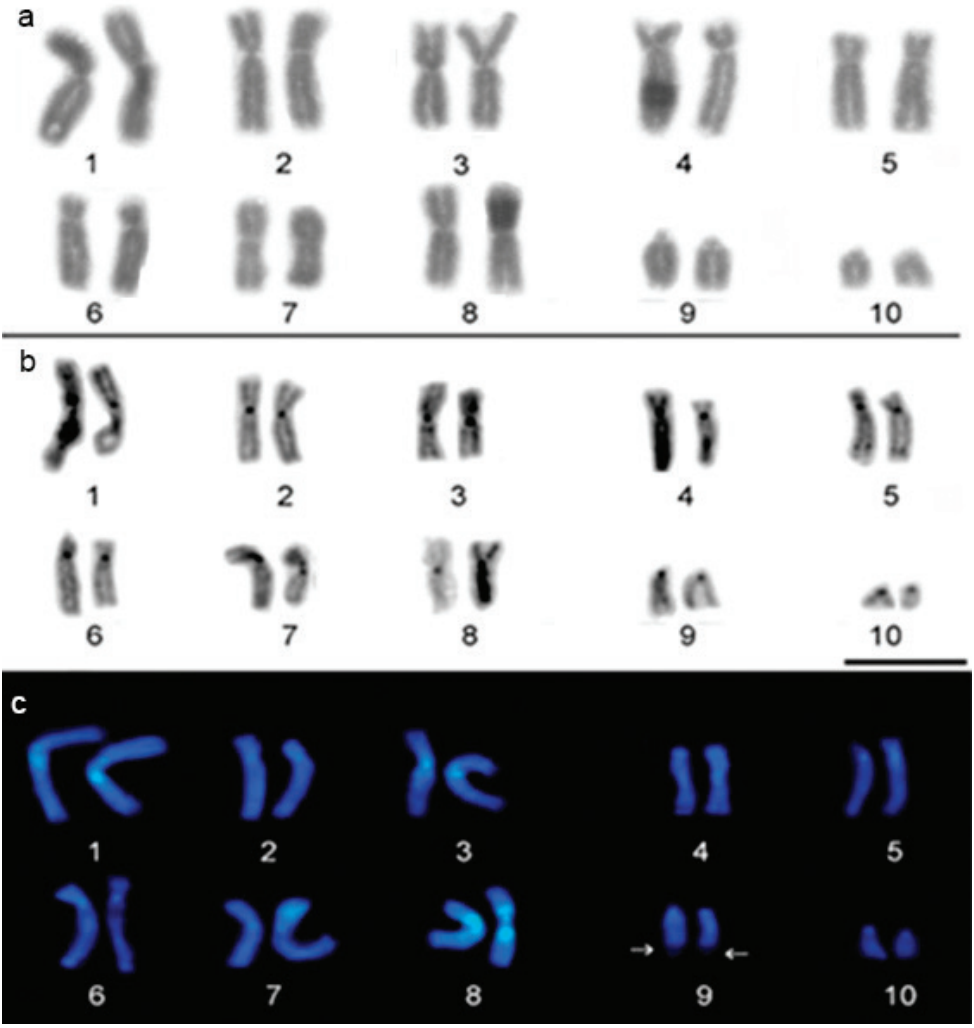

Figure 1. Karyotype of *P. carvalhoi*. **a** Prepared by conventional Giemsa staining **b** C-banding and **c** DAPI staining. The arrow indicates the NOR site.

tion, based on the karyotype of *Rhinophrynus dorsalis* Duméril & Bibron, 1841 (Bogart and Nelson 1976), the only member of the Rhinophrynidae.

Subsequently, Mezzasalma et al. (2015) proposed that the ancestral karyotype of Pipidae had a diploid number of 2n = 20, based on the conserved diploid numbers observed in *Xenopus* (= *Silurana*) *tropicalis* and *Hymenochirus boettgeri* + *Pseudhymenochirus merlini*. The phylogenetic inferences of Evans et al. (2004) and Irisarri (2011) indicated the existence of two clades in the clawed frogs (*Xenopus*), with a well-supported synapomorphy of the diploid number, which divides the species of this genus into two separate lineages: the subgenus *Silurana* (2n = 20) and the subgenus *Xenopus*, which has the primitive diploid number (2n = 18). The diploid number (2n = 20) found in

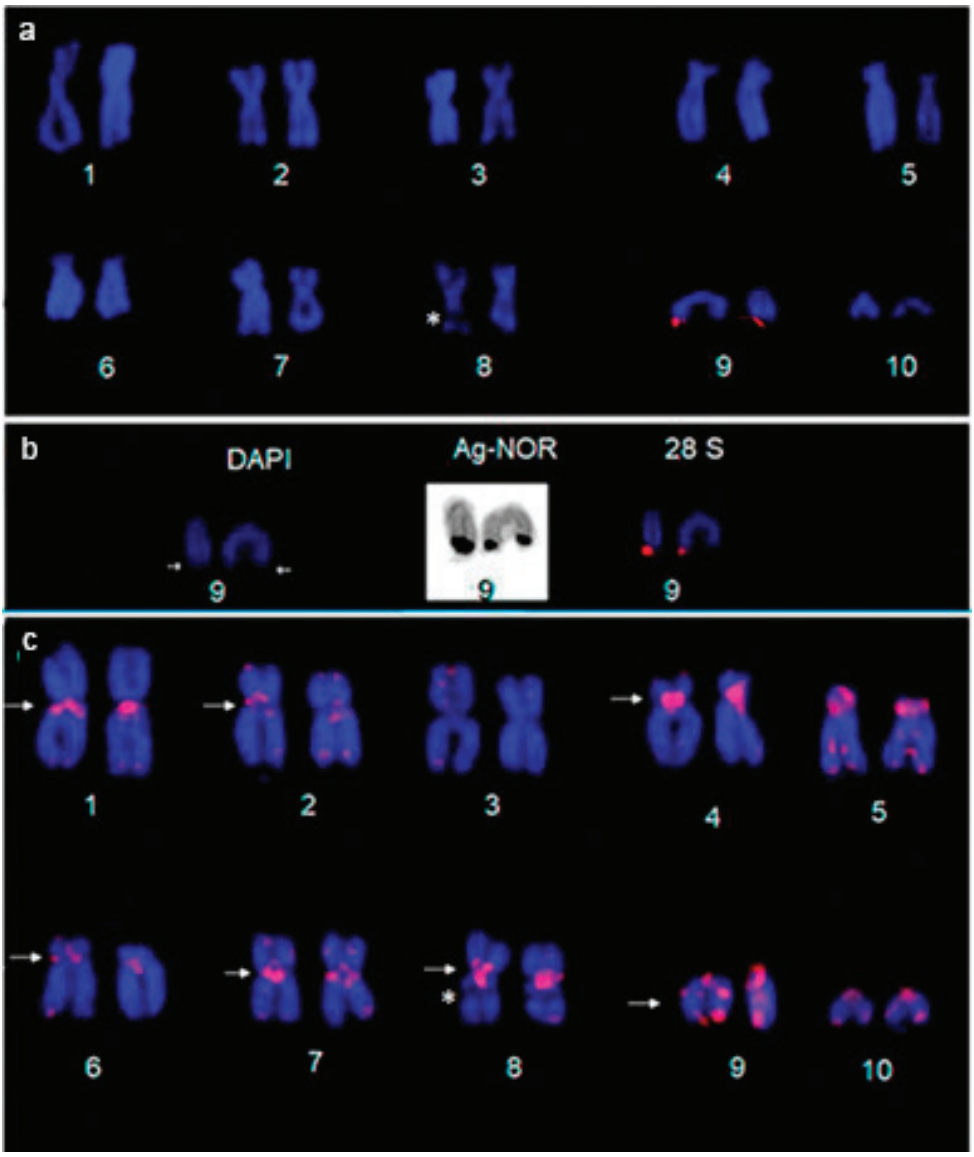

Figure 2. Fluorescence *in situ* hybridization in *P. carvalhoi* karyotype. **a** Hybridized with the 28S rDNA probe **b** the NOR-bearing chromosome highlighted by DAPI-staining, the Ag-NOR method, and FISH with 28S rDNA **c** *In situ* hybridization with the telomeric probe in the karyotype of *P. carvalhoi* from Pernambuco, Brazil. The arrows in **c** indicate the interstitial telomeric sequences (ITSs) and the constriction in chromosome 8 are indicates by asterisk.

Xenopus (= *Silurana*) *tropicalis* (Gray, 1864) and the polyploidy of the species derived from this form [2n = 4x = 40: *Xenopus* (= *Silurana*) *calcaratus* Peters, 1877; *Xenopus* (= *Silurana*) *epitropicalis* Fischberg, Colombelli and Picard 1982; *Xenopus* (= *Silurana*) *mellotropicalis* Evans et al. 2015] correspond to a retention of the plesiomorphic condition of the pipids (Mezzasalma et al. 2015).

Table 1. Detailed cytogenetic data available for species of the Pipidae family. NOR: Nucleolar Organizer Region; M= metacentric; SM= submetacentric; ST=subtelocentric; T=telocentric; p= short arm; q=long arm; (–) no data.

Species	Ploidy level	Karyotype formula	NOR site	Reference
***Xenopus tropicalis* group**				
X. tropicalis	2n = 20	2 M + 14 SM + 4 A	5q	Tymowska and Fischberg 1973; Uehara et al. 2002
X. epitropicalis	4n = 40	4M + 28 SM+ 8 A	5q	Tymowska and Fischberg 1982; Tymowska 1991
X. new tetraploid 1	4n = 40	4M + 28 SM+ 8 A	5q	Tymowska 1991; Evans et al. 2004
X. new tetraploid 2	4n = 40	4M + 28 SM+ 8 A	5q	Evans et al. 2004
***Xenopus laevis* group**				
X. borealis	4n = 36	6 M+ 14 SM+ 2 ST + 14 T	4p	Tymowska and Fischberg 1973; Tymowska 1991
X. clivii	4n = 36	6 M+ 14 SM+ 2 ST + 14 T	4p	Tymowska and Fischberg 1973; Tymowska 1991
X. fraseri	4n = 36	6 M+ 14 SM+ 2 ST + 14 T	6q	Tymowska and Fischberg 1973; Tymowska 1991
X. gilli	4n = 36	6 M+ 14 SM+ 2 ST + 14 T	12p	Tymowska and Fischberg 1973; Tymowska 1991
X. laevis laevis	4n = 36	6 M+ 14 SM+ 2 ST + 14 T	12p	Tymowska 1991
X. laevis bunyoniensis	4n = 36	6 M+ 14 SM+ 2 ST + 14 T	–	Tymowska 1991
X. laevis petersi	4n = 36	6 M+ 14 SM+ 2 ST + 14 T	–	Tymowska and Fischberg 1973; Tymowska 1991
X. laevis poweri	4n = 36	6 M+ 14 SM+ 2 ST + 14 T	–	Tymowska 1991
X. laevis sudanensis	4n = 36	6 M+ 14 SM+ 2 ST + 14 T	–	Tymowska 1991
X. laevis victorianus	4n = 36	6 M+ 14 SM+ 2 ST + 14 T	–	Tymowska and Fischberg 1973; Tymowska 1991
X. largeni	4n = 36	6 M+ 14 SM+ 2 ST + 14 T	–	Tymowska 1991
X. muelleri	4n = 36	6 M+ 14 SM+ 2 ST + 14 T	4p	Tymowska and Fischberg 1973; Tymowska 1991
X. pygmaeus	4n = 36	6 M+ 14 SM+ 2 ST + 14 T	6q	Loumont 1986
X. sp. nov. VI	4n = 36	6 M+ 14 SM+ 2 ST + 14 T	4p	Tymowska 1991
X. sp. nov. IX	4n = 36	6 M+ 14 SM+ 2 ST + 14 T	12p	Tymowska 1991
X. amieti	8n = 72	12 M + 28 SM + 4 ST + 28 T	5q	Kobel et al. 1980
X. andrei	8n = 72	12 M + 28 SM + 4 ST + 28 T	18q	Loumont 1983
X. boumbaensis	8n = 72	12 M + 28 SM + 4 ST + 28 T	6p+ 4p	Loumont 1983
X. itombwensis	8n = 72	12 M + 28 SM + 4 ST + 28 T	–	Evans et al. 2008
X. lenduensis	8n = 72	12 M + 28 SM + 4 ST + 28 T	–	Evans et al. 2011
X. vestitus	8n = 72	12 M + 28 SM + 4 ST + 28 T	12p	Tymowska 1991
X. wittei	8n = 72	12 M + 28 SM + 4 ST + 28 T	12p	Tymowska 1991
X. sp. nov. X	8n = 72	12 M + 28 SM + 4 ST + 28 T	18q	Tymowska 1991
X. longipes	12n = 108	18 M + 42 SM + 6 ST + 42 T	7p	Loumont and Kobel 1991
X. ruwenzoriensis	12n = 108	18 M + 42 SM + 6 ST + 42 T	11q	Tymowska and Fischberg 1973; Tymowska 1991
X. cf. *boumbaensis*	12n = 108	18 M + 42 SM + 6 ST + 42 T	7p	Evans 2007
X. sp. nov. VIIIa	12n = 108	18 M + 42 SM + 6 ST + 42 T	7p	Tymowska 1991
Genus *Pseudhymenochirus*				
P. merlini	2n = 20	8 M + 4 SM + 6 ST + 2 T	10q	Mezzasalma et al. 2015
Genus *Hymenochirus*				
H. boettgeri	2n = 20	14 M + 2 SM + 4 ST	4p	Mezzasalma et al. 2015
Genus *Pipa*				
P. carvalhoi	2n = 20	6 M+ 4 SM+6 ST + 4 T	9q	Present study
		8 M + 8 SM + 4 T[†]		Mezzasalma et al. 2015
P. pipa	2n = 22	8 M + 14 A	–	Wickbom 1950
		6M + 2ST + 14A		Morescalchi et al. 1970
P. parva	2n = 30	30 T	–	Morescalchi 1981

[†]Chromosomal formula shown by Mezzasalma et al. 2015 was based in Pfeuffer-Friederich 1980 and Sachsse 1980.

The diploid number (2n = 20) recorded here in *P. carvalhoi* also corresponds to a retention of the plesiomorphic condition of the pipids, and an overview of all the known karyotypes of pipid species indicates that the morphology of pairs 1, 2, 3, and 4 is highly conserved, as it is in the outgroup, *Rhinophrynus dorsalis* (Mezzasalma et al. 2015). Despite the conservative karyology of the principal pipid clades, the known diploid numbers of *Pipa* species vary considerably. The two other species for which data are available are *P. parva*, which has a karyotype (2n = 30) composed entirely of telocentric pairs (Wickbom 1950, Morescalchi 1968), and *P. pipa*, which has a diploid number of 2n = 22 (Morescalchi et al. 1970).

The comparison of the karyotypes of *P. carvalhoi* and *P. pipa* (Wickbom 1950, Morescalchi et al. 1970) indicates interspecific chromosomal homologies of the metacentric and submetacentric pairs 1, 2, 3, and 4. The minor differences between the *P. pipa* karyotypes published by Wickbom (1950) and Morescalchi et al. (1970) are derived from variation in the chromosomal nomenclature adopted in the two studies, rather than any real karyotype differences among the *P. pipa* populations. As the *P. parva* karyotype contains only telocentric pairs, the recognition of chromosome homologies with other *Pipa* species are currently restricted by the lack of appropriate markers.

The pericentromeric heterochromatin block in the homologs of pair 3 of *P. carvalhoi* could be a common feature of pipid karyotypes. Interestingly, this heterochromatin block, is also present in *Xenopus* (= *Silurana*) *tropicalis* (Tymowska & Fischberg, 1982), *Hymenochirus boettgeri*, and *Pseudhymenochirus merlini* karyotype (Mezzasalma et al. 2015), which all have a diploid number of 2n = 20 chromosomes. As the configuration of the heterochromatin is a valuable marker for the interspecific comparison of karyotypes, the unique non-centromeric heterochromatin blocks found in some of the chromosomes of *P. carvalhoi* constitute an important diagnostic trait for the analysis of the interspecific variation in the pipids, based on C-banding.

We detected interstitial telomeric sequences (ITSs) in the centromeric/pericentromeric region of the metacentric and submetacentric chromosomes of the *P. carvalhoi* karyotype. Based in Mezzasalma et al. (2015) hypothesis, the *P. carvalhoi* karyotype have been diversification from primitive Pipidae karyotype mainly by pericentromeric inversion involved pairs 3, 6, 8-10. In our data, the pericentromeric ITS detected in homologues of pairs 6, 8 and 9 validated this hypothesis, highlights the role of the intrachromosomal rearrangements shaping karyotype diversification in Pipidae. The pericentromeric inversion involved pair 3 occurred without repositioned telomeric repeats that justify absence of the ITS in this metacentric pair. Canonical telomeric repeats are located in the terminal regions of the chromosomes, but several vertebrate species have blocks of (TTAGGG)n repeats in non-terminal regions of their chromosomes (Meyne et al. 1990, Bolzán 2017). Non-telomeric (TTAGGG) n repeats have been described frequently in anuran species see (Bruschi et al. 2014, Schmid and Steinlein 2016, Schmid et al. 2018). For example, Nanda et al. (2008) reported the presence of ITSs in pipid chromosomes for the first time, detecting a wealth of non-telomeric (TTAGG)n repeats in the chromosomes of *Xenopus clivii*

Peracca, 1898, in pair 17 of the *Xenopus Laevis* (Daudin, 1802) karyotype, and associated with the NOR in *X. borealis* and *X. muelleri* (Peters, 1844). Interestingly, the ITS markers were fundamental to the discrimination of the karyotypes of these four species, which all share the same diploid number (2n = 36) and have highly uniform chromosome morphology, when analyzed using a classical cytogenetic approach. The ITSs distinguish *X. clivii*, which has much more numerous ITSs in comparison with the other *Xenopus* karyotypes.

Despite being an unusual feature of vertebrate genomes, we found ITS sites in euchromatic regions (in pair 9, for example), as found in some other anuran species. Schmid and Steinlein (2016) proposed 'large ITSs in restricted euchromatic regions (restricted eu-ITSs)' as a new category of ITS in anuran karyotypes. These euchromatic ITSs have already been documented in chromosome pairs 2 and 9 of *Hypsiboas boans* (Linnaeus, 1758) (Schmid and Steinlein 2016), which is consistent with the presence of these markers in pair 9 of *P. carvalhoi*.

Adopting the parsimony criterion, we rejected the hypothesis that the ITSs detected in the *P. carvalhoi* karyotype are remnants of centric (Robertsonian) fusions, given that *P. carvalhoi* has the plesiomorphic pipid diploid number. However, for some chromosomes (pairs 6, 8 and 9) theses ITS to confirm occurrence of the intrachromosomal rearrangements during evolution of this karyotype. Already, for others ITS signals, our data support the conclusion that the presence of the intrachromosomal telomeric motif (TTAGGG)n represents a component of the repetitive DNA sequences spread throughout these chromosomes. Furthermore, the ITSs found in the *P. carvalhoi* chromosomes coincide with the heterochromatic blocks detected by C-banding in chromosomes 1, 2, 4, 5 and 7. The role of telomeric repeats as repetitive motifs of part of the satellite DNA has already been described in a number of rodent genera, with a unique signal being found in the pericentromeric heterochromatin together with Msat-160 or in telomeric probes, in experiments with co-located het-ITSs and the Msat-160 satellite DNA (Rovatsos et al. 2011).

Ruiz-Herrera et al. (2008) proposed a model to account for the presence of short ITSs in the genome of vertebrates, in which the sequences originate from the insertion of telomeric repeats during the repair of double-strand breaks (DBSs) in the DNA, which may occur either with or without the intervention of telomerase, with the telomerase-mediated repair of the DSBs possibly leading to the appearance of ITSs. Bolzán and Bianchi (2006) concluded that the amplification of these sequences may be related to (i) the insertion of telomeric repeats during the repair of double-strand breaks or (ii) transposable elements. In the former case (i), the telomerase may catalyze the addition of telomeric sequences directly to non-terminal regions through the direct addition of (TTAGGG)n repeats to the ends of broken chromosomes (chromosome healing). The amplification of the ITSs may also occur through unequal crossing over between the repeats of sister chromatid breakage-fusion-bridge cycles, replication slippage (Lin and Yan 2008), gene conversion, and excision and reintegration events through the 'rolling circle' mechanism (Bolzán 2017).

Conclusion

Overall, then, the results of the present study indicate that *P. carvalhoi* has a karyotype of 2n = 20 chromosomes, supporting that this chromosome formula represents the pleiomorphic condition of the pipids, with interspecific chromosomal homologies indicating a highly conserved karyotype configuration. The presence of ITSs in some chromosomes may have originated independently during the chromosomal evolution of this species which in others pairs correspond to evidences of the pericentromeric inversions occurred during Pipidae karyotype diversification. The findings of the present study provide important insights into the mechanisms of chromosomal evolution in the genus *Pipa* and the diversification of the family Pipidae as a whole.

Acknowledgements

We thank the Fundação de Amparo a Pesquisa do Estado de São Paulo (FAPESP 2016/07717-6), Coordenação de Aperfeiçoamento de Pessoal de Nível Superior (CAPES/PROAP – Finance Code 001) for the scholarships provided to MLZ, LL, ID and DY, and Conselho Nacional de Desenvolvimento Científico e Tecnológico (CNPq/PQ/309904/2015-3). We thank the Multi-User Confocal Microscopy Center of the Federal University of Paraná for the capture of the images included in this study.

References

Araújo OGS, Pugener LA, Haddad CFB, Da Silva HR (2017) Morphology and development of the hyolaryngeal apparatus of *Pipa arrabali* (Anura: Pipidae). Zoologischer Anzeiger 269: 78–88. https://doi.org/10.1016/j.jcz.2017.07.001

Bogart JP, Nelson CE (1976) Evolutionary implications from karyotypic analysis of frogs of the families Aficrohylidae and Rhinophrynidae. Herpetologica 32: 199–208. https://www.jstor.org/stable/3891738

Bolzán AD, Bianchi MS (2006) Telomeres, interstitial telomeric repeat sequences and chromosomal aberrations. Mutation Research 612: 189–214. https://doi.org/10.1016/j.mrrev.2005.12.003

Bolzán AD (2017) Interstitial telomeric sequences in vertebrate chromosomes: Origin, function, instability and evolution. Mutation Research – Reviews in Mutation Research 773: 51–65. https://doi.org/10.1016/j.mrrev.2017.04.002

Bruschi DP, Busin CS, Siqueira S, Recco-Pimentel SM (2012) Cytogenetic analysis of two species in the *Phyllomedusa hypochondrialis* group (Anura, Hylidae). Hereditas 149: 34–40. https://doi.org/10.1111/j.1601-5223.2010.02236.x

Bruschi DP, Rivera M, Lima AP, Zúñiga AB, Recco-Pimentel SM (2014) Interstitial Telomeric Sequences (ITS) and major rDNA mapping reveal insights into the karyotypical evolution of Neotropical leaf frog species (*Phyllomedusa*, Hylidae, Anura). Molecular Cytogenetics 7(1): 22. https://doi.org/10.1186/1755-8166-7-22

Cannatella DC, Trueb L (1988) Evolution of pipoid frogs: Intergeneric relationships of the aquatic frog family Pipidae (Anura). Zoological Journal of the Linnean Society 94: 1–38. https://doi.org/10.1111/j.1096-3642.1988.tb00880.x

Cannatella DC, De Sá RO (1993). *Xenopus laevis* as a Model Organism. Systematic Biology 42(4): 476–507. https://doi.org/10.1093/sysbio/42.4.476

Cannatella D (2015) *Xenopus* in Space and Time: Fossils, Node Calibrations, Tip-Dating, and Paleobiogeography. Cytogenetic and Genome Research 145(3–4): 283–301. https://doi.org/10.1159/000438910

De Sá RO, Hillis DM (1990) Phylogenetic relationships of the pipid frogs *Xenopus* and *Silurana*: an integration of ribosomal DNA and morphology. Molecular Biology and Evolution 7: 365–376. https://doi.org/10.1093/oxfordjournals.molbev.a040612

Evans BJ, Kelley DB, Tinsley RC, Melnick DJ, Cannatella DC (2004) A mitochondrial DNA phylogeny of clawed frogs: phylogeography on sub-Saharan Africa and implications for polyploid evolution. Molecular Phylogenetics and. Evolution 33: 197–213. https://doi.org/10.1016/j.ympev.2004.04.018

Evans BJ (2007) Ancestry influences the fate of duplicated genes millions of years after polyploidization of clawed frogs (*Xenopus*). Genetics 176: 1119–1130. https://doi.org/10.1534/genetics.106.069690

Evans BJ, Carter TF, Tobias ML, Kelley DB, Hanner R, Tinsley RC (2008) A new species of clawed frog (genus *Xenopus*) from the Itombwe Massif, Democratic Republic of the Congo: implications for DNA barcodes and biodiversity conservation. Zootaxa 1780: 55–68. https://doi.org/10.5281/zenodo.182322

Evans BJ, Greenbaum E, Kusamba C, Carter TF, Tobias ML, Mendel SA, Kelley DB (2011) Description of a new octoploid frog species (Anura: Pipidae: *Xenopus*) from the Democratic Republic of the Congo, with a discussion of the biogeography of African clawed frogs in the Albertine Rift. Journal of Zoology 283: 276–290. https://doi.org/10.1111/j.1469-7998.2010.00769.x

Evans BJ, Carter TF, Greenbaum E, Gvoždík V, Kelley DB, McLaughlin PJ, Pauwels OSG, Portik DM, Stanley EL, Tinsley RC, Tobias ML, Blackburn DC (2015) Genetics, Morphology, Advertisement Calls, and Historical Records Distinguish Six New Polyploid Species of African Clawed Frog (*Xenopus*, Pipidae) from West and Central Africa. PLoS ONE 10(12). https://doi.org/10.1371/journal.pone.0142823

Frost DR (2019) Amphibian Species of the World: An Online Reference. American Museum of Natural History, New York. [Electronic Database] http://research.amnh.org/herpetology/amphibia/index.html [Version 6.0 accessed 15. March 2019]

Green DM, Sessions SK (1991) Nomenclature for chromosomes. In: Amphibian cytogenetics and evolution. Academic Press, San Diego, 431–432. https://doi.org/10.1016/B978-0-12-297880-7.50021-4

Howell WM, Black DA (1980) Controlled silver staining of nucleolar organizer regions with a protective colloidal developer: a –1 step method. Experientia 36: 1014–1015. https://doi.org/10.1007/BF01953855

Ijdo JW, Wells RA, Baldini A, Reeders ST (1991) Improved telomere detection using a telomere repeat probe (TTAGGG)n generated by PCR. Nucleic Acids Research 19(17): 4780. https://doi.org/10.1093/nar/19.17.4780

Irisarri I (2011) Reversal toair-driven sound production revealed by a molecular phylogeny of tongueless frogs, family Pipidae. BMC Evolutionary Biology 11: 114. https://doi.org/10.1186/1471-2148-11-114

King M, Rofe R (1976) Karyotypic variation in the Australian gecko *Phyllodactylus marmoratus* (Gray) (Gekkonidae: Reptilia). Chromosoma 54: 75–87. https://doi.org/10.1007/BF00331835

Kobel HR, Du Pasquier L, Fischberg M, Gloor H (1980) *Xenopus amieti* sp. nov. (Anura: Pipidae) from the Cameroons, another case of tetraploidy. Revue Suisse Zoologie 87: 919–926. https://doi.org/10.5962/bhl.part.85562

Lin KW, Yan J (2008) Endings in the middle: Current knowledge of interstitial telomeric sequences. Mutation Research 658: 95–110. https://doi.org/10.1016/j.mrrev.2007.08.006

Loumont C (1983) Deux espèces nouvelles de *Xenopus* du Cameroun (Amphibia, Pipidae). Revue Suisse Zoologie 90: 169–177. https://doi.org/10.5962/bhl.part.81970

Loumont C (1986) *Xenopus pygmaeus*, a new diploid pipid frog from rain forest of equatorial Africa. Revue Suisse Zoologie 93: 755–764. https://doi.org/10.5962/bhl.part.79511

Loumont C, Kobel HR (1991*) Xenopus longipes* sp. nov., a new polyploid pipid from western Cameroon. Revue Suisse Zoologie 98: 731–738. https://doi.org/10.5962/bhl.part.79810

Meyne J, Baker RJ, Hobart HH, Hsu TC, Ryder OA, Ward OG, Wiley JE, Wurster-Hill DH, Yates TL, Moyzis RK (1990) Distribution of non-telomeric sites of the (TTAGGG) n telomeric sequence in vertebrate chromosomes. Chromosoma: 99: 3–10. https://doi.org/10.1007/BF01737283

Mezzasalma M, Glaw F, Odierna G, Petraccioli A, Maria Guarino FM (2015) Karyological analyses of *Pseudhymenochirus merlini* and *Hymenochirus boettgeri* provide new insights into the chromosome evolution in the anuran family Pipidae. Zoologischer Anzeiger 258: 47–53. https://doi.org/10.1016/j.jcz.2015.07.001

Morescalchi A (1968) Initial cytotaxonomic data on certain families of amphibious Anura (Diplasiocoela, after Noble). Experientia 24: 280–283. https://doi.org/10.1007/BF02152819

Morescalchi A, Gargiulo G, Olmo E (1970) Notes on the chromosomes of some Amphibia. Journal of Herpetology 4: 77–79. https://doi.org/10.2307/1562706

Nanda I, Fugate M, Steinlein C, Schmid M (2008) Distribution of (TTAGGG) n telomeric sequences in karyotypes of the *Xenopus* species complex. Cytogenetic and Genome Research 122: 396–400. https://doi.org/10.1159/000167828

Pagnozzi JM, De Jesus Silva MJ, Yonenaga-Yassuda Y (2000) Intraspecific variation in the distribution of the interstitial telomeric (TTAGGG)(n) sequences in *Micoureus demerarae* (Marsupialia: Didelphidae). Chromosome Research 8: 585–591. https://doi.org/10.1023/A:1009229806649

Pough FH, Andrews RM, Cadle JE, Crump ML, Savitzky AH, Wells KD (2001) Herpetology. Prentice-Hall, New Jersey, 544 pp.

Pyron RA, Wiens JJ (2011) A large-scale phylogeny of Amphibia including over 2800 species, and a revised classification of extant frogs, salamanders, and caecilians. Molecular Phylogenetic and Evolution 61: 543–583. https://doi.org/10.1016/j.ympev.2011.06.012

Rovatsos MT, Marchal JA, Romero-Fernández I, Fernández FJ, Giagia-Athanosopoulou EB, Sánchez A (2011) Rapid, independent, and extensive amplification of telomeric repeats

in pericentromeric regions in karyotypes of arvicoline rodents. Chromosome Research 19: 869–882. https://doi.org/10.1007/s10577-011-9242-3

Ruiz-Herrera A, Nergadze SG, Santagostino M, Giulotto E (2008) Telomeric repeats far from the ends: mechanisms of origin and role in evolution. Cytogenetic and genome Research 122: 219–228. https://doi.org/10.1159/000167807

Schmid M (1978) Chromosome banding in Amphibia. I. Constitutive heterochromatin and nucleolus organizer regions in *Bufo* and *Hyla*. Chromosoma 66: 361–368. https://doi.org/10.1007/BF00328536

Schmid M, Steinlein C (2016) Chromosome Banding in Amphibia. XXXIV. Intrachromosomal Telomeric DNA Sequences in Anura. Cytogenetic and Genome Research 148: 211–226. https://doi.org/10.1159/000446298

Schmid M, Bogart JP, Hedges SB (2018) The Arboranan Frogs: Evolution, Biology, and Cytogenetics. Cytogenetic Genome Research 155: 1–5. https://doi.org/10.1159/000492098

Sumner AT (1972) A simple technique for demostrating centromeric heterochromatin. Experimental Cell Research 83: 438–442. https://doi.org/10.1016/0014-4827(72)90558-7

Targueta CP, Vittorazzi SE, Gatto KP, Bruschi DP, Veiga-Menoncello AC, Recco-Pimentel SM, Lourenço LB (2018) Anuran Cytogenetics: an overview. In: Norris N, Miller C (Eds) An Essential Guide to Cytogenetics (Charper 1). Nova Science Publishers, 1–64.

Tymowska J, Fischberg M (1973) Chromosome complements of the genus *Xenopus*. Chromosoma 44: 335–342. https://doi.org/10.1007/BF00291027

Tymowska J, Fischberg M (1982) A comparison of the karyotype, constitutive heterochromatin, and nucleolar organizer regions of a new tetraploid species *Xenopus epitropicalis* Fischberg and Picard with those of *Xenopus tropicalis* Gray (Anura, Pipidae). Cytogenetic and Cell Genetics, 34: 149–157. https://doi.org/10.1159/000131803

Tymowska J (1991) Polyploidy and cytogenetic variation in frogs of the genus *Xenopus*: In: Green DM, Sessions SK (Eds) Amphibian Cytogenetics and Evolution. Academic Press, New York, 259–297. https://doi.org/10.1016/B978-0-12-297880-7.50016-0

Trueb L, Ross CF, Smith R (2005) A new pipoid anuran from the Late Cretaceous of South Africa. Journal of Vertebrate Paleontology 25: 533–547. https://doi.org/10.1671/0272-4634(2005)025[0533:ANPAFT]2.0.CO;2

Uehara M, Haramoto Y, Sekizaki H, Takahashi S, Asashima M (2002) Chromosome mapping of *Xenopus tropicalis* using the G- and Ag-bands: tandem duplication and polyploidization of larvae heads. Development, Growth & Differentiation 44: 427–436. https://doi.org/10.1046/j.1440-169X.2002.00656.x

Viegas-Péquignot E (1992) In situ hybridization to chromosomes with biotinylated probes. In: Wilkinson DG (Ed.) In Situ Hybridization: A Practical Approach. IRL Press, Oxford, 137–158.

Wickbom T (1950) The chromosomes of *Pipa pipa*. Hereditas 36: 363–366. https://doi.org/10.1111/j.1601-5223.1950.tb03386.x

CompCytogen 13(3): 311–319 (2019)
doi: 10.3897/CompCytogen.v13i3.46777
http://compcytogen.pensoft.net

SHORT COMMUNICATION

COMPARATIVE Cytogenetics
A peer-reviewed open-access journal
International Journal of Plant & Animal Cytogenetics, Karyosystematics, and Molecular Systematics

Karyotype reinvestigation does not confirm the presence of two cryptic species and interspecific hybridization in the *Polyommatus* (*Agrodiaetus*) *damocles* complex in the Crimea (Lepidoptera, Lycaenidae)

Vladimir A. Lukhtanov[1,2], Konstantin A. Efetov[3], Alexander V. Dantchenko[1,4]

1 *Department of Karyosystematics, Zoological Institute of the Russian Academy of Sciences, Universitetskaya nab. 1, St. Petersburg 199034, Russia* **2** *Department of Entomology, St. Petersburg State University, Universitetskaya nab 7/9, St. Petersburg 199034, Russia* **3** *Department of Biological Chemistry and Laboratory of Biotechnology, V. I. Vernadsky Crimean Federal University, Lenin blvd. 5/7, Simferopol 295051, Russia* **4** *Faculty of Chemistry, Lomonosov Moscow State University, GSP-1, Leninskiye Gory 1/11, Moscow119991, Russia*

Corresponding author: *Vladimir A. Lukhtanov* (lukhtanov@mail.ru)

Academic editor: *V.G. Kuznetsova* | Received 23 September 2019 | Accepted 30 September 2019 | Published 17 October 2019

http://zoobank.org/85EBFC36-8F4F-4BFD-B291-88AC8F111189

Citation: Lukhtanov VA, Efetov KA, Dantchenko AV (2019) Karyotype reinvestigation does not confirm the presence of two cryptic species and interspecific hybridization in the *Polyommatus* (*Agrodiaetus*) *damocles* complex in the Crimea (Lepidoptera, Lycaenidae). Comparative Cytogenetics 13(4): 311–319. https://doi.org/10.3897/CompCytogen.v13i3.46777

Abstract

The karyotype of the blue butterflies from the Angarskiy Pass (Crimea), previously attributed to *Polyommatus* (*Agrodiaetus*) *poseidon* (Herrich-Schäffer, 1851), was re-examined. In all 19 studied individuals, we found the haploid chromosome number n = 26, including 7 pairs of relatively large and 19 pairs of relatively small chromosomes. According to the chromosome number and karyotype structure, the studied population does not differ from *P.* (*A.*) *damocles krymaeus* (Sheljuzhko, 1928) from the eastern part of the Crimean Mountains. This result does not confirm the previously formulated hypotheses, according to which (1) two morphologically similar but karyologically different species, *P.* (*A.*) *poseidon* and *P.* (*A.*) *damocles krymaeus*, occur sympatrically in the Crimea and (2) there is hybridization between these taxa on the Angarskiy Pass. Thus, only three species of the subgenus *Agrodiaetus* Hübner, 1822 have been reliably established for the Crimea: *P.* (*A.*) *damone pljushtchi* Lukhtanov & Budashkin, 1993, *P.* (*A.*) *damocles krymaeus* (Sheljuzhko, 1928) and *P.* (*A.*) *ripartii budashkini* Kolev & de Prins, 1995.

Keywords

Biodiversity, chromosome, hybrids, meiosis, karyosystematics, taxonomy

Introduction

The subgenus *Agrodiaetus* Hübner, 1822 of the genus *Polyommatus* Latreille, 1804 is a diverse and taxonomically difficult group of blue butterflies of the subtribe Polyommatina (Talavera et al. 2013), consisting of a large number of species weakly differentiated in morphology (Eckweiler and Bozano 2016). At the same time, the subgenus demonstrates a high level of karyotypic differentiation with respect to the chromosome number (Przybyłowicz et al. 2014, Lukhtanov 2015, Vershinina and Lukhtanov 2017), chromosome size (Lukhtanov and Dantchenko 2002) and number of chromosomes bearing ribosomal DNA clusters (Vershinina et al. 2015). Therefore, cytogenetic studies are an absolutely necessary (although not always sufficient) approach for solving many problems of the taxonomy in the subgenus *Agrodiaetus* (de Lesse 1960, Lukhtanov and Dantchenko 2017, Lukhtanov and Shapoval 2017, Vishnevskaya et al. 2018).

Karyotypes of the Crimean *Agrodiaetus* were studied by Kandul (1997) who indicated three species for this territory: *P.* (*A.*) *damone pljushtchi* Lukhtanov & Budashkin, 1993 (with the haploid chromosome number, n = 67), *P.* (*A.*) *ripartii budashkini* Kolev & de Prins, 1995 (n = 90) and *P.* (*A.*) *poseidon* (Herrich-Schäffer, 1851). The latter species, according to Kandul, is represented by two karyomorphs in the Crimea. One of them, determined by Kandul as *P.* (*A.*) *poseidon krymaeus* (Sheljuzhko, 1928) [currently known as *P.* (*A.*) *damocles krymaeus* (Sheljuzhko, 1928), see Eckweiler and Bozano 2016], has n = 26. It is quite widespread in the southern Crimea from the Angarskiy Pass in the west to the village of Kurortnoye in the east. Another karyomorph, determined by Kandul (1997) as *P.* (*A.*) *poseidon poseidon* (Herrich-Schäffer, [1851]), has n = 19. According to Kandul, the latter karyomorph was found in four individuals collected by K. A. Efetov on the Angarskiy Pass in 1992 (see the Discussion section for the alternative possible origin of these specimens). In addition, abnormal meiotic metaphase plates were found in the specimens from the Angarskiy Pass presumably indicating hybridization between *P.* (*A.*) *damocles krymaeus* and *P.* (*A.*) *poseidon* (Kandul 1997).

Since these chromosomal morphs (n = 26 and n = 19) were reported to inhabit in sympatry, it could be assumed that they belong to different species. This is a plausible assumption given that (1) the distribution areas of *P.* (*A.*) *damocles* and *P.* (*A.*) *poseidon* overlap in Turkey (Eckweiler and Bozano 2016), (2) *P.* (*A.*) *poseidon* is distributed more widely and represented on its northern edge by extremely local populations which remain unknown until now even on the well-studied territories (Lukhtanov and Tikhonov 2015), and (3) the larval foodplant of *P.* (*A.*) *poseidon* also belongs to the genus *Hedysarum* Linnaeus, 1753 (Fabaceae) as it was reported before for *P.* (*A.*) *damocles krymaeus* (Budashkin 1990, Dantchenko 1995, 1997, Dantchenko, unpubl.). The presence of hybrid individuals does not preclude this assumption, since their meiosis was reported to be abnormal (Kandul 1997).

To test the hypotheses about the two karyomorphs and interspecific hybridization, we re-examined the karyotypes of the blues from the same population (Crimea, the Angarskiy Pass) that was previously studied by Kandul (1997).

Material and methods

Adult males were collected by K. A. Efetov on the Angarskiy Pass of the Crimean Mountains exactly in the same place where in 1993 (erroneously cited by Kandul as "1992") the Kandul's material (Kandul 1997) was collected. The collection of the new material was carried out during two summer seasons: in 1997 and in 1998.

Testes were extracted from the butterfly abdomens and fixed in a mixture of glacial acetic acid and 96% ethyl alcohol (1 : 3). The fixed material was stored at + 4°C for 5–6 months. The testes were stained with 2% orcein acetic acid for 8–30 days as previously described (Lukhtanov 2017, Efetov et al. 2004, 2015 and references therein). The stained material was placed in a drop of 40% lactic acid on a glass slide. The testes were macerated with thin pins. The slide was covered with a coverslip and the macerated testes were squashed between the two glasses. Excess lactic acid was removed with filter paper. Karyotypes were studied in 19 individuals. For determination of karyotype parameters, 175 metaphase plates of the highest quality and 2 cells at the stage of diakinesis were selected. Cells in which the chromosomes were not located on the same plane, as well as cells with overlapping or touching chromosomes and/or bivalents, were rejected and not used for analysis. Haploid chromosome number (n) was counted at metaphase I (MI), metaphase II (MII) and diakinetic cells. In some cases, diploid chromosome number (2n) was counted in spermatogonial mitotic metaphase plates and atypical meioses (see: Lorković 1990, Lukhtanov and Dantchenko 2017 for an explanation and illustration of atypical meiosis in Lepidoptera).

Results and discussion

Butterflies of the *P.* (*A.*) *damocles* species complex have a single generation in the Crimea (Budashkin 1990), and therefore the adults can be encountered there from the first to the last days of July. In 1997, only the karyomorph n = 26 was found among the butterflies collected at the end of July (i.e. at the end of the flying period). Since it was impossible to exclude that the karyomorph n = 19 has a different phenology, and butterflies with this karyotype fly earlier, then in 1998, individuals were collected in all parts of the flying period: from the first to the last days of July. However, the karyomorph n = 19 was never detected.

Summing up the analysis of the samples collected on the Angarskiy Pass, 26 bivalents were found in all studied individuals in all cells at the stages of MI and diakinesis, and 26 chromosomes at the stage of MII. The karyotype at these stages is sharply asymmetric and includes 7 relatively large and 19 relatively small bivalents. Diploid chromosome number 2n = 52 was found in spermatogonial mitosis and atypical meiosis. No variation in the chromosome number was observed. Therefore, we do not confirm the numbers n = 25 and n = 27 reported for this population by Kandul (1997) along with the modal number n = 26. The information obtained is summarized in the Table 1. Photos of karyotypes are shown in the Figures 1–4.

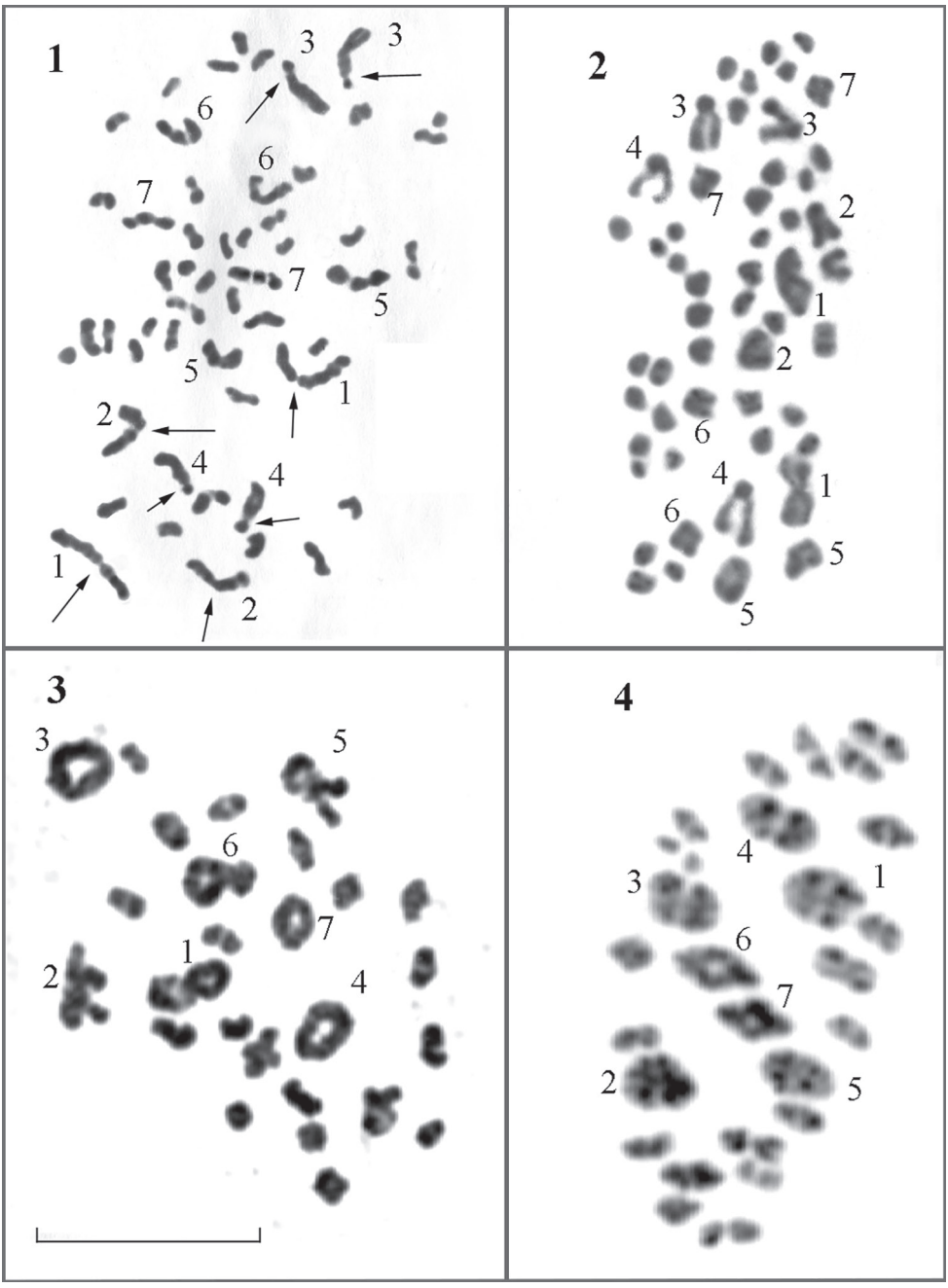

Figures 1–4. Karyotype in male mitosis and meiosis of *Polyommatus* (*Agrodiaetus*) *damocles krymaeus* from the Angarskiy Pass (Crimea). Numbers from 1 to 7 show the largest chromosome pairs in mitosis and the largest bivalents in meiosis. **1** metaphase of spermatogonial mitosis, 2n = 52 **2** early anaphase of spermatogonial mitosis, 2n = 52 **3** diakinesis, n = 26 **4** MI, n = 26. Scale bar: 10 μm.

Table 1. Chromosome numbers found in *P.* (*A.*) *damocles krymaeus* (Crimea, the Angarskiy Pass).

Code of specimen	Dates of collection	Chromosome number	Quantity and type of studied cells
1997-A	25.07.1997	n = 26	27 MI
1997-B	26.07.1997	n = 26	1 MI
1997-C	26.07.1997	n = 26	2 MI
1997-D	31.07.1997	n = 26	1 MI
1998-1	2.07.1998	n = 26	4 MI
1998-2	2.07.1998	n = 26	1 MI
1998-4	12.07.1998	n = 26	7 MI
1998-4	12.07.1998	n = 26	2 MII
1998-4	12.07.1998	2n = 52	2 atypical divisions
1998-4	12.07.1998	2n = 52	2 mitotic metaphases
1998-5	14.07.1998	n = 26	13 MI
1998-6	14.07.1998	n = 26	20 MI
1998-6	14.07.1998	n = 26	20 MII
1998-7	15.07.1998	n = 26	2 MI
1998-8	15.07.1998	n = 26	9 MI
1998-9	15.07.1998	n = 26	16 MI
1998-11	15.07.1998	n = 26	8 MI
1998-11	15.07.1998	n = 26	2 diakinetic cells
1998-12	15.07.1998	n = 26	7 MI
1998-13	15.07.1998	n = 26	4 MI
1998-14	21.07.1998	n = 26	4 MI
1998-51	23.07.1998	n = 26	5 MI
1998-54	23.07.1998	n = 26	7 MI
1998-55	23.07.1998	n = 26	9 MI
1998-55	23.07.1998	n = 26	4 MII

Analyzing the information at our disposal, as well as butterflies collected by K. A. Efetov on the Angarskiy Pass in 1993 (Kandul's material, cited by him as "1992") and 1997–1998 (our material), we conclude that, most likely, there are no blue butterflies of the subgenus *Agrodiaetus* with the karyotype n = 19 in the Crimea. Our conclusion is based on the following:

1) the presence of the karyomorph n = 19 is not confirmed by several studies, all 19 individuals studied from the Angarskiy Pass have n = 26;
2) males of *P.* (*A.*) *poseidon* and *P.* (*A.*) *damocles* are not identical in their appearance. Males of *P.* (*A.*) *damocles* have a darker blue coloration, and their veins on the wing upperside possess black scales (Eckweiler and Bozano 2016). If these two species are present on the Angarskiy pass, we expect to find both phenotypes here. However, this is not the case. The individuals E92003, E92012, E92014 and E92015, for which the karyotype n = 19 was reported (Kandul 1997), are identical in their external morphology to all other individuals from the Angarskiy Pass, for which n = 26 was established. All these individuals have the phenotype of *P.* (*A.*) *damocles krymaeus* (Figs 5–8).

   Additionally, our data do not confirm the conclusion (Kandul 1997) about chromosome number variation in *P.* (*A.*) *damocles krymaeus* from n = 25 to n = 27. We found the number n = 26 to be stable;

3) the conclusion about hybridization between the two putative chromosomal races was based on the analysis of the metaphase plates of insufficient quality (see: Kandul 1997: fig. 6). In the given micrographs, it is impossible to distinguish between bivalents and multivalents; we therefore conclude that the assumption of the presence of multivalents on these metaphase plates remains unsupported by the data.

In the end, we assume that the karyomorph n = 19 from the Angarskiy Pass does not actually exist and is an artifact, although it is rather difficult to explain the possible origin of this error. It cannot be excluded that it resulted from an accidental mix-up between the chromosomal preparations (but not between the butterfly samples) of *P.* (*A.*) *poseidon* from Turkey (n = 19) and *P.* (*A.*) *damocles krymaeus* from the Crimea (n = 26), since they were processed in parallel (see Kandul and Lukhtanov 1997).

In terms of the chromosome number and karyotype structure, the studied population found on the Angarskiy Pass is the same as that from the eastern Crimea (Sudak region) (Figs 5–8), although the wings of males of the Angarskiy Pass population are

Figures 5–8. *Polyommatus* (*Agrodiaetus*) *damocles krymaeus*, Crimea, Karadagh, Legener Mt. **5** male, upperside **6** male, underside **7** female, upperside **8** female, underside.

somewhat darker. We assign both these populations to the taxon originally described as "*Lycaena damone* Ev. *krymaea* (subsp. nov.) Sheljuzhko, 1928" (type locality: Agarmysh mountain near Stary Krym town, see Dantchenko 1997). In turn, this taxon is a subspecies of *P.* (*A.*) *damocles* to which it is most similar in terms of morphology (Dantchenko 1997), karyotype structure (Lukhtanov et al. 1997) and molecular characters (Kandul et al. 2007).

Acknowledgements

We thank Pavel Bogdanov (State Darvin Museum, Moscow) for important information on ecology *P.* (*A.*) *damocles crymaeus* and Yuri Budashkin for hospitality and help during the field studies in the Crimea. We thank Snejana Grozeva and Vladimir Gokhman for comments on the manuscript. The financial support for this study was provided by the grant no. 19-14-00202 from the Russian Science Foundation to the Zoological Institute of the Russian Academy of Sciences. The work was partially performed using equipment of the 'Chromas' Core Facility and the Centre for Molecular and Cell Technologies of St. Petersburg State University.

References

Budashkin YI (1990) Biology of *Agrodiaetus poseidon krymaeus* (Schelj.) (Lepidoptera, Lycaenidae). Vestnik Zoologii 1990(1): 85.

Dantchenko AV (1995) Notes on the biology of *Polyommatus* (*Agrodiaetus*) *damocles rossicus* Dantchenko & Lukhtanov, 1993 (Lepidoptera, Lycaenidae). Nachrichten des Entomologischen Vereins Apollo 16(2/3): 141–146.

Dantchenko AV (1997) Notes on the biology and distribution of the *damone* and *damocles* species-complexes of the subgenus *Polyommatus* (*Agrodiaetus*) (Lepidoptera: Lycaenidae). Nachrichten des Entomologischen Vereins Apollo, Supplement 16: 23–42.

de Lesse H (1960) Spéciation et variation chromosomique chez les Lépidoptères Rhopalocères. Annales des Sciences Naturelles Zoologie et Biologie Animale (12e série) 2: 1–223.

Eckweiler W, Bozano GC (2016) Guide to the butterflies of the Palearctic region. Lycaenidae part IV. Milano, Omnes artes. 132 pp.

Efetov KA, Parshkova EV, Koshio C (2004) The karyotype of *Illiberis* (*Primilliberis*) *rotundata* Jordan, [1907] (Lepidoptera: Zygaenidae, Procridinae). Entomologist's Gazette 55(3): 167–170.

Efetov KA, Parshkova EV, Tarasova LG, Tarmann GM (2015) The karyotypes of Procridinae (Lepidoptera: Zygaenidae), with the first record of the karyotype of *Pollanisus commoni* Tarmann, 2004, a representative of the tribe Artonini. Entomologist's Gazette 66(2): 121–125.

Kandul NP (1997) The karyology and the taxonomy of the blue butterflies of the genus *Agrodiaetus* Hübner, [1822] from the Crimea (Lepidoptera, Lycaenidae). Atalanta 28(1/2): 111–119.

Kandul NP, Lukhtanov VA (1997) Karyotype variability and systematics of blue butterflies of the species groups *Polyommatus* (*Agrodiaetus*) *poseidon* and *P.* (*A.*) *dama* (Lepidoptera, Lycaenidae). Zoologicheskii Zhurnal 76: 63–69. [In Russian with English abstract]

Kandul NP, Lukhtanov VA, Pierce NE (2007) Karyotypic diversity and speciation in *Agrodiaetus* butterflies. Evolution 61(3): 546–559. https://doi.org/10.1111/j.1558-5646.2007.00046.x

Lorković Z (1990) The butterfly chromosomes and their application in systematics and phylogeny. In: Kudrna O (Ed.) Butterflies of Europe, Vol. 2. Introduction to Lepidopterology. Aula-Verlag, Wiesbaden, 332–396.

Lukhtanov VA (2015) The blue butterfly *Polyommatus* (*Plebicula*) *atlanticus* (Lepidoptera, Lycaenidae) holds the record of the highest number of chromosomes in the non-polyploid eukaryotic organisms. Comparative Cytogenetics 9(4): 683–690. https://doi.org/10.3897/CompCytogen.v9i4.5760

Lukhtanov VA (2017) A new species of *Melitaea* from Israel, with notes on taxonomy, cytogenetics, phylogeography and interspecific hybridization in the *Melitaea persea* complex (Lepidoptera, Nymphalidae). Comparative Cytogenetics 11(2): 325–357. https://doi.org/10.3897/CompCytogen.v11i2.12370

Lukhtanov VA, Dantchenko AV (2002) Principles of highly ordered metaphase I bivalent arrangement in spermatocytes of *Agrodiaetus* (Lepidoptera). Chromosome Research 10(1): 5–20. https://doi.org/10.1023/A:1014249607796

Lukhtanov VA, Dantchenko AV (2017) A new butterfly species from south Russia revealed through chromosomal and molecular analysis of the *Polyommatus* (*Agrodiaetus*) *damonides* complex (Lepidoptera, Lycaenidae). Comparative Cytogenetics 11(4): 769–795. https://doi.org/10.3897/CompCytogen.v11i4.20072

Lukhtanov VA, Tikhonov VV (2015) Chromosomal and molecular evidence for presence of *Polyommatus* (*Agrodiaetus*) *poseidon* (Lepidoptera, Lycaenidae) in Caucasus region. Comparative Cytogenetics 9(2): 249–255. https://doi.org/10.3897/CompCytogen.v9i2.5020

Lukhtanov VA, Shapoval NA (2017) Chromosomal identification of cryptic species sharing their DNA barcodes: *Polyommatus* (*Agrodiaetus*) *antidolus* and *P.* (*A.*) *morgani* in Iran (Lepidoptera, Lycaenidae). Comparative Cytogenetics 11(4): 759–768. https://doi.org/10.3897/CompCytogen.v11i4.20876

Lukhtanov VA, Dantchenko AV, Kandul NP (1997) Die Karyotypen von *Polyommatus* (*Agrodiaetus*) *damone damone* und *P.* (*A.*) *damocles rossicus* nebst einigen Problemen bei *Agrodiaetus* (Lepidoptera, Lycaenidae). Nachrichten des Entomologischen Vereins Apollo, Supplement 16: 43–48.

Przybyłowicz Ł, Lukhtanov V, Lachowska-Cierlik D (2014) Towards the understanding of the origin of the Polish remote population of *Polyommatus* (*Agrodiaetus*) *ripartii* (Lepidoptera: Lycaenidae) based on karyology and molecular phylogeny. Journal of Zoological Systematics and Evolutionary Research 52(1): 44–51. https://doi.org/10.1111/jzs.12040

Talavera G, Lukhtanov VA, Pierce NE, Vila R (2013) Establishing criteria for higher-level classification using molecular data: the systematics of *Polyommatus* blue butterflies (Lepidoptera, Lycaenidae). Cladistics 29: 166–192. https://doi.org/10.1111/j.1096-0031.2012.00421.x

Vershinina AO, Lukhtanov VA (2017) Evolutionary mechanisms of runaway chromosome number change in *Agrodiaetus* butterflies. Scientific Reports 7: 8199. https://doi.org/10.1038/s41598-017-08525-6

Vershinina AO, Anokhin BA, Lukhtanov VA (2015) Ribosomal DNA clusters and telomeric (TTAGG)n repeats in blue butterflies (Lepidoptera, Lycaenidae) with low and high chromosome numbers. Comparative Cytogenetics 9(2): 161–171. https://doi.org/10.3897/CompCytogen.v9i2.4715

Vishnevskaya MS, Lukhtanov VA, Dantchenko AV, Saifitdinova AF (2018) Combined analysis of chromosomal and molecular markers reveals cryptic species: karyosystematics of the *Agrodiaetus* Hübner, [1822] blue butterflies. Comparative Cytogenetics 12(3): 325–326. https://doi.org/10.3897/CompCytogen.v12i3.27748

CompCytogen 13(3): 321–324 (2019)
doi: 10.3897/CompCytogen.v13i3.47366
http://compcytogen.pensoft.net

IN MEMORIAM

COMPARATIVE Cytogenetics
A peer-reviewed open-access journal
International Journal of Plant & Animal Cytogenetics, Karyosystematics, and Molecular Systematics

In Memoriam: Dr. Sergey V. Zhirov (1966–2017)

Valentina Kuznetsova[1], Natalia Golub[1], Ninel Petrova[1], Vladimir Lukhtanov[1], Boris Anokhin[1], Natalia Khabasova[1], Nazar Shapoval[1], Larissa Kupriyanova[1], Ilya Gavrilov-Zimin[1]

1 *Department of Karyosystematics, Zoological Institute, Russian Academy of Sciences, Universitetskaya nab. 1, 199034 St. Petersburg, Russia*

Corresponding author: *Valentina Kuznetsova* (valentina_kuznetsova@yahoo.com)

Academic editor: *V. Gokhman* | Received 16 October 2019 | Accepted 16 October 2019 | Published 21 October 2019

http://zoobank.org/2A4CBB57-6E2C-4E5F-B477-F39D776422D2

Citation: Kuznetsova V, Golub N, Petrova N, Lukhtanov V, Anokhin B, Khabasova N, Shapoval N, Kupriyanova L, Gavrilov-Zimin I (2019) In Memoriam: Dr. Sergey V. Zhirov (1966–2017). Comparative Cytogenetics 13(3): 321–324. https://doi.org/10.3897/CompCytogen.v13i3.47366

On October 26th, 2017, the Cytogenetic Science suffered a stunning loss: Dr. Sergey V. Zhirov, geneticist and cytogeneticist, passed away at the age of fifty-one.

Dr. Sergey V. Zhirov, the researcher of the Department of Karyosystematics of the Zoological Institute, Russian Academy of Sciences in St. Petersburg, died of a heart attack, on his way to the Institute. This was a sudden death, and we were shocked to learn it.

Sergey was born on June 8th, 1966 in the city of Starodub, Bryansk region, Russia, as a son of a schoolteacher and an engineer. His childhood passed in an ancient Russian city of Pskov, where Sergey graduated from a secondary school with a Gold Medal. At school, he enthusiastically studied biology, chemistry, physics, and mathematics. However, Sergey finally chose biology and, after graduating from the school, he entered the Pskov State Pedagogical Institute, the Faculty of Biology and Chemistry, and the Department of Natural Geography. After the first course, he was called up for the military service. He was doing this service at the Finnish border until 1986 and then he returned to his alma mater. Sergey's friends and tutors from the Institute recall him as a very capable, conscientious and active student. He participated in various activities of the student sci-

Figure 1. Dr. Sergey V. Zhirov (8.VI.1966 – 26.X.2017).

entific society, carrying out research projects and participating in student conferences. His Graduate Thesis entitled "The influence of electromagnetic fields on the embryogenesis of the Chudsky lake whitefish" represented an exemplary student work.

After graduating, Sergey remained at the Department of Zoology of the Institute. Being an associate professor, he organized and conducted field training of the students and supervised their research work. He wrote several manuals and used to teach at the Ecological and Biological Center. Simultaneously with the teaching activity, Sergey continued his scientific studies.

In 1989, Sergey married his classmate Diana, and in 1990, their daughter Uljana was born.

Sergey lived with a passion for science. His distinguished research career focused on studying giant polytene chromosomes of chironomid midges (Diptera, Chironomidae), including polymorphisms related to the environmental conditions. In 1991-1994, Sergey was pursuing postgraduate studies at the Herzen State Pedagogical University (St. Petersburg) and the Zoological Institute RAS. He received a PhD degree in Genetics at St. Petersburg State University with the thesis "Chromosomal and genomic polymorphism in chironomid populations of the Pskov region".

From 2008, Sergey continued his research in cytogenetics and karyosystematics of chironomids at the Department of Karyosystematics of the Zoological Institute RAS. Sergey was a talented researcher. He put forward interesting hypotheses and carefully and precisely conducted experiments to prove those hypotheses. Sergey had "golden hands" and created accurate and reliable research tools for his experiments. He published more than 20 articles in several peer-reviewed journals.

Among Sergey's many distinctions, we would like to note another two. He was a member of the Editorial Team of *Comparative Cytogenetics*. As a Subject Editor managing submissions on chironomid cytogenetics, he was strict but very helpful and friendly to the authors. In addition, he was a highly respected guide at the Zoological Museum of the Zoological Institute. He took his guide mission very seriously and was able to explain complex issues in a perfectly clear way. Sergey was therefore one of the most admired guides at the Museum.

Apart from Sergey's teaching and academic careers, he also was a talented person. He enjoyed literature and wrote a number of verses.

We were very fortunate to work and study together with Sergey. He will be sincerely missed by his friends and colleagues. Unfortunately, his wife outlasted Sergey for only two years; Diana passed away in October 2019. We send our heartfelt condolences to their daughter Uljana.

Main publications of Sergey V. Zhirov:

Petrova NA, Zhirov SV (2008) Cytogenetics of *Chironomus riparius* L. from the fishpond in Borok village (Diptera, Chironomidae, Diptera). Tsitologia 50(6): 535–538. [In Russian with English Summary]

Petrova NA, Zhirov SV (2008) Polytene chromosomes of salivary glands of chironomids (Diptera: Chironomidae) from the Wrangel Island (Russia). Comparative Cytogenetics 2(2): 127–130.

Petrova NA, Zhirov SV (2009) Inversion polymorphism in two Chironomidae species out of genera *Chironomus* and *Camptochironomus* (Diptera, Chironomidae, Chironomini) from different regions of Russia (Center and North-West). Vestnik of Saint Petersburg University (Series 3. Biology) 4: 29–39. [In Russian with English Summary]

Petrova NA, Zhirov SV (2010) Larva morphology, karyotype structure, and inversion polymorphism in a chironomid from the Republic of South Africa (Diptera, Chironomidae). Vestnik VOGiS 14(1): 70–78. [In Russian with English Summary]

Petrova NA, Zhirov SV, Zelentsov NI, Kachvoryan EA (2011) To the fauna of chironomids (Diptera, Chironomidae) from the Razdan River valley (Arnenia). Zoologicheskii Zhurnal 114: 445–451. [In Russian with English Summary]

Petrova NA, Zhirov SV (2011) Cytogenetic comparison of chironomid midge *Glyptotendipes glaucus* (Meigen, 1818) (Diptera, Chironomidae) populations from Northwest Russia and Ukraine (Chernobyl Zone). Ecological Genetics 9(2): 9–16. [In Russian with English Summary] https://doi.org/10.17816/ecogen1029-16

Petrova NA, Zhirov SV, Arutyunova KV, Arutyunova MV (2012) Morphological abnormalities of mouthparts in some species of subfamilies Orthocladiinae and Diamesinae (Diptera, Chironomidae). Biological Journal of Armenia 64(4): 48–52. [In Russian].

Zhirov SV, Petrova NA (2013) The chironomid midge *Dicrotendipes* sp. afr. (Diptera, Chironomidae) from the Republic of South Africa. Entomological Review 93(6): 695–702. [Originally published in Russian in Zoologicheskii Zhurnal, 2013, 92(4): 464–471] https://doi.org/10.1134/S0013873813060031

Petrova NA, Zhirov SV (2014) Characteristics of the karyotypes of three subfamilies of Chironomids (Diptera, Chironomidae: Tanypodinae, Diamesinae, Prodiamesinae) of the world fauna. Entomological Review 94(2): 157–165. [Originally published in Russian in Entomologicheskoe Obozrenie, 2013, 92(3): 505–516] https://doi.org/10.1134/S001387381402002X

Karmokov MKh, Belyanina SI, Zhirov SV, Petrova NA (2014) Karyotype and morphology of the midge *Stictochironomus crassiforceps* (Kieffer) (Diptera, Chironomidae) from several parts of the Palaearctic. Entomological Review 94(9): 1229–1238. [Originally published in Russian in Entomologicheskoe Obozrenie, 2014, 93(3): 555–563] https://doi.org/10.1134/S0013873814090048

Zhirov SV, Petrova NA (2015) Karyotypes and larval morphology of three species of midges (Diptera, Chironomidae) from lakes in the Southern part of Kunashir Island. Entomological Review 95(7): 881–890. [Originally published in Russian in Entomologicheskoe Obozrenie, 2015, 94(3): 599–607] https://doi.org/10.1134/S0013873815070064

Lobkova LE, Orel OV, Zhirov SV, Petrova NA (2015) *Chironomus* (*Chironomus*) *acidophilus* Keyl, 1960 (Diptera, Chironomidae, Chironominae): biology, morphology, karyotype and habitat conditions in the caldera of the Uzon Volcano (Kamchatka, Kronotsky Nature Reserve). Proceedings of the Kronotsky Nature Reserve 4: 92–119. [In Russian with English Summary]

Orel OV, Lobkova LE, Zhirov SV, Petrova NA (2015) A new record of *Chironomus* (*Chironomus*) *acidophilus* Keyl (Diptera, Chironomidae) from the Uzon volcanic caldera (Kronotsky Reserve, Kamchatka Peninsula, Russia), its karyotype, ecology and biology. Zootaxa 3981(2): 177–192. https://doi.org/10.11646/zootaxa.3981.2.2

Mylnikov SV, Zhirov SV (2015) Statistical approach to the problem of the taxonomic status and evolutionary potential of a non-biting midge *Prodiamesa olivacea* Meigen (1818) (Diptera, Chironomidae, Prodiamesinae) based on karyotype analysis. Ecological Genetics 13(1): 3–9. [In Russian with English Summary] https://doi.org/10.17816/ecogen1313-9

Petrova NA, Cornette R, Shimura S, Gusev OH, Pemba D, Kikawada T, Zhirov SV, Okuda T (2015) Karyotypical characteristics of two allopatric African populations of anhydrobiotic *Polypedilum* Kieffer, 1912 (Diptera, Chironomidae) originating from Nigeria and Malawi. Comparative Cytogenetics 9(2): 173–188. https://doi.org/10.3897/CompCytogen.v9i2.9104

Petrova NA, Zhirov SV (2015) The cytogenetic characteristic of some Palearctic populations of Holarctic midge *Glyptotendipes barbipes* Staeger (Diptera, Chironomidae). Tsitologia 57(11): 831–837. [In Russian with English Summary]

Zhirov SV, Mylnikov SV (2016) About approaches to studying the microevolutionary phenomena in connatural chironomids populations. Nonequilibrium of populations as stable state. Ecological Genetics 14(3): 35-46. [In Russian with English Summary] https://doi.org/10.17816/ecogen14335-46

Petrova NA, Zhirov SV (2017) Karyotype characteristics of *Chironomus fraternus* Wülker and *Ch. beljaninae* Wülker (Diptera, Chironomidae) from Northern Russia. Entomological Review 97(6): 730–734. [Originally published in Russian in Entomologicheskoe Obozrenie, 2017, 96(3): 429–435] https://doi.org/10.1134/S0013873817060033

Petrova NA, Zhirov SV, Krasheninnikov AB (2019) Larvae morphology and karyotype structure of *Chironomus* sp. (Diptera, Chironomidae) from Novaya Zemlya archipelago (Russia). Entomologicheskoe Obozrenie 98(4). [In press]